CNIC-01565
CNDC-0029
INDC(CPR)-053/L

COMMUNICATION OF NUCLEAR DATA PROGRESS

No. 25 (2001.6)

China Nuclear Data Center
China Nuclear Information Centre
China Nuclear Industry Audio & Visual Publishing House

COMMUNICATION OF NUCLEAR DATA PROGRESS

EDITORIAL NOTE

From this issue, the layout of CNDP has been changed to serve our reader better.The editors hope that our readers and colleagues will not spare their comments in order to improve this publication. If you have any, please contact us by following address:

Mailing Address: Profs. LIU Tingjin and ZHUANG Youxiang
China Nuclear Data Center
China Institute of Atomic Energy
P.O. Box 275 (41), Beijing 102413
People's Republic of China
Telephone: 86-10-69357729 or 69357830
Facsimile: 86-10-6935 7008
E-mail: tjliu @ iris.ciae.ac.cn or yxzhuang @ iris.ciae.ac.cn

Abstract: This is the 25th issue of *Communication of Nuclear Data Progress* (CNDP), in which the achievements in nuclear data field for the last year in China are carried. It includes the measurements of $^{10}B(n,\alpha)^{7}Li$ and $^{64}Zn(n,\alpha)^{61}Ni$ angular distributions and cross sections, $^{75}As(n,\gamma)^{76}As$ cross section and fission product yields of n+$^{235,238}U$; theoretical calculations of n+^{23}Na, $^{93,95}Nb$, ^{99}Tc, $^{99\sim105}Ru$, $^{132,134\sim138}Ba$, $^{133\sim135,137}Cs$, $^{136,138,140,142,Nat}Ce$, $^{142\sim148,150}Nd$, $^{175,176,Nat}Lu$, $^{174,176\sim180,Nat}Hf$; evaluations of reference fission yield data and n+$^{93,95}Nb$, $^{99,100}Ru$, $^{121,123}Sb$, $^{127,135}I$ and $^{241,242}Pu$ complete data; method to set up file 6 in neutron data library of light nuclei, Kerma factor calculation, a code for automatically searching optimal optical potential parameters below 300 MeV, internal conversion electrons data calculation, a code for composition of a nuclear data file of natural element from its isotope files; and the developments of CWIMS code and its 69-group library. Also the activities and cooperation on nuclear data in China are summarized.

Communication of Nuclear Data Progress
No. 25 (2001) Beijing

CONTENTS

Angular Distribution and Cross Section Measurement for $^{10}B(n,\alpha)^{7}Li$ Reaction

TANG Guoyou ZHANG Guohui CHEN Jinxiang SHI Zhaomin

Key Laboratory of Heavy Ion Physics, Ministry of Education, Beijing

YUAN Jing CHEN Zemin

Department of Physics, Tsinghua University, Beijing

YU.M.Gledenov M.Sedysheva G.Khuuknenkhuu

Joint Institute for Nuclear Research, Dubna 141908, Russia

【abstract】 *Using a gridded ionization chamber, the differential cross section for $^{10}B(n,\alpha)^{7}Li$ reaction were measured at 4.0, 5.0, 5.7 and 6.7MeV. The neutrons were produced through $D(d,n)^{3}He$ reaction. Absolute neutron flux was determined through $^{238}U(n,f)$ reaction. The differential cross sections are obviously backward peaked in the center of mass reference system.*

Introduction

The differential cross section data for $^{10}B(n,\alpha)^{7}Li$ reaction are important for the study of reaction mechanism and practical application. Since there are few existing data of cross section for $^{10}B(n,\alpha)^{7}Li$ reaction in lower than 5.0 MeV region, however, there are no differential data except in 14 MeV energy region.

Using a gridded ionization chamber, we performed the measurement of angular distribution and total cross sections for $^{10}B(n,\alpha)^{7}Li$ reaction at 4.0, 5.0, 5.7 and 6.7 MeV.

1 Experimental Details

The gridded ionization chamber was described in reference [1]. For present experiment, the working gas was Kr+4.73%CH_4 to exclude the interference from $^{16}O(n,\alpha)$ reaction. The distances from cathode to grid, grid to anode and anode to shield were 4.5, 2.2 and 1.1 cm, respectively.

The sample material was ^{10}B with the abundance of 99.9%. For present measurement two samples were used, they were evaporated on the tungsten backing (thickness:186 μg/cm^2), their weights were 1.78 and 1.84 mg respectively. They were back to back set on the sample changer in the ionization chamber, there was also a tungsten film placed in the sample changer of the gridded ionization chamber for background measurement. A ^{238}U sample (total weight 7.85±0.1 mg, *Φ*4.5 cm) were employed for absolute neutron flux measurement.

Since the thermal cross section for $^{10}B(n,\alpha)$ ^{7}Li reaction is as large as 3838 b, the interference of thermal neutron is very strong. In order to reduce this interference, the gridded ionization chamber was packed with Cd slice in thickness about 0.5 mm.

For the measurement in 5~6.5 MeV neutron energy region the working pressure of ionization chamber was 1.2 atm (1atm=101325 Pa). It was 1.1 atm at 4.0 MeV.

A BF_3 long counter was used as relative neutron flux monitor. The ^{238}U sample was employed to determine absolute neutron flux. The cross sections of $^{238}U(n,f)$ reaction were taken from CENDL-2 library.

The experiment was performed at the 4.5 MV Van de Graaff Accelerator of the Heavy Ion Physics, Peking University. Monoenergetic neutrons were produced through D(d,n) reaction with a gas target of 2.0 cm long and 1.5 to 2.0 atm in pressure separated from the vacuum tube by a molybdenum film 5 μm in

thickness. The energies of the beam deuterons are 1.0, 2.4, 3.0, and 3.7 MeV and the correspondence neutron energies are 4.0±0.2 , 5.03±0.26 , 5.75±0.15 and 6.5±0.20 MeV.

The deuteron beam was about 3.0 μA during experiment. The chamber was placed at 0 degree to the beam line, and the distance from its cathode to the center of the neutron source was about 38.0 cm. The samples were attached to the cathode, used as sample changer.

For the measurement at each energy point, the procedures are :

(1) Check the stability of the experiment using Pu-α source.

(2) Measure signal (including background).

(3) Measure background by using W-backing.

(4) Calibrate absolute neutron flux by using ^{238}U-target.

Total run time is about 15 to 30 hours for each neutron energy.

2 Results and Discussion

In Fig.1 and Fig.2 the two dimensional spectra for forward and backward angles at 5.7 MeV are shown respectively.

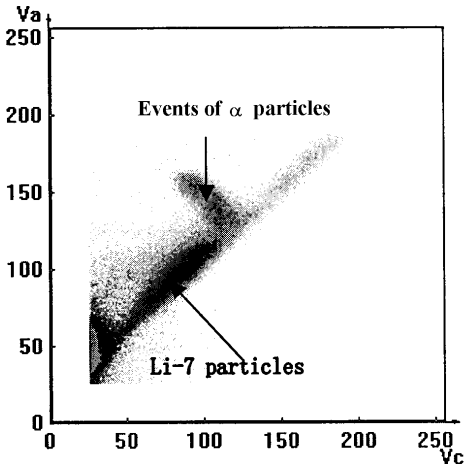

Fig. 1 The two dimensional spectra of forward for ^{10}B(n,α) ^{7}Li reaction at E_n=5.7±0.20 MeV
(Anode channel vs. cathode channel)

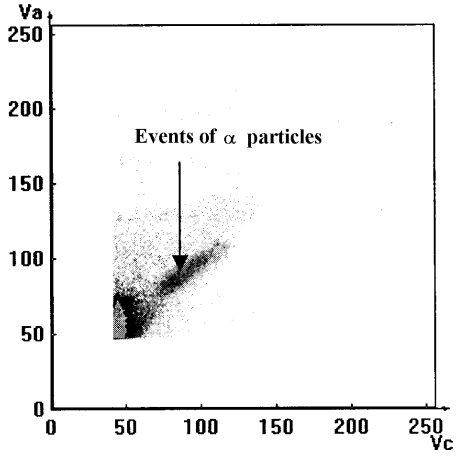

Fig.2 The two dimensional spectra for backward for ^{10}B(n,α) ^{7}Li reaction at E_n=5.7±0.20 MeV

In Figs. 3~6 the measured angular distributions in the center of mass system at 4.0, 5.0, 5.7 and 6.5 MeV are given respectively. The data larger than 70° in Lab-system are not included because of interference from ^{7}Li particles and thickness of target.

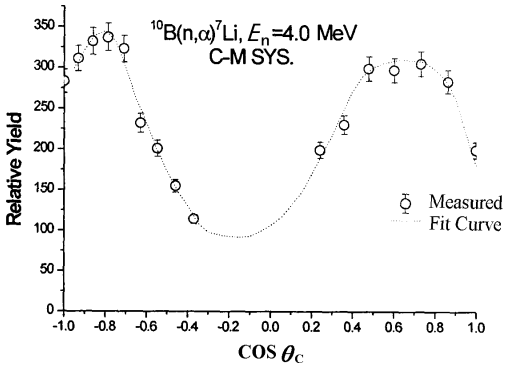

Fig. 3 Angular distribution for ^{10}B(n,α)^{7}Li reaction at 4.0±0.20 MeV

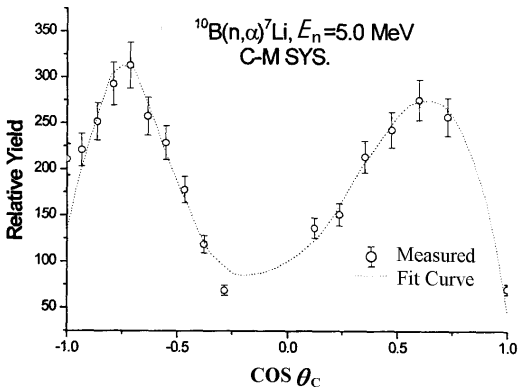

Fig. 4 Angular distribution for ^{10}B(n,α)^{7}Li reaction at 5.0±0.26 MeV

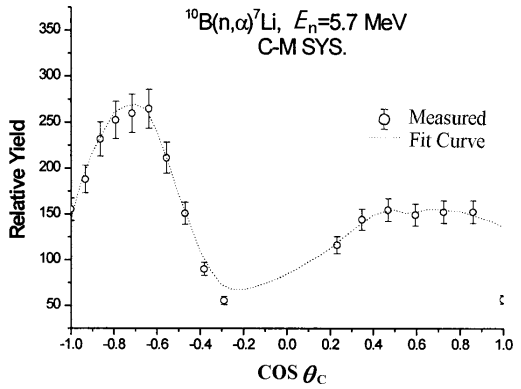

Fig. 5 Angular distribution for ^{10}B(n,α)^{7}Li reaction at 5.7±0.15 MeV

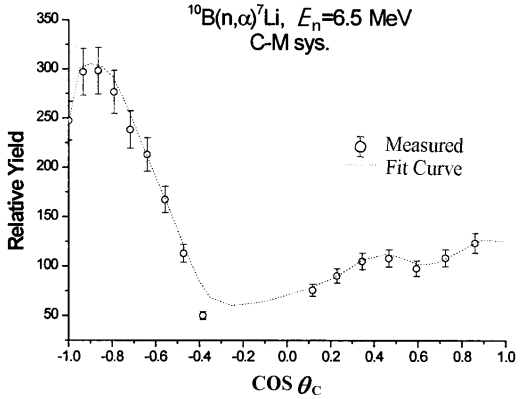

Fig. 6 Angular distribution for ^{10}B(n,α)^{7}Li reaction at 6.5±0.20 MeV

The principal errors of the angular distributions are from statistics for counts, background subtraction or subtraction of ^{7}Li particles, and uncertainty of 0 degree line. Total error for each datum point is about 5~10 percent.

The principal error of the cross section is from uncertainty of angular distribution shape, the error of absolute neutron flux and the nuclear number of targets. Total error of the cross section is about 10 percent.

From Figs.3~6, it can be seen that the angular distributions in the center of mass reference system are obviously backward peaked and that the higher energy, the more severe.

The cross sections for ^{10}B(n,α) ^{7}Li reaction at 4.0 , 5.0 ,5.7 and 6.5 MeV were derived from the angular distributions in laboratory system and the absolute counts of event. They are 32.6±3.3, 24.0±2.4, 23.2±2.4 and 26.0±2.6 mb at 4.0±0.2, 5.0±0.26, 5.7±0.15 and 6.5±0.2 MeV respectively

In Fig. 7, the result is compared with the data of H.Bichsel et. al, measured in 1957 with BF_3 proportion counter. It can be seen that present result is lower than the data of H.Bichsel′s, but our data measured in 1999 are in agreement with his data.

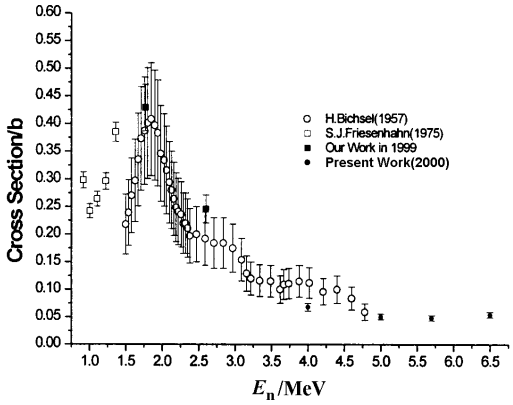

Fig. 7 Cross section comparison between present work and other measurements for ^{10}B(n,α) ^{7}Li reaction

Acknowledgment

The authors are indebted to China Nuclear Data Center for financial support. We also would like to thank the crew of 4.5 MV Van de Graaff of Peking University.

References

[1] TANG Guoyou, ZHANG Guohui et al., INDC(CPR)-043/L (1997)

[2] H.Bichsel et al., Phys. Rev, 108,1025(1957)

[3] S.J. Friesenhahn et al., INTEL-RT-7011-001,(1974)

Fission Product Yields from 22 MeV Neutron-induced Fission of ^{235}U

FENG Jing LIU Yonghui YANG Yi BAO Jie LI Ze QI Bujia TANG Hongqing ZHOU Zuying
CUI Anzhi RUAN Xichao SUN Hongqing ZHANG Shengdong GUO Jingru
CIAE,P.O. Box 275-46, Beijing

【**abstract**】*The chain yields of 28 product nuclides were determined for the fission of ^{235}U induced by 22 MeV neutrons for the first time. Absolute fission rate was monitored with a double-fission chamber. Fission product activities were measured by HPGe γ-ray spectrometry. Time of flight technique was used to measure the neutron spectrum in order to estimate fission events induced by break-up neutrons and scattering neutrons. A mass distribution curve was obtained and the dependence of fission yield on neutron energy is discussed.*

Introduction

The fission product mass distribution of ^{235}U has been extensively investigated, but few of these investigations deal with fission induced by neutrons with energy higher than 20 MeV. This is partly because it is very difficult to attain mono-energetic neutron source. In this work, fission product yields at 22MeV were acquired to help understanding the dependence of fission product yields on energy of incident neutrons. The second, third and fourth chance fission become important at this neutron energy .

Experimental

The experiment was carried out with the HI-13 Tandem at CIAE. The tritium gas chamber was of size Φ10×40 mm and made of stainless steel. The chamber was filled with the purified tritium gas of 0.22 MPa. The deuteron energy was 6.0 MeV and neutron spectrum was measured with TOF technique in order to estimate the fission events induced by the background neutrons. The ratio of fission events induced by neutrons with energy less than 21 MeV and fission events induced by 22 MeV neutrons is 0.38. The samples used in the irradiation were Φ16 mm disks of uranium metal with isotopic composition of 1.1% ^{234}U, 90.2% ^{235}U, 0.3% ^{236}U, and 8.4% ^{238}U. The uranium disk was sealed in a pure aluminum foil of 0.2 mm thickness. The sample, which was sandwiched between two standardized thin samples to monitor the fission rate absolutely, was mounted in the double fission chamber. The standardized thin samples were made of the same uranium as the thick ones. The double fission chamber was covered with Cd of 1 mm thickness to shield thermal neutrons in the environment. Two samples were irradiated for 20 or 40 hours at a distance of about 5 cm from the neutron source in the direction of zero degree.

After the irradiation, the γ-ray spectra of the samples were recorded directly by using HPGe γ-ray spectrometer. The γ-ray spectra were recorded successively over a period of two months to encompass the wide range of half-life involved, and to eliminate the cross interfering of the γ-rays from the product nuclides of almost the same energy, which can not be resolved by the HPGe detector. And then, the spectra were analyzed with the computer program SPAN[1] to obtain the intensities of the resolved photopeaks . The measured fission product γ-ray activities and fission rate were then analyzed by program FYAUTOLS to obtain the fission yields.

Results and Discussion

The chain yields of 28 product nuclides were obtained and they are presented in Table 1. Corrections were made for the self-absorption of the γ-rays, the cascade coincidence losses, the influence of background neutrons, the independent yields and the fission from ^{238}U. Uncertainties (1σ) of the yields were given by considering all known sources of random errors according to the error propagation law. The mass distribution is shown in Fig. 1, compared with evaluated data from Ref. [2]. The sum of the yields directly measured is (53.8±2.7%) for the light mass group, and (49.3±4.9%) for the heavy mass group. The sum of not only measured ones but also ones obtained by interpolating or extrapolating is 101.0% for the light mass group and 99.0% for the heavy mass group, where the limit mass number of the two groups is 117 and 118. The mean mass numbers are 98.2 and 135.8 for the light and heavy mass group respectively, which give the mean fission neutron number $\bar{\nu} = 2$. It can be seen from the results that multiple-chance fission plays a very important role in fission with neutrons' energy increasing to 22 MeV. Mean fission neutron number could not be derived in traditional way, since it could not be so small. The results of this experiment show that the fission yields of valley have positive correlation with the energy of neutron, while the fission yield decrease with increasing neutron energy for the product nuclides in the peak region of the mass distribution.

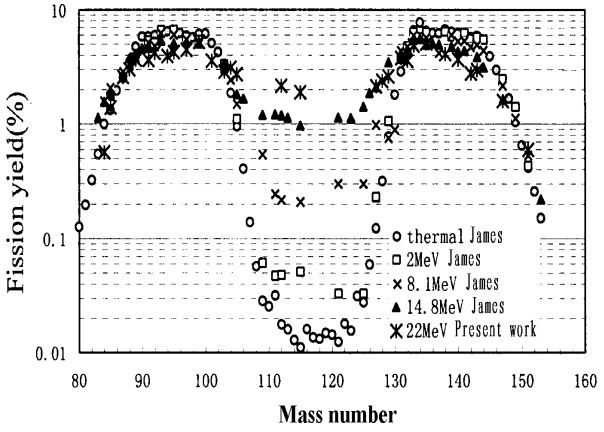

Fig1. Fission yields from monoenergetic-neutron induced fission of ^{235}U

Table 1 Chain yields from 22 MeV neutron induced fission of ^{235}U

Mass number	Fission yield(%)	error
85	0.99	0.08
87	2.61	0.11
88	3.26	0.15
89	4.22	0.25
91	4.25	0.16
92	4.93	0.24
94	4.85	0.22
95	4.67	0.18
97	5.08	0.19
99	4.90	0.18
101	4.14	0.17
104	3.10	0.18
105	2.47	0.15
112	1.51	0.15
115	1.20	0.14
127	1.49	0.13
128	2.06	1.45
129	2.37	0.50
131	3.70	0.83
132	4.16	0.15
133	5.66	0.25
135	5.84	0.29
138	5.85	0.59
140	4.45	0.17
142	3.76	0.18
143	4.25	0.18
147	2.10	0.12
151	0.45	0.02

References

[1] WANG Liyu. Multiple Processing in High Resolution Gamma Spectroscopy[J]. Appl Radiat Isot, 1989,40:575-579.

[2] James MF, Mills RW, Weaver DR. A New Evaluation of Fission Product Yields and the Production of a New Library (UKFYZ) of Independent and Cumulative Yields. Part II. Tables of Measured and Recommended Fission Yields: AEA-TRS-1018.1991.

Angular Distribution and Cross Section Measurement for $^{64}Zn(n,\alpha)^{61}Ni$ Reaction

YUAN Jing CHEN Zemin

Department of Physics, Tsinghua University, Beijing

TANG Guoyou ZHANG Guohui CHEN Jinxiang SHI Zhaomin

Key Laboratory of Heavy Ion Physics, Ministry of Education, Beijing

YU.M.Dledenov M.Sedysheva G.Khuuknenkhuu

Joint Institute for Nuclear Research, Dubna 141908, Russia

【abstract】 *Using a gridded ionization chamber, the differential cross section for $^{64}Zn(n,\alpha)$ ^{61}Ni reaction was measured at 5.0, 5.7and 6.7MeV. The neutrons were produced through D(d,n) ^{3}He reaction. Absolute neutron flux was determined through $^{238}U(n,f)$ reaction. The results show obviously backward peak in the center of mass reference system.*

Introduction

The differential cross section data for $^{64}Zn(n,\alpha)$ ^{61}Ni reaction are important for the study of reaction mechanism and in practical applieation. There are no data of cross sections for ^{64}Zn (n,α) (n,n) and (n,p) reactions .

Using a gridded ionization chamber, we performed the measurements of angular distributions and cross sections for $^{64}Zn(n,\alpha)^{61}Ni$ reaction at 5.0, 5.7 and 6.7 MeV.

1 Experimental Detail

The gridded ionization chamber was described in reference [1]. For our present experiment, the working gas was Kr+4.71% CH_4 to exclude the interference from $^{16}O(n,\alpha)$ reaction. The distances from cathode to grid, grid to anode and anode to shield were 4.5, 2.2 and 1.1 cm respectively.

The sample material was ^{64}Zn with the abundance 99.4%. For present measurement, two samples were used, which were evaporated on the tungsten backing. The thickness of each sample was 266.36 μg/cm^2 for the two samples. They were back to back set on the sample changer of ionization chamber. There was also a tungsten film placed on the sample changer in the gridded ionization chamber for background measurement. A ^{238}U sample (total weight 7.85±0.1 mg, Φ4.5 cm) was employed inside the chamber for absolute neutron flux measurement. The cross section of $^{238}U(n,f)$ reaction was taken from CENDL-2 library. A BF_3 long counter was used as relative neutron flux monitor.

For the measurements at 5, 5.7, and 6.5 MeV, the working pressure of ionization chamber were 1.2, 1.4 ,and 1.6 atm (1 atm=101325 Pa) respectively.

The experiment was performed at the 4.5 MV Van de Graaff accelerator of the Heavy Ion Physics, Peking University. Monoenergetic neutrons were produced through D(d,n) reaction with a deuteron gas target of 2.0 cm long and 1.5 to 2.0 atm in pressure, separated from the vacuum tube by a molybdenum film of 5 μm in thickness. The energies of the deuterons were 2.4, 3.0, and 3.7 MeV and the correspondence neutron energies were 5.03±0.26 , 5.75±0.15 and 6.5±0.20 MeV.

The deuteron beam was about 3.0 μA during experiment. The chamber was placed at 0 degree to the beam line, and the distance from its cathode to the center of the neutron source was about 38.0 cm. The samples were attached to the cathode.

The measurement at each energy point include:

(1) Check the stability of the experiment using Pu-α source.

(2) Measure the signal including background.

(3) Measure background using W-backing.

(4) Calibrate absolute neutron flux using ^{238}U-target.

Total run time was about 30 to 40 h for each neutron energy.

2 Results and Discussion

In Fig.1 and Fig.2 are shown the two dimensional spectra for forward and backward at 5.7 MeV respectively. It can be seen clearly that there are two groups of α particles.

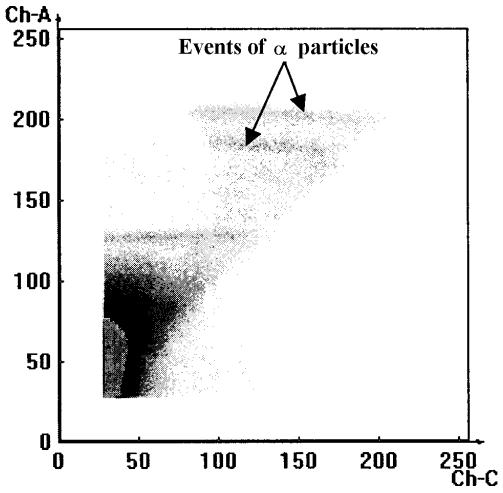

Fig.1 The two dimensional spectra of forward alpha particles of ^{64}Zn(n,α) ^{61}Ni reaction at E_n=5.7 MeV(Anode Channel vs. Cathode Channel)

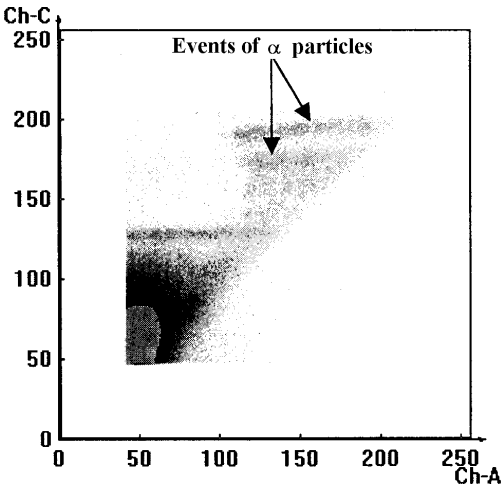

Fig.2 The two dimensional spectra of backward alpha particles at E_n=5.7 MeV

In Fig.3 to 5 are shown the measured angular distributions in the laboratory system at 5.0, 5.7 and 6.5 MeV respectively. The data near 90° in Lab-system could not be measured since interference from thickness of target.

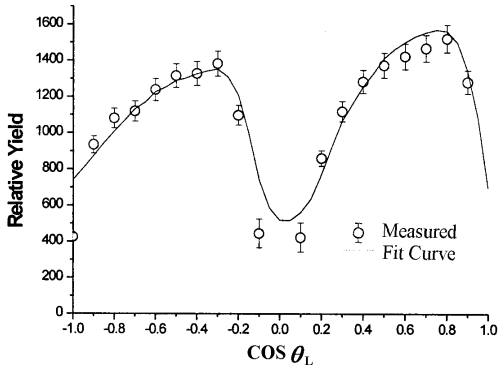

Fig. 3 Angular Distribution of ^{64}Zn(n,α)^{61}Ni reaction at 5.0±0.26 MeV

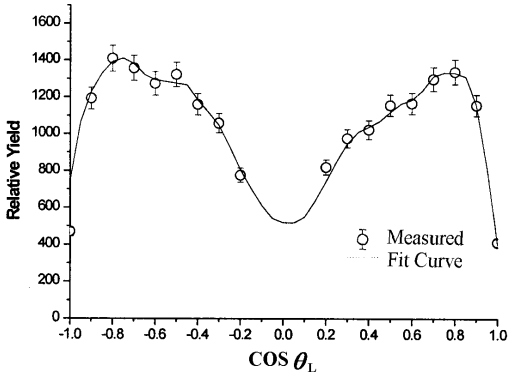

Fig. 4 Angular Distribution of ^{64}Zn(n,α)^{61} reaction at 5.7±0.15 MeV

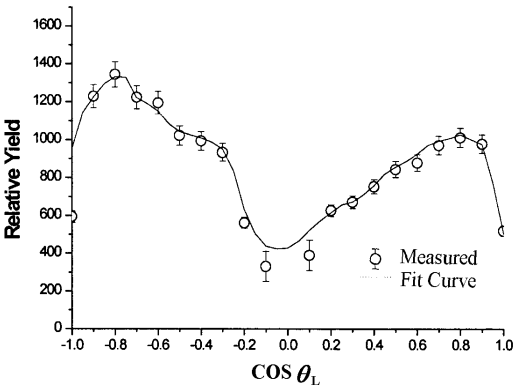

Fig. 5 Angular Distribution for ^{64}Zn(n,α)^{61} reaction at 6.5±0.20 MeV

Principal error of the angular distribution comes from statistics for counts, background subtraction and uncertainty of 0 degree line. Total error of each datum point is about 2~5 percent.

Principal error of the cross section comes from uncertainty of angular distribution shape, the error of absolute neutron flux and the nuclear number of the samples. Total error of the cross section is about 10 percent.

From Fig.3 to 5, it can be seen that the angular distribution in the laboratory system is obviously backward peaked, the higher the neutron energy, the more backward.

The cross sections for ^{64}Zn(n,α) ^{61}Ni reaction at 5.0, 5.7 and 6.5 MeV were derived from the angular distribution in laboratory system and absolute counts of event. They are 72.5±7.0, 72.0±7.0 and 70.8±7.0 mb at 5.00±0.26, 5.70±0.15 and 6.50±0.20 MeV respectively:

In Fig. 6, the result is compared with the data of JEF (there is no this data in other evaluated data libraries). It can be seen that our result in the energy region from 5.0 to 6.5 MeV is 10^2 larger than the data of JEF. The cross sections should be measured at more energy points, such as 2, 3, 4, 10, 13, 15 and 20 MeV to study the cross section change trend with neutron energy.

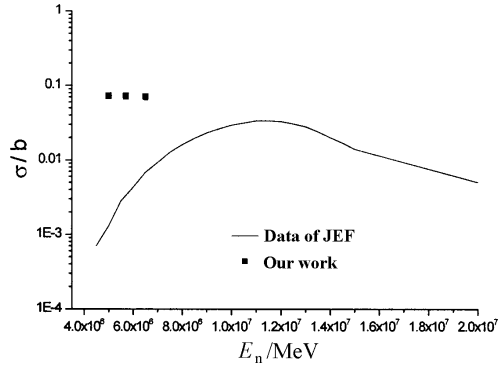

Fig. 6 The cross section of ^{64}Zn(n,α) ^{61}Ni reaction compared with JEF evaluated data

Acknowledgment

The authors are indebted to China nuclear data center for financial support. We would like to thank the crew of 4.5 MV Van de Graaff of Peking University too.

References

[1] TANG Guoyou, ZHANG Guohui et al., INDC(CPR)-043/L(1997)

Measurement of Neutron Capture Cross Section of ^{75}As in the Energy Range from 29 to 1100 keV

XIA Yijun YANG Zhihua LUO Xiaobing

Institute of Nuclear Science and Technology, Sichuan University, Chengdu

Zheng Yiyun

Department of Physics, Sichuan University, Chengdu

【abstract】 *The cross sections for the ^{75}As(n,γ) ^{76}As reaction were measured relatively to that of ^{197}Au in neutron energy range from 29 to1100 keV, using the activation technique. Neutrons were produced via the ^{7}Li(p,n) ^{7}Be and T(p,n) ^{3}He reactions with a 2.5 MV Van de Graaff accelerator at Sichuan University. The activities after irradiation were measured with a calibrated high resolution HPGe detector. The errors of the measurements are 6.7%~7.8%. The experiment results were compared with existing data.*

Introduction

The chemical elements heavier than Fe are predominantly synthesized by neutron capture reactions in stars. The neutron capture cross sections of ^{75}As are important in the s-process nucleosynthesis.

So far, only one comparatively complete set of data given by Macklin[1] for the ^{75}As(n,γ)^{76}As reaction is available in the energy range from 3 to 700 keV. A model calculation[2] is in energy region above 10 keV, which is 25% lower than the data of Macklin. In order to clarify the discrepancy, in present work the capture cross sections of ^{75}As were measured by using the activation method in the neutron energy range from 29 to 1100 keV, using the ^{197}Au(n,γ) reaction as a standard.

Measurement

The samples were made of As_2S_3 powder which was pressed into a disk with 20 mm in diameter and 2.5 mm in thickness packed in Al film. The gold disks of 20 mm in diameter and 0.1 mm in thickness were used as the neutron fluence monitors. Each sample was sandwiched between two gold disks, and wrapped in cadmium foils of 0.5 mm thickness. A group of samples mounted on the surface of Al ring (100 mm in diameter) centered at the neutron source were irradiated simultaneously at 0, 30, 60, 90, and 120 degrees with relation to the incident proton beam. The neutrons between 29 to 230 keV were produced by the ^{7}Li(p,n)^{7}Be reaction, and 215 to1100 keV by the T(p,n)^{3}He reaction. The proton beam current was generally 8 to 12 μA and the duration of irradiation was about 20 to 40 h in each run . The neutron fluence was monitored by using a long counter placed at 0 degree at a distance of 1.8 m from the source. In order to record the neutron fluence as a function of irradiation time, the count rate of the long counter per 2 minutes was recorded continuously by microcomputer multiscaler and stored on magnetic disk for calculating the correction of non-uniformity irradiation history. To determine the effect of back ground neutron, another As sample was placed at a distance of 1.8 m from the target and irradiated simultaneously.

The activities of the samples and the gold disks were measured with a calibrated high resolution HPGe detector. Because the activities of samples were rather weak, they were placed on the surface of the detector for measurement. In Table 1 some parameters for calculation are listed.

Table 1 Decay data of products

product nucleus	$T_{1/2}$	E_γ /keV	I_γ / %
^{76}As	26.32 h	559.1	45
^{198}Au	2.6935	411.8	95.5

Results

The cross sections for the ^{75}As(n,γ)^{76}As reaction obtained with the standard cross section of ^{197}Au (n,γ) ^{198}Au reaction taken from ENDF/ B-6 are listed in Table 2 and plotted in Fig.1. The comparison among our measurements, the the data measured by Macklin, and the evaluated data from ENDF/B-6 as well as the Gardner's model calculation[2] is shown in Fig.1.

Table 2 Measured cross sections

E_n / keV	σ / mb
29±7	284.0±19
59±16	209.0±14
121±27	132.8±8.9
196±30	114.2±7.7
215±44	107.3±7.2
230±12	98.5±6.6
376±87	52.9±3.8
655±134	27.6±2.1
962±135	20.4±1.6
1100±83	18.6±1.4

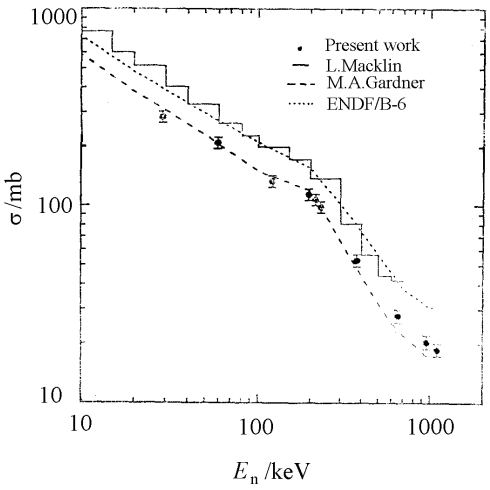

Fig. 1 The neutron capture cross section of ^{75}As

It can be seen from Fig.1 that our results for ^{75}As(n,γ)^{76}As reaction are in good agreement with a

recent model calculation within the uncertainties, but lower than the data of Macklin and ENDF/B-6. The data of Macklin are 20% higher than the data of ENDF/B-6 at the lower energies, but agree well above 100 keV.

The support of the Van de Graaff crew in providing the neutron beams is gratefully appreciated.

Reference

[1] R. L. Macklin, Nucl. Sci. Eng ., 99,133(1988)
[2] M. A. Gardner and D. G. Gardner, Capture Cross Section and Spectrum Calculations for Medium Weight Nuclei, Proc. Int. Conf.Nuclear Cross Sections for Technology, Knoxville, Tennessee,october 22-26,1979, NBS Special Publication 594, p. 752,U.S. National Bureau of Standards(1980)

Fission Product Yields from 19.1 MeV Neutron Induced Fission of ^{238}U

YANG Yi LIU Yonghui BAO Jie FENG Jing LI Ze CUI Anzhi SUN Hongqing
ZHANG Shengdong GUO Jingru
CIAE,P.O. Box 275-46, Beijing

【**abstract**】*36 chain yields were determined for the fission of ^{238}U induced by 19.1 MeV neutrons for the first time. Absolute fission rate was monitored with a double-fission chamber. Fission product activities were measured by HPGe γ-ray spectrometry. Threshold detector method was used to measure the neutron spectrum in order to estimate the fission events induced by break-up neutrons and scattering neutrons. A mass distribution curve was obtained and the dependence of fission yield on neutron energy was discussed.*

Introduction

The fission product mass distribution of ^{238}U has been extensively investigated, but only a few of those investigations deal with fission induced by mono-energetic neutrons. S. Nagy et al. studied the mass distribution of ^{238}U with essentially mono-energetic neutrons of 1.5, 2.0, 3.9, 5.5, 6.9, and 7.7 MeV[1].T.C. Chapman et al. determined the mass distribution for the fission of ^{238}U induced by neutrons with energies of 6.0, 7.1, 8.1, and 9.1 MeV[2]. On the other hand, a lot of work about the determination of the fission product yields of ^{238}U induced by neutrons have been done in China. For instance, Li Ze et al. measured the mass distribution for the fission of ^{238}U with 8.3 MeV neutrons[3]. Zhang Chunhua et al. investigated the mass distribution with 3.0 MeV neutrons[4] and Wang Xiuzhi et al. measured the yields of 9 fission products with 5.0 MeV neutrons[5]. And Su Shuxin et al. measured the mass distribution for the fission of ^{238}U with fission spectrum neutrons[6]. Several other measurements of the mass distribution are 14 MeV neutrons[7,8] since with 14 MeV neutrons are readily available. At present work, the experiment was carried out for the fission yields of 39 product nuclides from ^{238}U fission induced by 19.1 MeV neutrons.

Experimental

The experiment was carried out with the 5SDH-2.2×1.7 MV minim tandem at CIAE. The tritium-Ti target, bombarded by the deuteron beam to produce neutrons, was of the size Φ10mm, thickness of about 5.5 mg/cm^2, and the adsorption of tritium was 4.0~4.5 Ci (1Ci=3.7×10^{10} Bq) for every target. The deuteron beam energy was 3 MeV and the neutron spectrum was measured by threshold detector in order to estimate the fission events induced by the background neutrons in the energy region 2~8 MeV from the T(d,np)^{3}H reaction and from scattering by the environment. The ratio of background fission events to 19.1 MeV neutron fission events was

estimated to correct the yield. The samples used in the irradiation were Φ16 mm disks made of natural uranium metal about 2 g. The uranium disk was sealed in a pure Aluminum foil of 0.2 mm thickness. The sample sandwiched between two standardized thin samples to monitor the fission rate absolutely was mounted in the double fission chamber. The standardized thin samples were made of the same uranium as the thick ones. The double fission chamber was covered with Cd of 1 mm thickness to shield the thermal neutrons in the environment. Four samples were irradiated for periods about 30 h, every time 2 samples were irradiated, one had a distance of about 5 cm from the neutron source in the direction of zero degree (in the chamber), another one 5 mm from the neutron source, 0 degree. During the irradiation, fission rate was monitored and recorded. After the irradiation, the γ-ray spectra of the samples were recorded directly by using HPGe γ-ray spectrometer. The γ-ray spectra were recorded successively over a period of two months to encompass the wide range of half-life involved and to eliminate the cross interfering of the γ-rays from the product nuclides of almost the same energy that can not be resolved by the HPGe detector. And then, the spectra were analyzed with the computer program SPAN[9] to obtain the intensities of the resolved photopeaks. The measured fission product γ-ray activities and fission rate were then analyzed by program FYAUTOLS to obtain the fission yields. Decay data comes from Table of Isotopes, 8th edition.

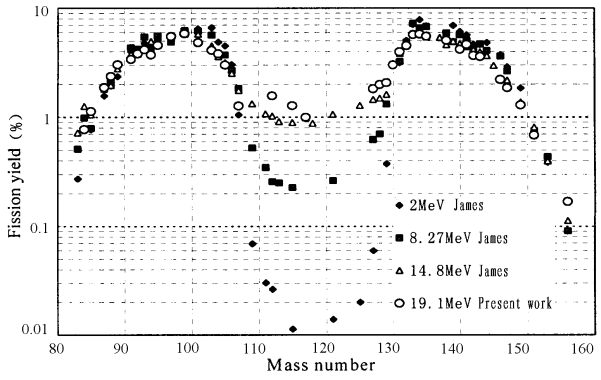

Fig.1 Fission yields from mono energetic-neutron-induced fission of ^{238}U

Results and Discussion

The 36 chain yields were obtained and they are presented in Table 1. Corrections were made for the self-absorption of the γ-rays, the cascade coincidence losses, the influence of the background neutrons, the independent yields and fission from ^{235}U. Uncertainties (1σ) of the fission yields were given by considering all known sources of random errors according to the error propagation law. A comparison for the mass distribution characteristic parameters of ^{238}U induced by neutrons from 1.5 MeV to 19.1 MeV are listed in Table 2. It can be seen from Table 2 that with increasing neutron energies, the ratios for peak/valley decrease. The mass distribution was derived from the yields as shown in Fig.1, compared with the evaluated data from Ref. [10]. The integral values of the fission from measurement for light and heavy groups are 61.0% and 61.7% respectively, after interpolating and extrapolating the values are 101.0% and 99.4%. The result of this work proves the experience rule that the fission yields at valley and wings have positive correlation with the energy of neutron.

Table 1 Chain yields by 19.1 MeV neutron induced fission of ^{238}U

Mass number	Fission yield(%)	Error
85	1.130	0.099
87	1.871	0.070
88	2.370	0.107
89	3.024	0.173
91	3.392	0.105
92	3.815	0.165
93	4.159	0.251
94	3.730	0.170
95	4.564	0.139
97	5.498	0.165
99	5.824	0.206
101	4.822	0.211
103	4.110	0.138
104	3.823	0.175
105	3.011	0.097
112	1.570	0.065
115	1.277	0.075
127	1.818	0.073
128	1.987	0.161
129	2.066	0.086
130	3.000	0.985
131	3.969	0.141
132	4.529	0.157
133	5.704	0.181
134	5.762	0.302
135	5.503	0.326
138	5.046	0.448
140	4.178	0.136
141	4.632	0.301
142	3.663	0.145
143	3.595	0.162
146	2.212	0.121
147	1.859	0.063
149	1.296	0.089
151	0.686	0.033
156	0.169	0.072

Table 2 Comparison of he mass distribution characteristic parameters of fission of ^{238}U

E_n (MeV)	Peak (valley)	Mean mass		ν_a	ν_b
		Light group	Heavy group		
1.5	600	97.5	139.0	2.5	2.6
2.0	600	97.5	139.0	2.5	2.6
3.9	200	97.4	138.9	2.7	2.9
5.5	80	97.4	138.6	3.0	3.2
6.9	50	97.5	138.4	3.1	3.4
7.7	40	97.4	138.3	3.3	3.5
14.0	7	98.0	136.8	4.2	4.5
19.1	4.5	98.88	135.88	4.24	No

(1) Light group: mass<=117, heavy group: mass>=118;
(2) Light group: 81<=mass<=107, heavy group: 128<=mass<=156;
(3) ν_a — Calculated from conservation of mass;
(4) ν_b — Experimental values based on direct measurement.

References

[1] S. Nagy et al., Mass distribution in monoenergetic neutron induced fission of ^{238}U. Phys, Rev.C 17, 163(1978)

[2] Champman, T.C, et al., Fission product yields from 6~9 MeV neutron induced of ^{235}U and ^{238}U. Phys, ReV.C 17, 1089(1978).

[3] LI Ze et al., Mass distribution in 8.3 MeV neutron induced fission of ^{238}U. Chinese J. Nucl. Radiochem. 7, 97(1985)

[4] ZHANG Chunhua et al., Distribution of fission yields in the 3.0 MeV neutron induced fission of ^{238}U. Chinese J. Nucl. Radiochem. 7,1(1985)

[5] WANG Xiuzhi et al.,The absoluted determination of the cumulative yield of several nuclides from induced fission of ^{238}U by 5 MeV neutrons. Chinese J. Nucl.Radiochem. 6, 183(1984)

[6] SU Shuxin et al., The mass distribution in fission spectrum neutron induced fission of ^{238}U. Chinese J. Nucl. Radiochem.13, 129(1991)

[7] LIU Chonggui et al., The mass distribution in 14.9 MeV neutron induced fission of ^{238}U. Chinese J. Nucl.Phys. 7,235(1985)

[8] Nethaway et al., Low yield products from fission of ^{232}Th, ^{235}U,and ^{238}U with 14.8 MeV neutrons. Phys. Rev. 182, 1251(1969)

[9] WANG Liyu. Mutiple Processing in High Resolution Gamma Spectroscopy[J]. Appl Radiat Isot, 1989,40:575-579.

[10] James MF,Mills RW,Weaver DR. A New Evaluation of Fission Product Yields and the Production of a New Library (UKFYZ) of Independent and Cumulative Yields.Part II.Tables of Measured and Recommended Fission Yields:AEA-TRS-1018.1991.

[11] Richard B.Firestone. Table of Isotopes (EIGHTH EDITION), CDROM Edition,Version 1.0,March 1996.

The Method to Set up File-6 in Neutron Data Library of Light Nuclei Below 20 MeV

ZHANG Jingshang HAN Yinlu
China Nuclear Data Center, CIAE, Beijing

Introduction

The light nuclei imply the 1P-shell elements in this paper. So far there is no file-6 (double-differential cross section data, DDX) of the light nuclei in the main evaluated neutron nuclear data libraries in the world, including ENDF/B-6, except ^{9}Be, of which the file-6 was obtained by using a Monte Carlo technique to fit the measured double-differential cross sections[1]. For the other 1P-shell elements, only neutron spectra are given. For the reaction channels, such as (n,nx)p, (n,nx)d, (n,nx)t and (n,nx)α, their outgoing isotropic neutron spectra were obtained by means of the phase space method and given in the file-5, meanwhile, by using the pseudo-levels for supplement of the information of neutrons in the file-4 as the inelastic scattering process. In this case, all of the information on the double-differential cross sections of outgoing charged particles could not be obtained from the library. Therefore, locating a proper description on the double differential cross sections of all kinds of outgoing particles from neutron induced light nucleus reactions below 20 MeV is necessary, even it is a very complex problem for theorists and evaluators. The motivation for this work is to introduce a way to set up the file-6 in the neutron data library.

In view of the reactions at incident neutron energies $E_n \leq 20$ MeV all of the first outgoing particles are emitted from compound nucleus to the discrete levels of the residual nuclei. All of the discrete level schemes used in the opened reaction channels at $E_n \leq 20$ MeV can be obtained from Ref. [2].

The first particle emissions can be described with pre-equilibrium and equilibrium mechanism. To conserve angular momentum, the angular momentum coupling effect must be taken into account, which is presented in Sec. 2. The linear momentum dependent exciton state density was employed for calculating the angular distribution of the first nucleon emissions[3]. In this method, the leading particle is not assumed; instead, a statistical population of all states compatible with energy and momentum conservation is proposed. The effects of the Fermi motion, as well as Pauli blocking by the 'sea' of nucleons, are included. In particular, the angular distribution from the first pre-equilibrium state is identical to that obtained with the Kikuchi-Kawai scattering kernel[4,5]. The pickup mechanism is used for calculating the cluster pre-formation factors[6,7] and double-differential cross sections of composite particle emissions[8,9].

Because of the strong recoil effect in light nucleus reactions, the energy balance must be taken into account strictly. Only in this way the file-6 could be set up with full energy balance.

There are many measurements for DDX in EXFOR file. In terms of the model calculation to reproduce the measured data of total outgoing neutron energy-angular spectra satisfactorily, the file-6 could be set up for application.

1 Dynamics

Besides the equilibrium mechanism, the pre-equilibrium mechanism must be taken into account. The model calculations indicate that the pre-equilibrium mechanism dominates the reaction processes, so that only the Hauser-Feshbach model could not work to reproduce the measured DDX data. This kind of reactions can be described with the unified Hauser-Feshbach and exciton model[10].

From the Heisenberg's uncertainty relation $\Delta E \Delta t \approx \hbar$, as very known, the ΔE is in the order of magnitude of few eV for heavy nuclei, corresponding the life-time Δt of the compound nucleus is about 10^{-16} seconds. For the light nucleus reaction, the fitting procedure drops a hint that the ΔE of the compound nucleus is in the order of magnitude of few hundred keV, corresponding the life-time Δt is about 10^{-21} seconds. Therefore, in light nucleus reactions, the behavior of the pre-equilibrium emissions is very much similar to the direct reactions calculated by the DWBA method.

Since the pre-equilibrium emission is an important reaction mechanism from the compound nucleus to

the discrete levels of the residual nucleus, each of which has its individual spin and parity, so the angular momentum coupling should be taken into account for the angular momentum conservation in pre-equilibrium emission mechanism. The formulation of the angular momentum dependent exciton model can be found in Refs.[11,12]. With this procedure the emissions to the discrete level, which is marked by $j\pi$, can be treated. However, the j-independent exciton model could not deal with this kind reaction mechanism.

2 Kinematics

Because of light mass, very strong recoil effect appears in the light nucleus reaction processes. Therefore, the consideration of the kinematics in a strict way plays a very important role in the angular-energy spectrum calculations.

There are many opened reaction channels below 20 MeV. Besides the sequential particle emissions, the cluster separation of the residual nucleus and three-body breakup processes also exist. The total neutron energy-angular spectra consists of the outgoing neutrons from various reaction channels, which strongly differ from each other in their respective energy-angular distributions. The double differential cross sections could provide the information for analysing the components from the differential reaction mechanism.

The research indicates that the kinematics of various emission processes can be described with the four possible types in light nucleus reactions.

(1) From discrete level to discrete level (D to D),
(2) From continuum spectrum to discrete level (C to D),
(3) From discrete level to continuum spectrum (D to C)
(4) From continuum spectrum to continuum spectrum (C to C)

The first two terms are used in the sequential particle emissions, because all final states are in discrete levels, while the last two terms are used for the three-body breakup processes, because the final states are continuum spectra to go through three-body breakup.

The formulation on the description of the outgoing particle spectra with the energy balance has been obtained analytically, which is straightforward but tedious. All of the formula can be found in Refs. [13~16].

The summation over all the energies carried by the outgoing particles and recoil nucleus, as well as gamma ray gives the total released energy analytically in the center of mass system as follows

$$\sum_i E^{\mathrm{c}}(m_i) = \frac{M_{\mathrm{T}}}{M_{\mathrm{c}}} E_{\mathrm{n}} + Q$$

And in the laboratory system, the total released energy is analytically given by

$$\sum_i E^{\mathrm{l}}(m_i) = E_{\mathrm{n}} + Q$$

where E_{n} stands for the incident neutron energy in laboratory system, M_{T} and M_{C} are the masses of target and compound nucleus, respectively. Q refers to the Q-value of the reaction channel.

3 Model and LUNF Codes

The optical model is involved in the unified Hauser-Feshbach and exciton model. The phenomenological spherical optical potential is employed in the optical model calculations. The optical model parameters of neutrons are determined by fitting total, elastic and non-elastic cross section, as well as elastic-scattering angular distributions. The optical model parameters of charged particles like protons, deuterons, tritons, and alpha particles are determined by fitting the corresponding reaction cross sections.

The LUNF code for light nucleus reactions are developed for calculating reaction cross sections and energy-angular spectra of all kinds of outgoing particles from each reaction channel below 20 MeV. Being very different opened reaction channels with variety status of the residual nuclei, each light nucleus has its own edition. The physical quantities calculated numerically by the LUNF code given in ENDF/B-6 format are as follows:

(1) Total, elastic and non-elastic scattering cross sections as well as elastic-scattering angular distributions.
(2) All kinds of reaction cross sections with a different reaction mechanism and angular distributions of outgoing particles, like neutrons, protons, alpha particles, and deuteron.
(3) Double-differential cross sections of the outgoing particles from each reaction mechanism and total double-differential cross sections of the emitted particles.
(4) Partial kerma factors of outgoing particles and recoil nuclei, and the total kerma factor.

4 Summary

In terms of this approach, the model calculations for fitting the double-differential measurements of outgoing neutrons have been performed for the light elements from lithium to oxygen. The calculated

results indicate that this method can reproduce the double-differential measured data of outgoing neutrons. The fitting results can be found in Refs. [17~21]. Since lack of the double-differential cross section measurements of outgoing charged particles, only the comparisons of the total double-differential cross sections of the outgoing neutrons have been performed.

Because of the level widths and energy resolution in the measurements, according to the Heisenberg's uncertainty relation, the measured data are always in a broadening form. Therefore, the broadening effect must be taken into account in the fitting procedure. The Gaussian expansion form is adopted. The standard deviation consists four components:

(1) Energy resolution of the neutron source;

(2) Energy spread caused by the finite timing resolution of time-of-flight method[22];

(3) Life-time of the compound nucleus;

(4) Level widths. All of the level widths are taken from the experimental data as fixed parameters.

The formulation of the broadening expansions can be found in Ref.[12]. Of course in the establishment of the file-6 for the double-differential cross sections any uncertainty expansions are not needed at all.

Since the calculated double-differential cross sections are in center of mass system, so the transformation from the center of mass system to the laboratory system must be performed in fitting procedure. The related formalism can be found in Ref. [12].

Taking n+^{9}Be reaction as an example, the comparisons of the normalized neutron angular-energy spectra of 60 deg. in file-6 between ENDF/B-6 and CENDL-3 at E_n=5.9, 14.1 MeV are shown in Figs. 1~2, respectively. By using a Monte Carlo technique to fit the double-differential measurements ENDF/B-6 gives a smooth curve of the angular-energy spectra, while this approach gives discrete structure. The peak at the high-energy part mainly comes from the second excited level in Perkins approach[1]. In our model calculation, there are many peaks from different excited levels, including the first excited level.

In general, as the second nucleon emissions (neutron or proton) give small energy region with several hundred keV in the ring-type spectra in center of mass system; while the triton or alpha particle emissions give the large energy region with a few MeV due to the relative heavier mass. All of the ring-type spectra must be treated as the continuum spectra, only in this way one can keep the energy balance[12].

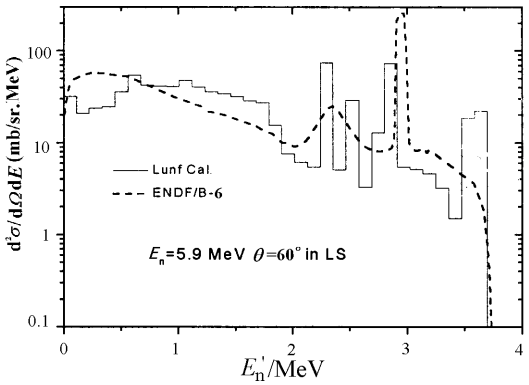

Fig. 1 The neutron angular-energy spectrum of θ=60° at E_n=5.9 MeV for ^{9}Be

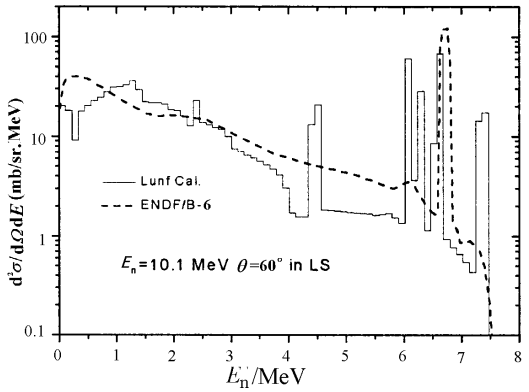

Fig. 2 The neutron angular-energy spectrum of θ=60° at E_n =14.1 MeV for ^{9}Be

The statistical reaction model is often used in the evaluation of nuclear data for medium or heavy nuclei, while the model calculations indicate that it still can be applied to the light nuclei. However, the pre-equilibrium emission processes from the excited compound nucleus to the discrete levels dominate the reaction processes. As long as the angular momentum and parity conservation as well as the recoil effect is taken into account in whole reaction processes, the optical model still works well to give the emission branch from level to level in the light nucleus reactions. The angular momentum coupling approach has been proposed for conserving the angular momentum in the pre-equilibrium emission mechanism.

The optical model parameters are important in the model calculations. Besides neutron optical parameters, the optical model parameters of the charged particles can be adjusted to improve the fitting results of the partial spectra, as well as fitting the corresponding reaction cross sections in the reasonable area.

Since all of the particles are emitted to the discrete levels, we do not need the level density parameters.

Based on the fitting to the double-differential

measurements, the file-6 can be established by using the LUNF code with full energy balance in the neutron library CENDL-3. All of the double differential cross sections of the outgoing particles are given in the Legendre coefficients in center of mass system in ENDFB-6 format. The files-6 needed to be set up for 1P-shell elements are listed in the Table.1. From this Table one can see that n+^{9}Be is the easiest one, because the total neutron angular-energy spectra is just equivalent to that of the (n,2n) reaction channel. However, for the other nuclei, the outgoing neutrons come from more than two reaction channels, so the fitting method by Monte Carlo technique is unable to mark off the different reaction channels.

Limited by this statistical reaction model, the resonance phenomenon in the reaction cross sections could not be obtained, so the evaluated experimental data of cross sections are employed in the neutron library. This approach is mainly used for setting up the file-6 for the double-differential cross sections.

Table 1 The file-6 needed to be set up of the 1-p shell elements[1)]

Target	Channel	(MT)	Channel	(MT)	Channel	(MT)	Channel	(MT)
^{6}LI	(n,nd)α	(32)	(n,2np)α	(41)				
^{7}Li	(n,2n)^{6}Li	(16)	(n,nα)t	(22)	(n,2nd)α	(24)	(n,3np)α	(25)
	(n,np) ^{6}He	(28)						
^{9}Be	(n,2n)2α	(16)						
^{10} B	(n,2n)p2α	(16)	(n,nα) ^{6}He	(22)	(n,np) ^{9}Be	(28)	(n,nd)2α	(32)
	(n,pα) ^{6}He	(112)	(n,t)2α	(33)				
^{11}B	(n,2n) ^{10}B	(16)	(n,nα) ^{7}Li	(22)	(n,np) ^{10}Be	(28)	(n,nd) ^{9}Be	(32)
	(n,nt)2α	(33)						
^{12}C	(n, np) ^{11}B	(28)	(n,n3α)	(29)				
^{14}N	(n,2n) ^{14}N	(16)	(n,nα)^{10}B	(22)	(n,np) ^{13}C	(28)	(n,nd)^{12}C	(32)
	(n,2np) ^{12}C	(41)	(n,2α) ^{7}Li	(29)	(n,t)3α	(33)		
^{16}O	(n,2n) ^{15}O	(16)	(n,nα) ^{11}C	(22)	(n,np) ^{15}N	(28)	(n,2α)^{9}Be	(29)

Note: 1) The corresponding MT numbers are given in the parentheses.

Reference

[1] S.T. Perkins et al., *Nucl. Sci. Eng.,* 90, 83 (1985).

[2] R.B.Firestone et al., John Wiley & Sons (1996).

[3] M. B. Chadwick et al., *Phys. Rev*. C. 44 1740(1991).

[4] K.Kikuchi et al., *Nuclear Matter and Nuclear Reaction,* North-Holland, Amsterdam, p.44 (1968).

[5] Z.Sun et al., *Z. Phys*. A. 305,61(1982).

[6] A.Iwamoto et al., *Phys. Rev*. C. 26 1828(1982).

[7] ZHANG Jingshang *Proc. Int. Conf. Nuclear Data for Science and Technology,* Gatinburg, Tennessee, May 9-13 1994, Vol.2p.932, American Nuclear Society (1994); see also Zhang Jingshang et al., *Chin. J. Nucl. Phys*.18,28(1996).

[8] ZHANG Jingshang, *Nucl. Sci. Eng.,* 116, 35 (1994).

[9] ZHANG Jingshang, *Chin. J. Nucl. Phys*.15,347(1993).

[10] ZHANG Jingshang, *Nucl. Sci. Eng.,* 114, 55 (1993).

[11] ZHANG Jingshang, *Chin. J. Nucl. Phys*.16,153(1994).

[12] ZHANG Jingshang et al., *Commu. in Theor, Physics* (2001)

[13] ZHANG Jingshang, CNIC-01460, (2000). (in Chinese).

[14] ZHANG Jingshang et al., *Nucl. Sci. Eng.,* 133, 218 (1999).

[15] ZHANG Jingshang, *Commu. of Nucl. Data Progress*, 22,1(1999).

[16] ZHANG Jingshang, *Commu. of Nucl. Data Progress*, 22,5(1999).

[17] ZHANG Jingshang et al.. *Commu. of Nucl. Data Progress*, 20,5(1998).

[18] ZHANG Jingshang et al., *Commu. of Nucl. Data Progress*, 20,17(1998).

[19] ZHANG Jingshang et al.. INDC(CPR)-052/L *Commu. of Nucl. Data Progress*, 24,6(2000).

[20] ZHANG Jingshang et al.. *Commu. of Nucl. Data Progress*, 24,13(2000).

[21] ZHANG Jingshang et al.. *Commu. of Nucl. Data Progress*, 24,20(2000).

[22] S.Chiba et al., *Phys. Rev. C* 58, 2203 (1998)

Kerma Factors Calculated with UNF Code

ZHANG Jingshang HAN Yinlu

China Nuclear Data Center, CIAE,Beijing

【**abstract**】*As a new function is developed in UNF code, the kerma factors from every reaction channels including elastic scattering process can be calculated. Since the recoil effects have been taken into account strictly for energy balance with the analytical form, so it is easy to give the kerma factors. The formula for each reaction mechanism is given. As an example, for n+^{56}Fe the comparison of the calculated result with measurement is shown in the figure.*

Introduction

Since nuclear materials have strong stopping power, charged particles are easy to be detained in nuclear material and to transform the kinetic energy into heat. Information on the energy of charged particles produced in the nuclear reactions is needed in several applications. For example, the kerma factor is of specific interest regarding the heat produced in fusion reactors as well as regarding the calculation of radiation dose in radiobiology.

In UNF code, one particle emission, two particle sequential emission, as well as the three particle emission (only for (n,3n) channel) are involved in the model calculations.

The emission mechanism includes the emissions from continuum state to continuum state and from continuum state to discrete levels. All of the residual nuclei are charged particles and contribute to the kerma factors. Because the angular distributions and the double differential cross sections can be obtained by UNF code calculation in the Legendre expansion form in CMS, with the analytical form for energy balance[1~3], the kerma factors can also be calculated. In the first section the expressions of the kerma factors for the elastic scattering and one particle emission processes are given. The formula of the kerma factors of the multi-particle emissions from continuum state to continuum state, and from continuum state to discrete levels are given in section 2.

The three motion system are used, the physical quantities are indicated by the superscripts l, c and r for the laboratory system (LS), center of mass system (CMS) and recoil residual system (RNS), respectively. The energies carried by emitted particle and recoil nucleus are denoted by ε and E, respectively.

1 Kerma Factor of Elastic Scattering and One Particle Emissions

The kerma factor of the recoil nucleus by elastic scattering is given by Ref. [2]

$$E_{\mathrm{el}} = 2\sigma_{\mathrm{el}} \frac{m_{\mathrm{n}} M_{\mathrm{T}}}{M_{\mathrm{c}}^2} (1 - f_1^{\mathrm{c}}(\mathrm{el})) E_{\mathrm{n}} \tag{1}$$

where m_{n}, M_{T}, M_{c} stand for the masses of incident neutron, target and compound nuclei, respectively. E_{n} is the incident energy in LS. $f_1^{\mathrm{c}}(\mathrm{el})$ refers to the Legendre coefficient of the partial wave l=1 in CMS.

In the case of the first particle emission to the discrete level, the energies carried by the particle and its recoil nucleus in CMS, respectively, are

$$\varepsilon_k^{\mathrm{c}} = \frac{M_1}{M_{\mathrm{c}}} (E^* - B_1 - E_k) \tag{2}$$

$$E_k^{\mathrm{c}} = \frac{m_1}{M_{\mathrm{c}}} (E^* - B_1 - E_k) \tag{3}$$

where m_1, M_1 are the masses of the emitted particle and its residual nucleus, respectively, E^* is the excitation energy, B_1 is the binding energy of the particle 1 in the compound, E_k is the energy of the discrete level of residual nucleus.

In LS the energies are given by

$$\varepsilon_k^{\mathrm{l}} = \frac{m_{\mathrm{n}} m_1}{M_{\mathrm{c}}^2} E_{\mathrm{n}} + \varepsilon_k^{\mathrm{c}} + \frac{2}{M_{\mathrm{c}}} \sqrt{m_{\mathrm{n}} m_1 E_{\mathrm{n}} \varepsilon_k^{\mathrm{c}}}\, f_1^{\mathrm{c}}(k) \tag{4}$$

$$E_k^{\mathrm{l}} = \frac{m_{\mathrm{n}} M_1}{M_{\mathrm{c}}^2} E_{\mathrm{n}} + E_k^{\mathrm{c}} - \frac{2}{M_{\mathrm{c}}} \sqrt{m_{\mathrm{n}} m_1 E_{\mathrm{n}} \varepsilon_k^{\mathrm{c}}}\, f_1^{\mathrm{c}}(k) \tag{5}$$

where $f_1^{\mathrm{c}}(k)$ is the Legendre coefficient in CMS of the angular distribution of the emitted particle reaching to the k level of the residual nucleus M_1.

With the same procedure, in the case of the first particle emission to continuum state, the energies carried by the emitted particle and its recoil nucleus in LS, respectively, are

$$\varepsilon_{\mathrm{c}}^{\mathrm{l}} = \int \{ [\frac{m_{\mathrm{n}} m_1}{M_{\mathrm{c}}^2} E_{\mathrm{n}} + \varepsilon_1^{\mathrm{c}}] f_0(\varepsilon_1^{\mathrm{c}}) + \frac{2}{M_{\mathrm{c}}} \sqrt{m_{\mathrm{n}} m_1 E_{\mathrm{n}} \varepsilon_1^{\mathrm{c}}}\, f_1(\varepsilon_1^{\mathrm{c}}) \} \mathrm{d}\varepsilon_1^{\mathrm{c}} \tag{6}$$

$$E_{\mathrm{c}}^{\mathrm{l}} = \int \{ [\frac{m_{\mathrm{n}} M_1}{M_{\mathrm{c}}^2} E_{\mathrm{n}} + E_1^{\mathrm{c}}] f_0(E_1^{\mathrm{c}}) - \frac{2}{M_{\mathrm{c}}} \sqrt{m_{\mathrm{n}} M_1 E_{\mathrm{n}} E_1^{\mathrm{c}}}\, f_1(E_1^{\mathrm{c}}) \} \mathrm{d}E_1^{\mathrm{c}} \tag{7}$$

Obviously, the Legendre coefficients of the recoil nucleus has the relation with that of the first particle emission as follows

$$f_l(E_1^{\mathrm{c}}) = \frac{M_1}{m_1} f_l(\varepsilon_1^{\mathrm{c}}) \tag{8}$$

Thus, the partial kerma factors can be obtained by multiplying the cross sections for every corresponding reaction channel and summing over them accordingly.

2 Kerma Factor of the Multi-particle Sequential Emissions

For the case of the secondary particle emissions, if the final state of the residual nucleus is in the continuum state, the energy carried by the first emitted particle in LS is given by Eq.(6). The energy carried by the second emitted particle and its recoil nucleus are obtained by[1,2]

$$\varepsilon_2^{\mathrm{l}}(\mathrm{cont}) = \frac{m_{\mathrm{n}} m_2}{M_{\mathrm{c}}^2} E_{\mathrm{n}} + \frac{m_1 m_2}{M_1^2} \int \mathrm{d}\varepsilon_1^{\mathrm{c}} \frac{\mathrm{d}\sigma}{\mathrm{d}\varepsilon_1^{\mathrm{c}}} \varepsilon_1^{\mathrm{c}} + \int \mathrm{d}\varepsilon_2^{r} f_0(\varepsilon_2^{r}) \varepsilon_2^{r} - 2 \frac{\sqrt{m_{\mathrm{n}} m_1}}{M_{\mathrm{c}}} \frac{m_2}{M_1} \sqrt{E_{\mathrm{n}}} \int \mathrm{d}\varepsilon_1^{\mathrm{c}} f_1(\varepsilon_1^{\mathrm{c}}) \sqrt{\varepsilon_1^{\mathrm{c}}} \tag{9}$$

$$E_2^{\mathrm{l}}(\mathrm{cont}) = \frac{m_{\mathrm{n}} M_2}{M_{\mathrm{c}}^2} E_n + \frac{M_2 m_1}{M_1^2} \int \mathrm{d}\varepsilon_1^{\mathrm{c}} \frac{\mathrm{d}\sigma}{\mathrm{d}\varepsilon_1^{\mathrm{c}}} \varepsilon_1^{\mathrm{c}} + \frac{m_2}{M_2} \int \mathrm{d}\varepsilon_2^{\mathrm{r}} f_0(\varepsilon_2^{\mathrm{r}}) \varepsilon_2^{\mathrm{r}} - 2 \frac{\sqrt{m_{\mathrm{n}} m_1}}{M_c} \frac{M_2}{M_1} \sqrt{E_{\mathrm{n}}} \int \mathrm{d}\varepsilon_1^{\mathrm{c}} f_1(\varepsilon_1^{\mathrm{c}}) \sqrt{\varepsilon_1^{\mathrm{c}}} \tag{10}$$

where m_2, M_2 are the masses of the second emitted particle and its residual nucleus, respectively. $\mathrm{d}\sigma / \mathrm{d}\varepsilon_1^{\mathrm{c}} = f_0(\varepsilon_1^{\mathrm{c}})$ stands for the normalized spectrum of the first emitted particle in CMS, while $f_0(\varepsilon_2^{\mathrm{r}})$ is the normalized spectrum of the second emitted particle in RNS.

When the final state is in the discrete level state, with analogy procedure all of the released energies can be obtained. If the residual nucleus is in E_{k2} level, the energy carried by the second emitted particle and its residual nucleus are obtained by [1,2]

$$\varepsilon_2^{\mathrm{l}}(k) = \frac{m_{\mathrm{n}} m_2}{M_{\mathrm{c}}^2} E_{\mathrm{n}} + \frac{M_2}{M_1} (E^* - B_1 - B_2 - E_{k_2}) - \left(\frac{M_2 M_{\mathrm{c}}}{M_1^2} - \frac{m_1 m_2}{M_1^2} \right) \int \mathrm{d}\varepsilon_1^{\mathrm{c}} f_0(\varepsilon_1^{\mathrm{c}}) \varepsilon_1^{\mathrm{c}} - 2 \frac{\sqrt{m_{\mathrm{n}} m_1}}{M_{\mathrm{c}}} \sqrt{E_n} \frac{m_2}{M_1} \int \mathrm{d}\varepsilon_1^{\mathrm{c}} f_1(\varepsilon_1^{\mathrm{c}}) \sqrt{\varepsilon_1^{\mathrm{c}}} \tag{11}$$

$$E_2^{\mathrm{l}}(k) = \frac{m_{\mathrm{n}} M_2}{M_{\mathrm{c}}^2} E_{\mathrm{n}} + \frac{m_2}{M_1} (E^* - B_1 - B_2 - E_{k_2}) - \left(\frac{m_2 M_{\mathrm{c}}}{M_1^2} - \frac{m_1 M_2}{M_1^2} \right) \int \mathrm{d}\varepsilon_1^{\mathrm{c}} f_0(\varepsilon_1^{\mathrm{c}}) \varepsilon_1^{\mathrm{c}} - 2 \frac{\sqrt{m_{\mathrm{n}} m_1}}{M_{\mathrm{c}}} \sqrt{E_n} \frac{M_2}{M_1} \int \mathrm{d}\varepsilon_1^{\mathrm{c}} f_1(\varepsilon_1^{\mathrm{c}}) \sqrt{\varepsilon_1^{\mathrm{c}}} \tag{12}$$

Thus, the partial kerma factors can be obtained by multiplying the cross sections for every corresponding reaction channel and summing over them accordingly.

The total kerma factors is given by the summing over every partial kerma factors for each incident energy.

3 Kerma Factor of n+^{56}Fe reaction

The kerma factor calculations of n+^{56}Fe have been performed up to 20 MeV. The relation of the

unit is 1b·MeV=1.722951×10^{-12} Gy·cm^2 for ^{56}Fe.

The calculated total kerma factor is shown Fig.1 with the measured data. At low energies, for an example of n+^{56}Fe, the dominant part is the kerma from elastic recoil below 5 MeV. With the increasing incident energies the kerma from non-elastic recoils becomes of important.

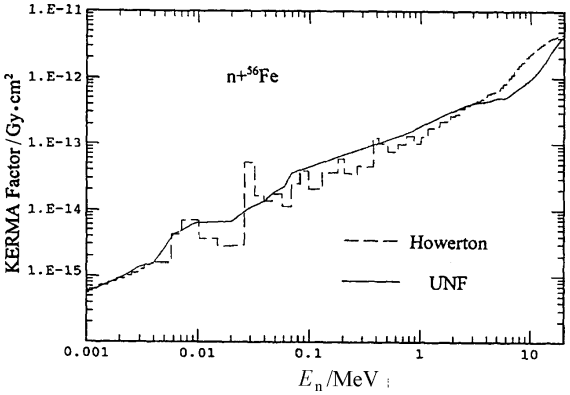

Fig.1 The total kerma factors of n+^{56}Fe, the data were taken from Ref.[4]

Since the cross sections of elastic scattering are in the resonance region at low energies, the calculation of them is not realistic, therefore the evaluated data of elastic scattering are adopted in the calculations.

4 Remarks

When the new function for calculating kerma factors is added in UNF code, a new file "kma.out" is opened for the kerma data outputting. The total kerma factors of proton, alpha-particle, triton, deuteron, ^{3}He, non-elastic recoils, elastic recoil, and the total kerma factors are given both in the unit of b·MeV and Gy·cm^2, respectively. Then the partial kerma factors of each reaction channel are also given for analysis.

Acknowledgments

The authors would like to thank Dr. T. Fukahori for providing the experimental data on kerma factor and dpa cross sections for analysis.

Reference

[1] ZHANG Jingshang, Commu. Nucl. Data Prog. 23, p18(2000)
[2] ZHANG Jingshang, CNIC-01460, (2000) (in Chinese)
[3] ZHANG Jingshang, Commu. Nucl. Data Prog. 22, p26 (1999)
[4] R. J. Howerton, UCRL-50400 Vol. 27 (1986)

A Code APMN for Automatically Searching Optimal Optical Potential Parameters below 300 MeV

SHEN Qingbiao
China Nuclear Data Center, CIAE, Beijing

The optical model is one of the most important evaluation tool in nuclear data calculations and evaluations. The calculated results of the optical model are mainly decided by its parameters. Thus, choosing and adjusting the optical potential parameters are the crucial steps.

APMN is a program for automatically searching a set of optimal optical potential parameters in E≤300 MeV energy region by means of the improved fastest falling method[1], which is suitable for non-fissile medium-heavy nuclei with the light projectiles, such as n, p, d, t, ^{3}He, and α. One set of optical potential parameters may be suitable from 1 to 40 target nuclei obtained based on their experimental data simultaneously.

The optical potentials considered here are Woods-

Saxon form for the real part, Woods-Saxon and derivative Woods-Saxon form for the imaginary parts corresponding to the volume and surface absorption respectively, and the Thomas form for the spin-orbit part[2,3]. Their potential parameters are presented as:

$$V = V_0 + V_1 E_{\rm L} + V_2 E_{\rm L}^2 + V_3 (N-Z)/A + V_4 Z/A^{1/3} \quad (1)$$

$$W_{\rm s} = W_{\rm s0} + W_{\rm s1} E_L + W_{\rm s2} (N-Z)/A \quad (2)$$

or

$$W_{\rm s} = W_{\rm s0} + W_{\rm s1} E_{\rm L} + W_{\rm s2} (N-Z)/A, \text{ when } E_{\rm L} \le E_{\rm ws} \quad (3)$$

$$W_{\rm s} = W_{\rm s0h} + W_{\rm s1h} E_{\rm L} + W_{\rm s2} (N-Z)/A, \text{ when } E_{\rm L} \ge E_{\rm ws} \quad (4)$$

$$W_{\rm s0h} = W_{\rm s0} + (W_{\rm s1} - W_{\rm s1h}) E_{\rm ws} \quad (5)$$

$$W_{\rm v} = W_{\rm v0} + W_{\rm v1} E_{\rm L} + W_{\rm v2} E_{\rm L}^2 \quad (6)$$

$$a_{\rm j} = a_{\rm j0} + a_{\rm j1} (N-Z)/A, \quad {\rm j = s, v} \quad (7)$$

Where $E_{\rm L}$ is the incident particle energy in laboratory system and in $E_{\rm L}$≤300 MeV energy region; Z, N and A are proton, neutron, mass number of the target nucleus. In order to improve the agreement between the theoretical and experimental values at the high energy part, the $E_{\rm L}^2$ term is included in the volume absorption potential $W_{\rm v}$. The 18 parameters V_0, V_1, V_2, V_3, V_4, $W_{\rm s0}$, $W_{\rm s1}$, $W_{\rm s2}$, $W_{\rm v0}$, $W_{\rm v1}$, $W_{\rm v2}$, $r_{\rm r}$, $r_{\rm s}$, $r_{\rm v}$, $a_{\rm r}$, $a_{\rm s0}$, $a_{\rm v0}$, $r_{\rm c}$ can be adjusted for W_s given by Eq.(2); the above 18 parameters and $W_{\rm s1h}$ can be adjusted for $W_{\rm s}$ given by Eqs.(3) and (4).

The adjustment of the optical potential parameters is performed automatically with computer to minimize a quantity of χ^2, which represents the deviation of the calculated nuclear data from the experimental values. The χ^2 is defined as follows:

$$\chi^2 = [\sum_{i=1}^{NN} W_i]^{-1} \sum_{i=1}^{NN} W_i \chi_i^2 \quad (8)$$

$$\chi_i^2 = [W_{i,\rm tot} + W_{i,\rm ne} + W_{i,\rm el}]^{-1} [W_{i,\rm tot}\chi_{i,\rm tot}^2 + W_{i,\rm ne}\chi_{i,\rm ne}^2 + W_{i,\rm el}\chi_{i,\rm el}^2], \quad (9)$$

$$\chi_{i,\rm tot}^2 = N_{i,\rm tot}^{-1} \sum_{j=1}^{N_{i,\rm tot}} [\frac{\sigma_{i,\rm tot}^{\rm T}(j) - \sigma_{i,\rm tot}^{\rm E}(j)}{\Delta\sigma_{i,\rm tot}^{\rm E}(j)}]^2 \quad (10)$$

$$\chi_{i,\rm ne}^2 = N_{i,\rm ne}^{-1} \sum_{j=1}^{N_{i,\rm ne}} [\frac{\sigma_{i,\rm ne}^{\rm T}(j) - \sigma_{i,\rm ne}^{\rm E}(j)}{\Delta\sigma_{i,\rm ne}^{E}(j)}]^2 \quad (11)$$

$$\chi_{i,\rm el}^2 = N_{i,\rm el}^{-1} \sum_{j=1}^{N_{i,\rm el}} K_{i,j,\rm el}^{-1} \sum_{k=1}^{K_{i,j,\rm el}} [\frac{\sigma_{i,j,\rm el}^{\rm T}(\theta_{i,j,k}) - \sigma_{i,j,\rm el}^{\rm E}(\theta_{i,j,k})}{\Delta\sigma_{i,j,\rm el}^{\rm E}(\theta_{i,j,k})}]^2 \quad (12)$$

Where N is the number of the nuclei to be considered. W_i is the weight of the i-th nucleus. $W_{i,\rm tot}$, $W_{i,\rm ne}$, $W_{i,\rm el}$ are the weights of the total cross sections, nonelastic scattering cross sections, elastic scattering angular distributions for the i-th nucleus, $W_{i,\rm tot}$=0 for the charged particle projectile. $N_{i,\rm tot}$, $N_{i,\rm ne}$, $N_{i,\rm el}$ are the energy point numbers of the experimental data of the total cross sections, nonelastic scattering cross sections, elastic scattering angular distributions for the i-th nucleus, respectively. $K_{i,j,\rm el}$ is the angle number of the experimental data of the elastic scattering angular distribution for the i-th nucleus and j-th energy point. The superscripts T and E represent the theoretical and experimental values, respectively. $\sigma_{i,\rm tot}(j)$ and $\sigma_{i,\rm ne}(j)$ are the total and nonelastic scattering cross sections for the i-th nucleus and j-th energy point, there is no total cross section for the charged particle projectile. $\sigma_{i,j,\rm el}(\theta_{i,j,k})$ is the elastic scattering angular distribution for the i-th nucleus, j-th energy point, and k-th outgoing angle. $\Delta\sigma$ stands for the experimental data error of the corresponding data.

We regard χ^2 as the function of the adjustable parameters. In order to search for the minimum of the χ^2, the adjusted parameters are constantly changing along the direction in which the χ^2 decreases fastest. In this program the fastest falling method is improved by the author, for which each parameter step length can be adjusted respectively and automatically. The calculations of the compound nucleus elastic scattering are within the framework of the width fluctuation corrected Hauser-Feshbach theory. This program allows user to fit the experimental data for up to 40 nuclei simultaneously. Thus, for those elements lack of experimental data, one can obtain its optical potential parameters based on the experimental data of neighbor nuclei with this program.

Many practical uses of this program in E≤20 MeV and E≤300 MeV energy regions show that the velocity of searching the best parameters is fast and rather successful results can be obtained.

The followings are some calculation results obtained with APMN code for the proton reactions with ^{208}Pb and ^{56}Fe.

Based on the experimental data of p+^{208}Pb reaction cross sections[4] and elastic-scattering angular distributions at energies of 16.0,[5] 21.0, 26.3, 30.3, 35.0, and 45.0,[6] 40.0,[7] 49.4,[8] 61.4,[9] 65.0,[10] 100.0,[11] 156.0,[12] and 160.0 and 182.0[13] MeV, a set of optimum proton optical potential parameters in the region of $E_{\rm P}$≤ 300 MeV is obtained by using the APMN code as follows:

$$V = 46.62447 - 0.32792E_{\rm p} - 0.0003875E_{\rm p}^2 + 24.0(N-Z)/A + 0.4(Z/A^{1/3}) \quad (13)$$

$$W_{\rm s} = \max\{0, 7.66757 + 0.004642E_{\rm p} + 12.0(N-Z)/A\} \quad (14)$$

$$W_{\rm v} = \max\{0, 0.42362 - 0.0032795E_{\rm p} - 0.0008046E_{\rm p}^2\} \quad (15)$$

$$U_{\rm so} = 6.2 \quad (16)$$

r_r =1.25970, r_s =1.09139, r_v =1.95,

r_{so} =1.25970, r_c =1.02222 (17)

a_r=0.63211, a_s=0.67536+0.7(*N*-*Z*)/*A*,

a_v=0.9+0.7(*N*-*Z*)/*A*,a_{so}=0.63211 (18)

Fig.1 compares the p+^{208}Pb reaction cross sections between the calculated values and the experimental data. Comparisons of the elastic-scattering angular distributions for the p+^{208}Pb reaction between the calculated values and the experimental data are given in Figs. 2, 3, and 4. In the whole E_p≤300 MeV energy region, the calculated values fit the experimental data very well.

The comparison of the elastic scattering angular distributions for the p+^{56}Fe reaction between the calculated values and the experimental data is shown in Fig. 5, the fitting agrees fairly well with each other.

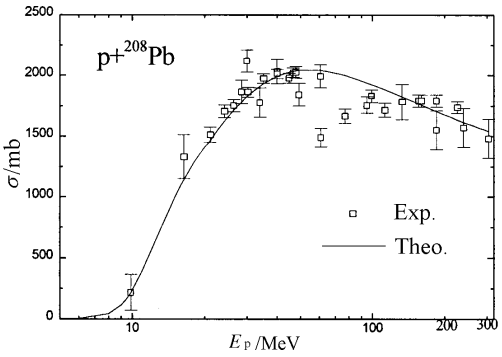

Fig. 1 Comparison of reaction cross sections between the calculated values and the experimental data for p+^{208}Pb reaction

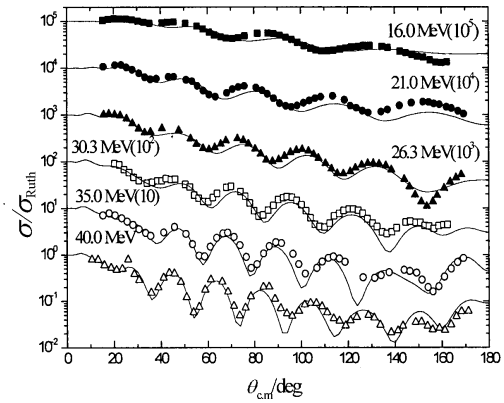

Fig. 2 Comparison of proton elastic scattering angular distributions between the calculated values and the experimental data for p+^{208}Pb reaction at E_p=16.0, 21.0, 26.3, 30.3, 35.0, and 40.0 MeV

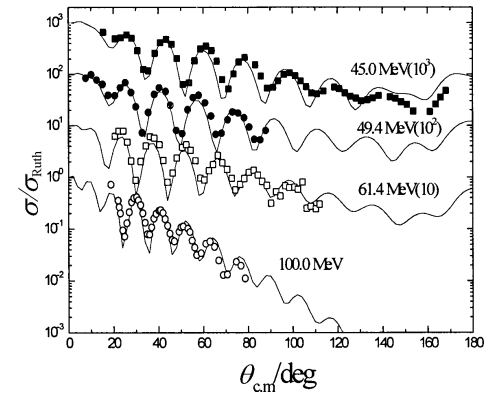

Fig. 3 Comparison of proton elastic scattering angular distributions between the calculated values and the experimental data for p+^{208}Pb reaction at E_p=45.0, 49.4, 61.4, and 100.0 MeV

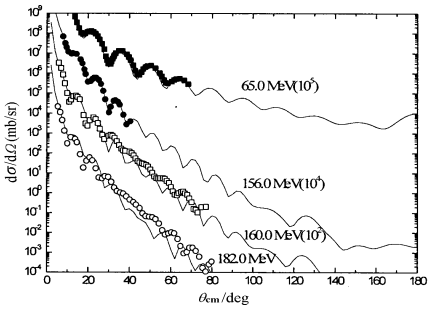

Fig. 4 Comparison of proton elastic scattering angular distributions between the calculated values and the experimental data for p+^{208}Pb reaction at E_p=65.0, 156.0, 160.0, and 182.0 MeV

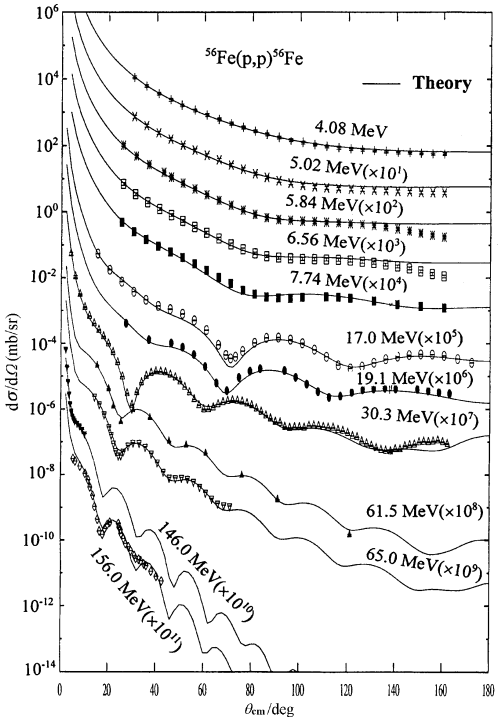

Fig. 5 Comparison of proton elastic scattering angular distributions between the calculated values and the experimental data for p+^{56}Fe reaction at E_p=4.08, 5.02, 5.84, 6.56, 7.74, 17.0, 19.1, 30.3, 61.5, 65.0, 146.0 and 156.0 MeV

In summary, APMN is a very useful code in nuclear data calculation. It has very strong function to search automatically a set of optimal optical potential parameters based on the experimental data in E≤300 MeV energy region, which is suitable for the light projectiles of n, p, d, t, ^{3}He, α and maximum 40 non-fissile medium-heavy target nuclei simultaneously.

The author would like to thank Prof. Cai Chonghai for providing some subroutines and Prof. Han Yinlu for providing some calculation results.

References

[1] B.Alder, S.Fernbach, and M.Rotenberg, Methods in Computational Physics, Vol.6, 1966, p.1, Academic Press, New York and London.

[2] F. D. Becchetti and G. W. Greenlees, Phys.Rev., 182, 1190 (1969).

[3] SHEN Qingbiao et al., Commu. of Nucl. Data Progress, No.7 41 (1992).

[4] W.Bauhoff., *Atomic Data and Nuclear Data Tables*., 35, 429 (1986)

[5] W. Makofske et al., *Phys. Rev*., C5, 780 (1972).

[6] W.T.H.Van Oers et al., *Phys. Rev*., C10, 307 (1974).

[7] J. J. H. Menetet al., *Phys. Rev*., C4, 1114 (1971).

[8] G.S. Mani et al., *Nucl. Phys*., A165, 384 (1971).

[9] C.B.Fulmer, J. B. Ball, *Phys. Rev*., 181, 1565 (1969).

[10] H.Sakaguchi et al., *Phys. Rev*., C26, 944 (1982).

[11] K.Kwiatrowski et al., *Nucl. Phys*., A301, 349 (1978).

[12] V.Comparat et al., *Nucl. Phys*., A221, 403 (1974).

[13] A.Nadasen et al., *Phys. Rev*., C23, 1023 (1981).

New Functions in UNF Code and Illustration

ZHANG Jingshang

China Nuclear Data Center, CIAE, Beijing

【**abstract**】*The information on the improvement of UNF code is issued as the additional illustration of UNF code revised version[1] in 2001.*

1 New Functions in UNF Code

(a) DGM is the parameter for direct gamma emission in the input parameter file UNF.DAT which is used to determine the component part in the capture radiation cross section.

(b) Selection of the used formula of level densities in the input parameter file:

KLD=1 for using Gilbert-Cameron level density formula;

KLD=2 for using Back-shifted level density formula.

(c) Including the calculation of kerma factors and outputting in KMA.OUT in both units of b·eV and Gy·cm^2.

(d) DPA calculation of the damage cross sections when the flag KDPA=1. All of the calculated results are written in the output file DPA.OUT.

(e) Checking the parameters of gamma ray emission branch ratios: Set KPDL=1 and run any one incident energy point calculation, then the Checked table is shown in UNF.OUT, in which the emitted gamma energies and the status of the normalization of the branch ratios are given. If it is not normalized, then user needs to correct them accordingly.

(f) When the user want to issue the ENDF/B-6 format outputting, the threshold energies for each reaction channels including the discrete levels of the residual nuclei are needed to be involved in the input incident energy points in file UNF.DAT. To do in this way, set flag KTEST=1 and run any one incident energy point calculation, then the threshold energies are given in output file UNF.OUT.

(g) In the UNF.DAT file the initial status of the target is labeled by
k=1 for ground state of target;
k>1 for excited state of the isomeric levels of target.

(h) Five angles are written in UNF.DAT as the input data. When the flag KDDCS=1, the angular-energy spectra are output in PLO.OUT file for fitting measured double-differential cross sections of the total outgoing neutrons in laboratory system.

(i) When users want to observe the gamma production cross sections from a discrete level to a discrete level in each reaction channel, then set the number of the discrete levels in the file UNF.DAT. The results are in output file UNF.OUT.

2 Flags Used in UNF code

Since the computer condition is improved, so the flags are simplified, and some new functions are added in UNF code. So far the remained flags are as follows:

KTEST=1 for doing some auxiliary calculation and outputting some medium results for analysis (=0 not).

KOPP=1 for outputting optical potential parameters (=0 not).

KPDL=1 for outputting the set of discrete levels (energy, spin and parity) of the residual nuclei and checking the gamma ray blanch rations (=0 not).

KDDCS=1 for calculating the double-differential cross sections, (=0 not).

KGYD=1 for calculating the gamma productions (=0 not).

KENDF=1 for outputting the files in ENDF/B-6 format (=0 not).

KDPA=1 for calculating dpa cross sections (=0 not).

Reference

[1] ZHANG Jingshang, Energy Balance in UNF Code, Commu. of Nucl. Data Progress, 23, 18(2000)

Calculation and Recommendation of n+$^{174,176\sim180,Nat}$Hf Reactions

HAN Yinlu

China Nuclear Data Center, CIAE, Beijing

【**abstract**】*Based on the experimental data of total, elastic scattering cross sections and elastic scattering angular distribution of natural Hf, a set of neutron optical potential parameter is obtained and all cross sections, angular distribution, double differential cross sections, γ-ray production cross sections and γ-ray production energy spectrum were calculated for n+ $^{174,176\sim180,nat}$Hf at incident neutron energies below 20 MeV. Theoretical results are compared with existing experimental data and evaluated data from ENDF/B6 and JENDL-3.*

Introduction

Natural Hf consists of six isotopes, i.e. ^{174}Hf (0.16%), ^{176}Hf (5.26%), ^{177}Hf (18.60%), ^{178}Hf (27.28%), ^{179}Hf (13.62%) and ^{180}Hf (35.08%). Because experimental data are scare, it is necessary to calculate all cross sections in theory.

1 Analysis of Experimental Data

The experimental data of total cross section were given in Refs. [1~5] for natural Hf in incident neutron energies 0.1~20 MeV. The experimental data are in basically agreement with all Refs.. The experimental data[6~9] of elastic scattering cross sections and elastic angular distribution were given at 0.9498, 1.0, 7.0 and 8.05 MeV, respectively, and the experimental data of elastic cross sections were also given in Ref. [10] in incident neutron energies 0.3~1.6 MeV. Above all of experimental data were used to guide adjusting optical potential parameters.

The experimental data of (n,γ) reaction cross sections were given in Refs. [11,12] for $^{176\sim180}$Hf, respectively. The experimental data of ^{180}Hf (n,γ) reaction cross sections were also given in Refs. [13~15]. The experimental data taken from Ref.[11] is agreement with those of Refs. [14,15] for ^{180}Hf (n,γ) reaction cross sections. The experimental data taken from Ref. [11] were used to guide theoretical calculation. The experimental data of ^{nat}Hf (n,γ) reaction cross sections were also given in Refs.[5,16~18], the experimental data are basically in agreement.

The experimental data of (n,p) reaction cross section were given in Refs. [19~23] for ^{178,179,180}Hf, respectively. The experimental data of ^{178,180}Hf (n,α) reaction cross sections were given in Refs. [21,24] , respectively. The experimental value taken from Ref. [24] is three times of those taken from Ref. [21] for ^{180}Hf (n,α) reaction, the experimental data taken from Ref. [24] were not considered in our calculation.

The experimental data of ^{174}Hf (n,2n) reaction cross sections were given in Refs. [24~27], respectively. The experimental value taken from Refs. [25,26] is larger than those taken from Ref. [27], and smaller than those taken from Ref. [25]. The experimental data taken from Refs. [25,26] were used to guide theoretical calculation. The experimental data of ^{176}Hf (n,2n) reaction cross sections were given in Refs. [24,25,28,29], respectively, and experimental data were analyzed in Ref. [28]. The experimental data taken from Ref. [28] were used in our calculation.

The evaluation of experimental data for total cross sections of ^{Nat}Hf and $^{176\sim180,nat}$Hf (n,γ) cross sections were given in Ref. [30]

2 Codes and Parameters

The code APOM[31] , by which the best neutron optical potential parameters can be searched automatically with fitting relevant experimental total, nonelastic scattering cross sections, elastic scattering cross sections and elastic scattering angular distributions, was used to obtain a set of optimum neutron optical potential parameters of Hf. Because there are no experimental data for isotopes, the experimental data of ^{nat}Hf were used to obtain a set of optimum neutron optical potential parameters of ^{180}Hf. Then, this set of optimum neutron optical potential parameters were used in n+$^{174,176\sim180,nat}$Hf reaction as fellows:

V=50.9999+0.3931E−0.02637E^2−24.0(N−Z)/A

W_s=10.2565−0.3203E−12.0(N−Z)/A

W_v=−1.2589+0.1257E+0.01170E^2

U_{so}=6.2

r_r= 1.1754, r_s=1.4030, r_v=1.6116, r_{so}=1.1754

a_r=0.5037, a_s=0.5418, a_v=0.4677, a_{so}=0.5037

Using this set of neutron optical potential parameters, adjusting charged particle optical potential parameters as well as giant dipole resonance parameters and level density parameters, all reaction cross sections, angular distribution, double differential cross sections, γ-ray production cross sections and γ-ray production energy spectrum were calculated for n+ $^{174,176\sim180,nat}$Hf at incident neutron energies below 20 MeV by code NUNF[32]. The direct inelastic scattering data were calculated by the code DWUCK4[33] . The exciton model parameter K was taken as 900 MeV^3 for all isotopes.

3 Calculated Results and Analysis

The comparison of calculated results of neutron total, elastic scattering cross sections and elastic scattering angular distribution with experimental data for n+^{Nat}Hf reaction are given in Figs.1~3. The calculated results of total cross sections and elastic scattering angular distribution are in good agreement with experimental data, while the calculated results of elastic scattering cross section pass through existing experimental data. Based on the above fitting, a set of neutron optical potential parameters were determined for n+^{180}Hf reaction.

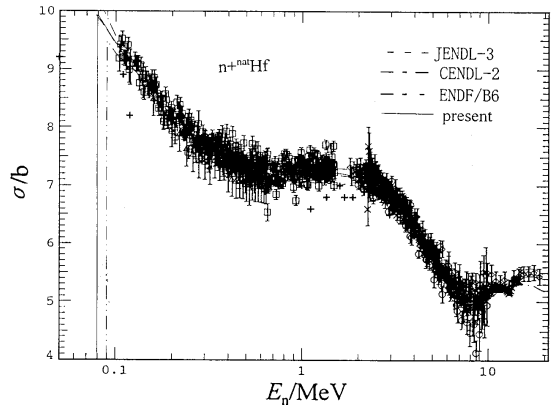

Fig. 1 The total cross section of n+NatHf reaction

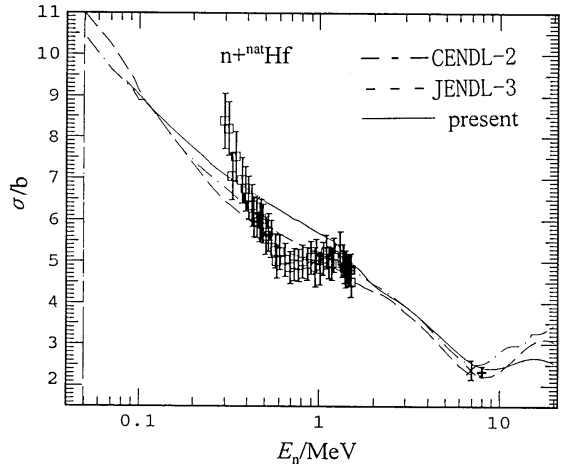

Fig. 2 The elastic scattering cross section of n+NatHf reaction

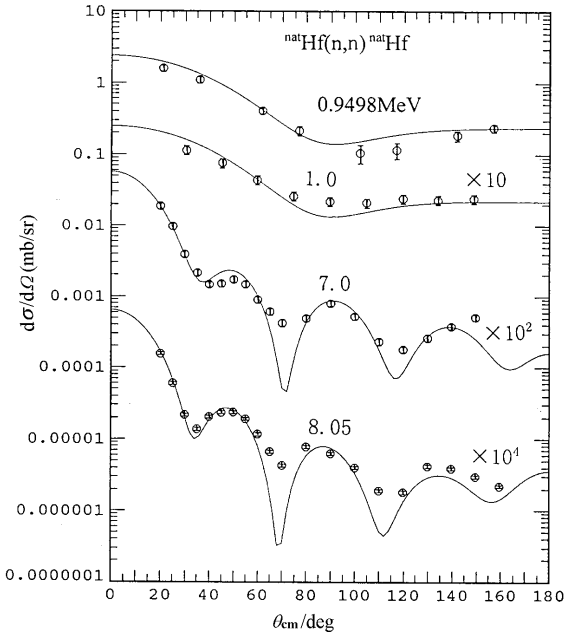

Fig. 3 The elastic scattering angular distribution of n+NatHf reaction

The comparison of calculated results of (n,γ) reaction cross section with experimental data for $^{176\sim180,nat}$Hf are given in Figs. 4~9, respectively. The calculated results of $^{176\sim180}$Hf(n,γ) reaction cross sections are in good agreement with experimental data taken from Ref. [11] in energy region 0.01~2 MeV, while for $E_n \geq 2$ MeV, it seems the present results are reasonable. The calculated results for ^{nat}Hf(n,γ) reaction cross sections are in good agreement with experimental data in energy region 0.01~3 MeV.

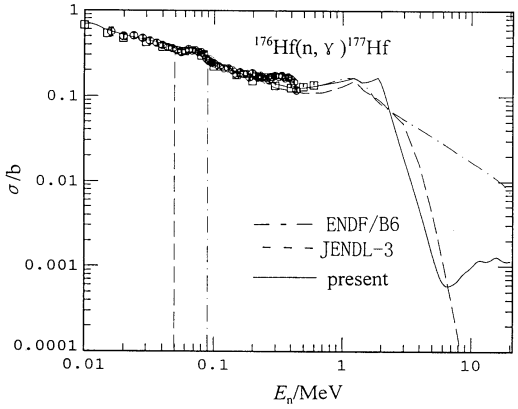

Fig. 4 The cross section of ^{176}Hf (n,γ) reaction

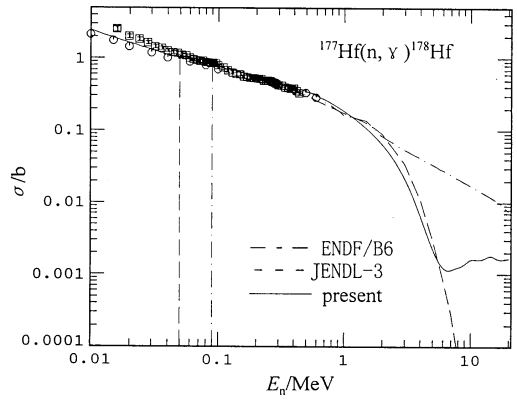

Fig. 5 The cross section of ^{177}Hf (n,γ) reaction

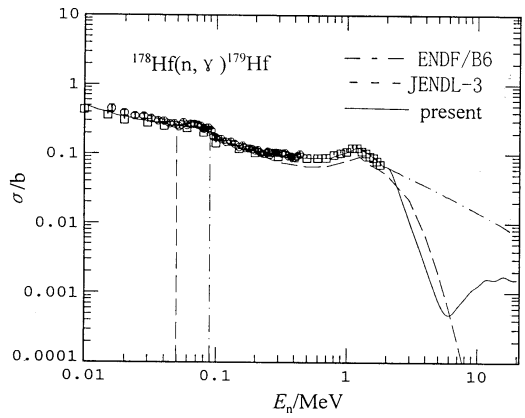

Fig. 6 The cross section of ^{178}Hf (n,γ) reaction

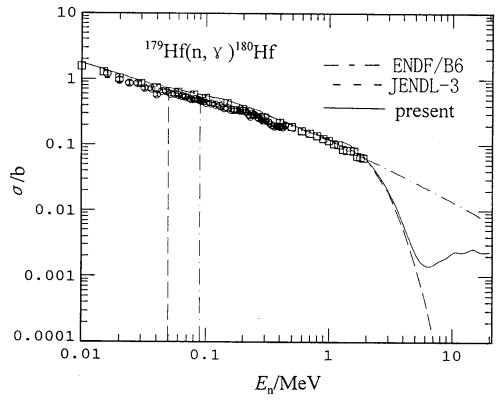

Fig. 7 The cross section of ^{179}Hf (n,γ) reaction

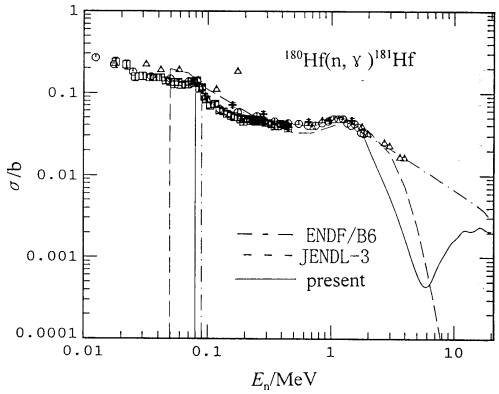

Fig. 8 The cross section of ^{180}Hf (n,γ) reaction

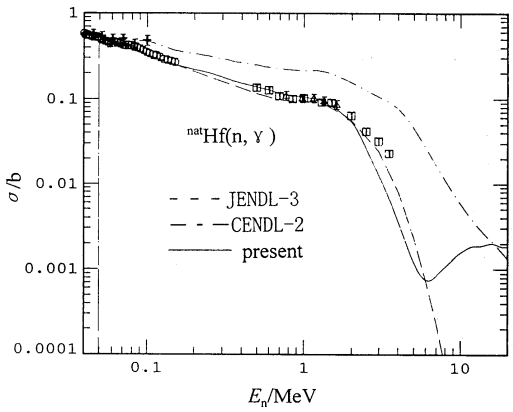

Fig. 9 The cross section of ^{Nat}Hf (n,γ) reaction

In Figs.10~12, the comparison of calculated results of ^{178,179,180}Hf(n,p) reaction cross sections with experimental data are given, respectively. The calculated curves pass through the experimental data within error bars. The comparison of calculated results and experimental data for ^{178,180}Hf(n,α) reaction cross sections are given in Figs.13 and 14, respectively. The calculated results fit the experimental data.

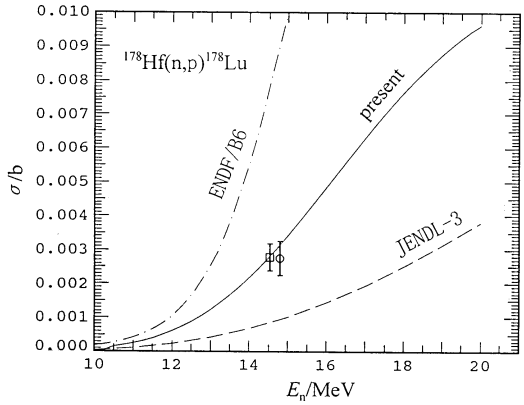

Fig. 10 The cross section of ^{178}Hf (n,p) reaction

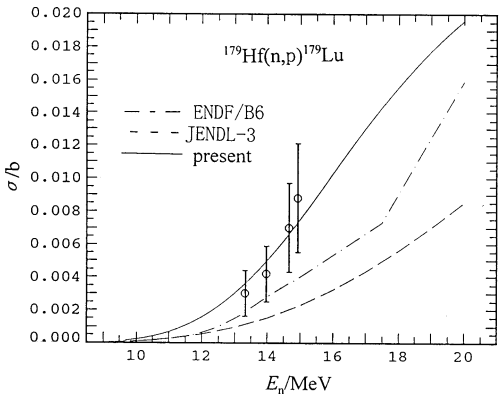

Fig. 11 The cross section of ^{179}Hf (n,p) reaction

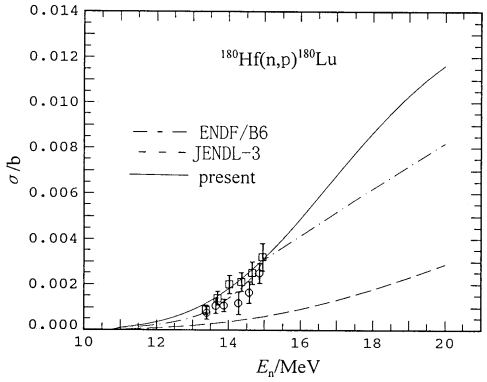

Fig. 12 The cross section of ^{180}Hf (n,p) reaction

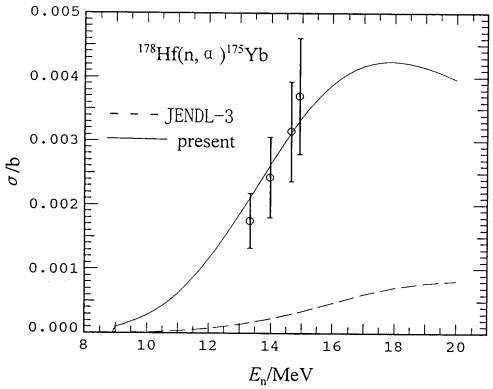

Fig. 13 The cross section of ^{178}Hf (n,α) reaction

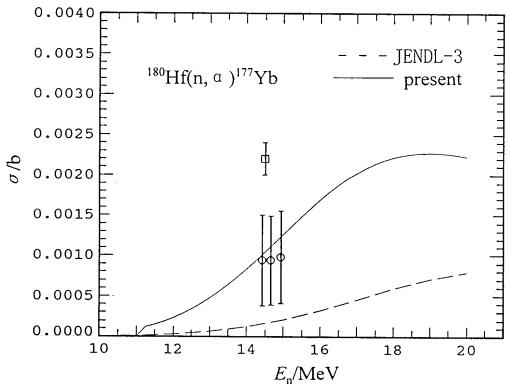

Fig. 14 The cross section of ^{180}Hf (n,α) reaction

The comparison of calculated results with experimental data for ^{174,176}Hf(n,2n) reaction cross sections are given in Figs.15 and 16, respectively. The calculated curves pass through the experimental data within error bars taken from Refs.[25,26] for ^{174}Hf(n,2n) reaction, the calculated results of ^{176}Hf(n,2n) reaction cross section are in good agreement with the experimental data.

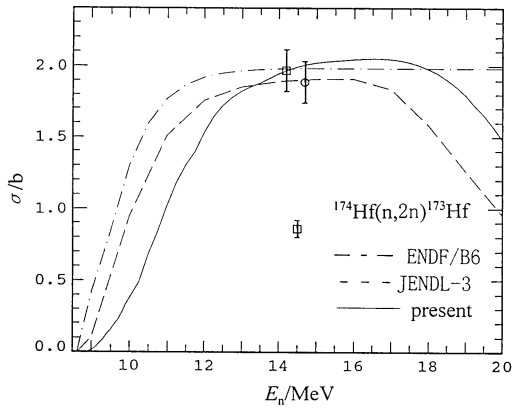

Fig. 15 The cross section of ^{174}Hf (n,2n) reaction

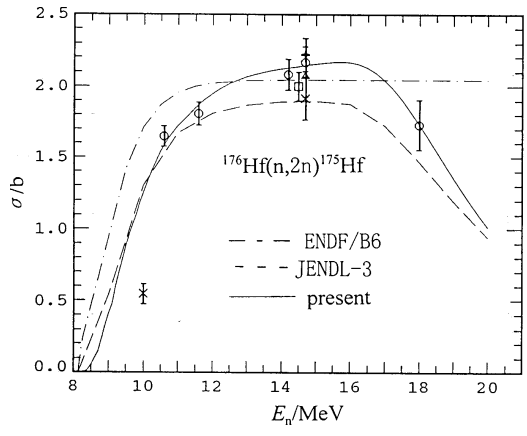

Fig. 16 The cross section of ^{176}Hf (n,2n) reaction

As example, the energy spectrum, γ-ray production cross section and γ-ray production energy spectrum for n+^{180}Hf reaction are given in Figs.17~20, respectively. The calculated results are reasonable.

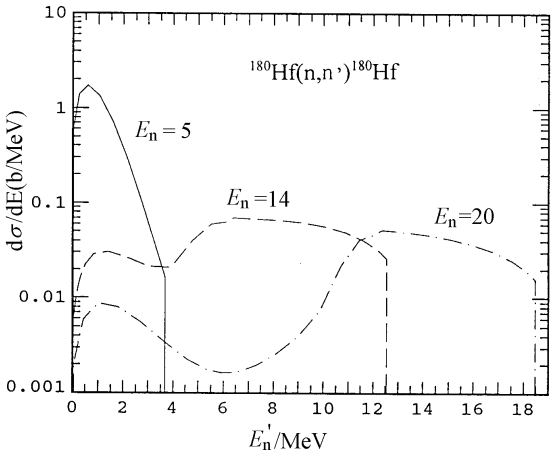

Fig. 17 The energy spectrum of ^{180}Hf (n,n') reaction

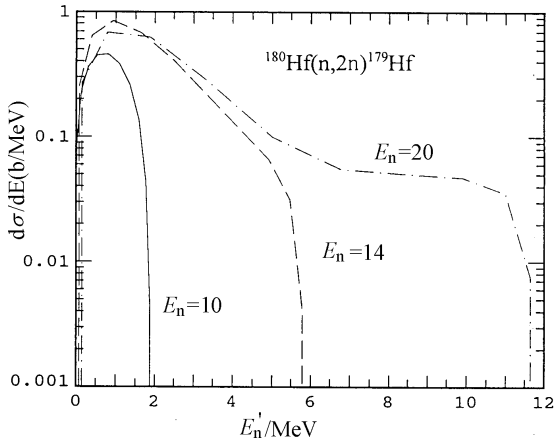

Fig. 18 The energy spectrum of ^{180}Hf (n,2n) reaction

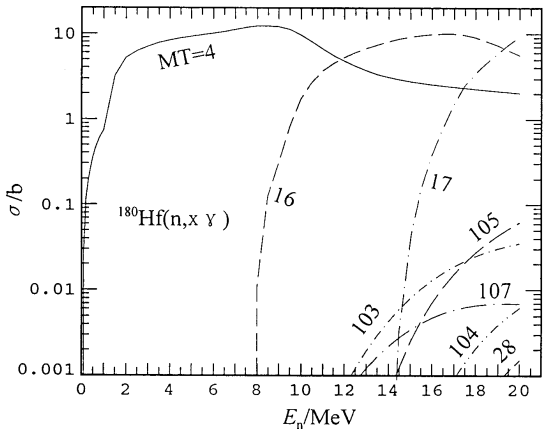

Fig. 19 The γ–ray production cross section of n+^{180}Hf reaction

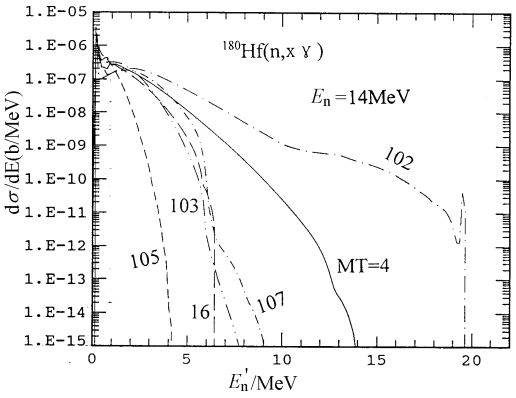

Fig.20 The γ–ray production energy spectrum of n+^{180}Hf reaction

4 Recommendation

Because theoretical calculated results are reasonable from above analysis, the calculated results are recommended in the energy range from 0.08 to 20 MeV; while for energy from 1.0^{-5} to 0.08 MeV, the evaluated data of ENDF/B6 library are adopted.

The final recommendations were accompished with the aid of combined adjustment in order to make the complete data of natural element and its isotopes satisfy the consistent relationships at the same time.

References

[1] D.G. Foster, et al., Phys. Rev., C3,576(1971)
[2] L. Green, et al., WAPD-TM-1073,1973
[3] M. Divadeenam, Dissertaion Abstr., B28,3834(1968)
[4] A. Okazaki, et al., Phys. Rev., 93,461(1954)
[5] W.P. Potenitz, et al., ANL-NDM-80,1983
[6] S.A. Cox, et al., ANL-7935,1972
[7] M. Walt, et al., Phys. Rev., 93,1062(1954)
[8] B. Holemad, et al., AE-430,1971
[9] M.A. Etemad, et al., AE-482,1973
[10] G.L. Sherwood, et al., Nucl. Sci. Eng., 39,67(1970)
[11] H. Beer, et al., Phys. Rev., C30,464(1984)
[12] M.V. Bokhovko, et al., FEI-2169-91,1991
[13] J.A. Miskel, et al., Phys. Rev., 128,2717(1962)
[14] ZHOU Zuying, et al., Chin. Nucl. Phys., 6,174(1984)
[15] ZHEN Jinxiang, et al., Chin. Nucl. Phys., 19,110(1997)
[16] D. Kompe, Nucl. Phys., A133,513(1969)
[17] MU Yunshan, et al., Chin. Nucl. Phys., 10,233(1988)
[18] WANG Chunhao, et al., Chin. Nucl. Phys., 12,89(1990)
[19] J.L. Meason, et al., Radiochimica Acta, 6,26(1966)
[20] A. Kirov, et al., Z. Phys., A245,285(1993)
[21] C. Konno, et al., NEANDC(J)-155,15,1990
[22] S. Murahira, et al., INDC(JPN)-157,268,1992
[23] Y. Kasugai, et al., 94GATLIN, 935, 1990
[24] M. Hillman, et al., J. of Inorganic and Nucl. Chem., 31, 909 (1969)
[25] S.M. Qaim, Nucl. Phys., A224,319(1974)
[26] N. Lakshmana DAS, et al., Annals of Nucl. Energ., 8, 283 (1981)
[27] B.H. Patrick, et al., INDC(NDS)-232,69(1990)
[28] LU Hanlin, et al., Commun. Nucl. Data Prog., 19,10 (1998)
[29] J.W. Meadows, et al., Annals of Nucl. Energ., 23, 877 (1996)
[30] WANG Tingtai, et al., Commun. Nucl. Data Prog., 24, 103 (2000)
[31] SHEN Qingbiao, Commun. Nucl. Data Prog., 7,43 (1992)
[32] ZHANG Jingshang, Private Commun., 1998
[33] P.D. Kunz, DWUCK4 Code.

Calculations of Complete Data for n+^{99}Tc Reaction in E_n=0.01~20 MeV Region

CAI Chonghai
Department of Physics, Nankai University, Tianjin
ZHUANG Youxiang
China Nuclear Data Center, CIAE, Beijing

The code APMN[1] is used to automatically get the optimal parameters of the optical potential for neutron channel. The experimental σ_{tot} in E_n<0.1 MeV region are considered unreliable, only the experimental σ_{tot} in 2~15 MeV energy region were used in automatically searching for the optimal optical potential parameters which are:

V_0=52.19657516, V_1=−0.18551011,

V_2=−0.02026110, V_4=−0.17908059,
W_0=6.96990824, W_1=0.70658392,
U_0=−3.24499989, U_1=0.13205899, U_2=−0.00668700,
a_r=0.61835420, a_s=0.50631952, a_v=0.61555803,
r_r=1.28659534, r_s=1.31162643, r_v=1.17986906.

The DWBA code DWUCK4[2] is used to calculate the direct inelastic scattering cross sections and the angular distributions of the four levels for ^{99}Tc. These direct inelastic scattering data and above optimum set of optical potential parameters are taken as the input data of the kernel program SUNF[3]. Through adjusting some parameters in the input data of SUNF by hand again and again, we can make $\sigma_{n,\gamma}$, $\sigma_{n,n'}$, $\sigma_{n,2n}$, $\sigma_{n,p}$, $\sigma_{n,\alpha}$ and $\sigma_{n,n\alpha}$ in optimum agreement with experimental data.

The final optimal values of the adjusted parameters we got are: Ck (the parameter for exciton model)=220.0, Ce1(the multiplied factor in $\sigma_{n,\gamma}$) =0.30. The change of energy level density parameter is as follows: $a_{n,n'}$ from 15.49548 to 15.99548, $a_{n,p}$ from 15.05988 to 13.05988; $a_{n,\alpha}$ from 14.04595 to 13.04595; $a_{n,2n}$ from 14.25234 to 13.25234; $a_{n,n\alpha}$ from 13.32280 to 15.32280; $a_{n,3n}$ from 13.51792 to 15.51792. The change of pair energy correction is as follows: $\Delta_{n,\alpha}$from 0.0 to 0.7; $\Delta_{n,d}$ from 2.32 to 1.32; $\Delta_{n,2n}$ from 0.15 to -0.10; $\Delta_{n,n\alpha}$ from 1.12 to 0,0; $\Delta_{n,3n}$ from 0.97 to 0.0. The change of some optical potential parameters is as follows: r_s=r_v of p channel from 1.32 to 1.22; r_s=r_v of α channel from 1.442 to 1.20.

The calculated σ_{tot}, σ_{non} and σ_{el} as well as the experimental σ_{tot} are given in Fig.1, $\sigma_{n,\gamma}$ in Fig. 2, from which we can see that the calculated values are in pretty good agreement with experimental data. Besides, the calculated $\sigma_{n,n'}$, $\sigma_{n,p}$, $\sigma_{n,\alpha}$ and $\sigma_{n,n\alpha}$ are also in rather good agreement with few experimental data, though their figures are not given here.

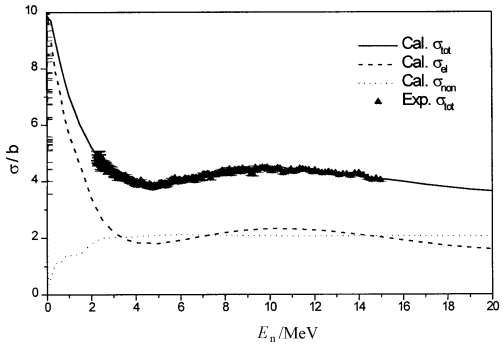

Fig. 1 σ_{tot}, σ_{el} and σ_{non} of ^{99}Tc

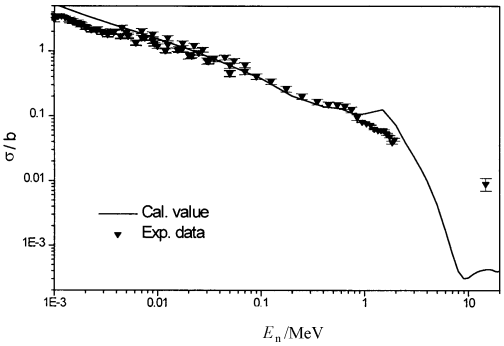

Fig. 2 Radioactive capture cross sections of ^{99}Tc

References

[1] SHEN Qingbiao, APMN96, a code for automatically searching for a set of optimal optical potential parameters of many medium and heavy nucleus (unpublished);

[2] P.D.Kunz, DWBA code DWUCK4, University of Colorado, USA (unpublished);

[3] ZHANG Jingshang, SUNF, a code for comprehensive calculations of fission product nucleus based on unified model, CNDC, CIAE (unpublished);

Calculation and Recommendation of n+$^{142\sim148,150}$Nd Reactions in the Energy Region up to 20 MeV

SHEN Qingbiao ZHUANG Youxiang LIANG Qichang

China Nuclear Data Center, CIAE, Beijing

【**abstract**】*The neutron data of $^{142-148,150}$Nd were calculated and recommended in the energy region 10^{-5} eV to 20 MeV. The data include total, elastic, (n,γ), total inelastic, discrete level and continuum inelastic, (n,2n), (n,3n), (n,p), (n,α), (n,t), (n,^{3}He), (n, n'p+pn'), (n,n'α+αn') cross sections. The angular distributions and the spectra of the secondary neutrons and the resonance parameters were also included.*

Introduction

The neodymium (Nd) is an important fission product nucleus. The natural neodymium consists of 7 isotopes, ^{142}Nd (27.2%), ^{143}Nd (12.2%), ^{144}Nd (23.8%), ^{145}Nd (8.3%), ^{146}Nd (17.2%), ^{148}Nd (5.7%), ^{150}Nd (5.6%). The evaluated neutron nuclear data of the various neodymium isotopes including some unstable nuclei (such as ^{147}Nd) in the energy region up to 20 MeV are useful in the design of the nuclear engineering.

Some experimental data of total, (n,γ), (n,2n), (n,p), (n,α) cross sections and elastic scattering distributions are available for even nuclei ^{142}Nd, ^{144}Nd, ^{146}Nd, ^{148}Nd and ^{150}Nd in the energy region up to 20 MeV. But there are only some experimental data of (n,γ), (n,p) and (n,α) cross sections for odd nuclei ^{143}Nd and ^{145}Nd. All the experimental data were taken from EXFOR library.

1 Theoretical Calculation

Firstly, the code APMN[1] was used to automatically get the optimal optical potential parameters for neutron channel based on various neutron experimental data. The optical potential forms are as follows:

$$V=V_0+V_1E_n+V_2E_n^2+V_3(N\text{-}Z)/A+V_4Z/A^{1/3} \quad (1)$$

$$W_s=\max\{0,W_0+W_1E_n+W_2(N\text{-}Z)/A\} \quad (2)$$

$$W_v=\max\{0,U_0+U_1E_n+U_2E_n^2\} \quad (3)$$

where E_n is the incident neutron energy and Z, N, A are the number of proton, neutron, mass of the target nucleus, respectively. The obtained optical potential parameters for ^{142}Nd, ^{143}Nd, ^{144}Nd, ^{145}Nd, ^{146}Nd, ^{148}Nd and ^{150}Nd are listed in Table 1. The optical potential parameters of ^{147}Nd are taken as the same with isotope ^{145}Nd. The spin-obit potential parameters are taken as: V_{so}=6.2, $r_{so}=r_r$, $a_{so}=a_r$.

The code DWUCK4[2] was used to calculate the direct inelastic scattering cross sections and angular distributions. The main code SUNF[3] was used to calculate the various data. In our calculations the Gilbert-Cameron level density formula[4] was applied. The obtained level density parameters for (n,γ), (n, n'), (n,2n), (n,3n), (n,p), (n,α) channels through fitting the experimental data are listed in Table 2. The exciton model constants K are given in Table 3.

Table 1 The obtained optical potential parameters of various isotopes of element neodymium

Isotope	^{142}Nd	^{143}Nd	^{144}Nd	^{145,147}Nd	^{146}Nd	^{148}Nd	^{150}Nd
V_0	52.2797	51.3048	52.0414	51.3308	52.0720	51.9998	52.6031
V_1	0.12242	0.29459	0.21032	0.30931	0.19889	0.17513	-0.35163
V_2	-.02963	-.026481	-.02965	-.026248	-.027631	-.025027	.008689
V_3	-24.0	-28.3580	-20.2199	-28.3235	-19.6094	-19.9663	-19.6464
V_4	0.0	-.021802	-.056216	-.021573	-.056528	-.050219	.008309
r_r	1.19815	1.19665	1.19029	1.19767	1.18541	1.18289	1.17869
a_r	0.77643	0.86728	0.75238	0.85312	0.75224	0.75139	0.71996
W_0	8.00865	9.17282	6.01072	9.28461	6.74306	7.32856	8.80026
W_1	0.26144	0.12610	0.19879	0.14908	0.15511	0.13483	-0.01057
W_2	-12.0	-4.88630	0.97448	-4.81538	-0.29927	-1.52729	-8.01776
r_s	1.31647	1.31591	1.29040	1.32555	1.28033	1.27429	1.21281
a_s	0.50009	0.44904	0.53828	0.44419	0.55718	0.57686	0.59411
U_0	-1.16537	-1.27231	-1.12540	-1.28093	-1.07960	-1.05403	-0.41800
U_1	0.10517	0.12150	0.11340	0.12034	0.11284	0.11067	0.17000
U_2	-.001379	.000346	-.001971	.000367	-.002004	-.002097	-.001797
r_v	1.9500	1.60239	1.91978	1.50603	1.81996	1.76192	1.68053
a_v	0.94210	0.31945	0.94710	0.34290	0.95000	0.94954	0.29000

Table 2 The obtained level density parameters of various iisotopes of element neodymium

Isotope	^{142}Nd	^{143}Nd	^{144}Nd	^{145}Nd	^{146}Nd	^{147}Nd	^{148}Nd	^{150}Nd
(n,γ)	11.602	15.816	15.943	13.491	22.008	15.589	23.374	22.390
(n,n')	10.615	14.002	12.116	10.043	14.591	14.508	18.589	19.359
(n,2n)	22.148	13.015	13.902	18.116	19.343	20.591	16.008	18.374
(n,3n)	18.451	20.848	18.715	22.902	18.116	23.343	15.591	27.589
(n,p)	12.290	15.630	20.701	11.052	20.860	13.239	22.709	22.224
(n,α)	15.334	11.425	15.059	10.353	18.418	14.360	18.548	20.357

Finally, through changing some other parameters of level density and charged particle optical potential, the calculated various cross sections are in good agreement with the experimental data and some systematic rules of the calculated data are obtained.

2 Data Recommendation

The recommendation of complete neutron nuclear data of $^{142\sim148,150}$Nd were made on the basis of both the experimental data and the theoretical calculation results.

2.1 Thermal Cross Sections and Resonance Parameters

The resolved resonance parameters and the unresolved resonance parameters for $^{142\sim148,150}$Nd were taken from JENDL-3.2 library, but certain adjustment for them was made in order to get good thermal cross sections in agreement with the experimental data and good conjunction at the resonance boundaries. Since the unresolved resonance parameters used here presented the smooth cross sections, they were adjusted in order to fit the (n,γ) experimental data in this energy region. Table 4 gives the comparisons of thermal cross sections and (n,γ) resonance integrals $I_{n,\gamma}$ (0.5 eV cutoff) between the libraries JENDL-3.2 (J3), ENDF/B-6 (B6), this work(C3) and the experimental data[5] for ^{147,148,150}Nd. The agreement with experimental data of our results are evidently better than those in JENDL-3.2 and ENDF/B-6 libraries, except $I_{n,\gamma}$ of ^{150}Nd which should be improved in the future. Table 5 shows the total (TOT), elastic (EL), radiation capture (GM) cross section conjunction of JENDL-3.2 and this work at resonance boundaries for ^{147,148,150}Nd. Here Er and Eu are the conjunction energies between the resolved resonance region and unresolved resonance region, unresolved resonance region and the smooth cross section region, respectively. The cross sections at resonance boundaries, calculated by PSY code, are the average cross sections over a small energy region nearby the boundaries. From Table 5 one can see that the conjunction at E_r of this work is obviously better than JENDL-3.2.

Table 3 The exciton model constant *K* of various isotopes of element neodymium

Isotope	^{142}Nd	^{143}Nd	^{144}Nd	^{145}Nd	^{146}Nd	^{147}Nd	^{148}Nd	^{150}Nd
K (MeV^3)	2300	1000	600	1700	600	600	600	600

Table 4 Comparisons of thermal cross sections and (n,γ) resonance integrals between various libraries and experimental data

		^{147}Nd	^{148}Nd	^{150}Nd
σ_{tot} / b	J3	510.3	6.997	5.981
	B6	524.1	2.202	5.052
	C3	520.3	6.503	4.700
	EXP.		6.5	4.7
σ_{el} / b	J3	79.28	4.505	4.780
	B6	84.21	-0.299	3.852
	C3	80.33	4.000	3.500
	EXP.		4.0±0.5	3.5±0.5
$\sigma_{n,\gamma}$ / b	J3	431.0	2.493	1.202
	B6	439.9	2.500	1.200
	C3	440.0	2.503	1.200
	EXP.	440±150	2.5±0.2	1.2±0.2
$I_{n,\gamma}$ / b	J3	628.58	14.762	15.823
	B6	573.49	19.360	15.943
	C3	653.52	13.896	10.424
	EXP.		14±1	14±2

Table 5 Comparisons of cross section conjunction at resonance boundaries between JENDL-3.2 and this work(C3)

		^{147}Nd		^{148}Nd		^{150}Nd	
		J3	C3	J3	C3	J3	C3
	Er(eV)	3.6E+1	3.52E+1	8.0E+3	8.0E+3	1.369E+4	1.369E+4
	Eu(eV)	1.0E+5	1.0E+5	1.0E+5	1.0E+5	1.0E+5	1.0E+5
TOT	σ_r-(b)	4.8619E+1	2.3478E+2	3.1220E+1	2.0750E+1	2.9789E+1	1.5037E+1
	σ_r+(b)	2.0788E+2	2.3503E+2	2.0553E+1	2.0724E+1	1.6625E+1	1.5037E+1
	σ_u-(b)	9.4059E+0	8.7974E+0	9.4769E+0	9.2078E+0	9.6474E+0	8.1677E+0
	σ_u+(b)	9.4762E+0	8.8089E+0	9.4762E+0	9.2113E+0	9.6469E+0	8.2000E+0
EL	σ_r-(b)	3.5083E+1	7.0034E+1	3.1066E+1	2.0278E+1	2.9551E+1	1.4717E+1
	σ_r+(b)	7.2719E+1	7.0255E+1	2.0357E+1	2.0251E+1	1.6417E+1	1.4717E+1
	σ_u-(b)	8.4596E+0	7.9000E+0	9.3898E+0	9.1065E+0	9.5273E+0	8.0565E+0
	σ_u+(b)	8.5409E+0	7.9118E+0	9.3887E+0	9.1100E+0	9.5274E+0	8.0885E+0
GM	σ_r-(b)	1.3537E+1	1.6475E+2	1.5383E-1	4.7224E-1	2.3802E-1	3.1974E-1
	σ_r+(b)	1.3516E+2	1.6478E+2	1.9623E-1	4.7224E-1	2.0781E-1	3.1995E-1
	σ_u-(b)	4.8031E-1	2.3032E-1	8.7119E-2	1.0130E-1	1.2007E-1	1.1123E-1
	σ_u+(b)	4.6929E-1	2.3003E-1	8.7489E-2	1.0130E-1	1.1960E-1	1.1150E-1

2.2 Smooth Cross sections

2.2.1 Total Cross Sections

The total cross sections of ^{142,144,146,148,150}Nd were measured by R. E. Shamu et al.[6] in 0.745 to 13.89 MeV region in 1980 and A. N. Djumin et al.[7] at 14.2 MeV in 1973. There are many experimental data of total cross sections up to 20 MeV for ^{Nat}Nd. Fig.1 shows the comparison of the recommended and the calculated total cross sections in smooth region with those in JENDL-3.2 and ENDF/B-6 libraries as well as the experimental data for ^{145}Nd, but the experimental data of ^{Nat}Nd were used. Fig.2 shows the comparison of the recommended total cross sections in smooth and unresolved resonance regions with those in JENDL-3.2 and ENDF/B-6 libraries as well as the experimental data for ^{150}Nd. The calculated total cross sections above 0.4 MeV for ^{150}Nd are recommended since they are in good agreement with the experimental data.

2.2.2 Radiation Capture Cross Sections

There are some experimental data of radiation capture cross sections for $^{142\sim146,148,150}$Nd below 3.0 MeV. Obviously, the (n,γ) cross sections of the odd nuclei at low energy region are higher than even one.

Fig. 3 shows the measured radiation capture cross sections of ^{148}Nd from 0.01 to 2.0 MeV. From Fig.3 one can note that the experimental data by A.E.Johnsrud (1959), Y.Nakajima(1978) and B.V.Thirumala (1972) are too high. The measured data by A.R.Delmusgrove (1978) were compared with others for several Nd isotopes, one found they were too low and were removed from the new

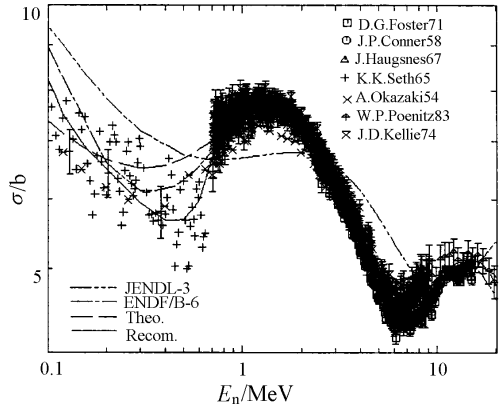

Fig. 1 Comparison of the recommended and the calculated total cross sections in smooth region with those in JENDL-3.2 and ENDF-B6 libraries as well as the experimental data for ^{145}Nd

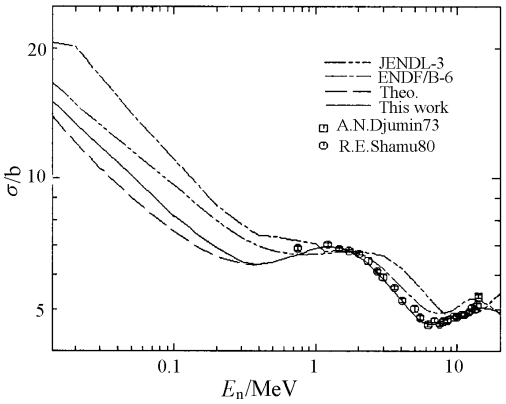

Fig. 2 Comparison of the calculated total cross sections with those in JENDL-3.2 and ENDF-B6 libraries as well as the experimental data for ^{150}Nd

EXFOR library. The measured data by T. Bradley (1979)[8], S. S. Hasan (1968)[9], K. Siddappa (1974)[10], V. N. Kononov (1977)[11], YU.N.Trofimov (1987)[12] and YU.N.Trofimov (1993)[13] were used for the data recommendation. Fig. 4 shows the comparisons of the recommended (n,γ) cross sections in smooth and unresolved resonance regions with those in JENDL-3.2 and ENDF/B-6 libraries as well as the experimental data for ^{148}Nd. Obviously the recommended data here are in better agreement with the experimental data than those in JENDL-3.2 and ENDF/B-6 libraries.

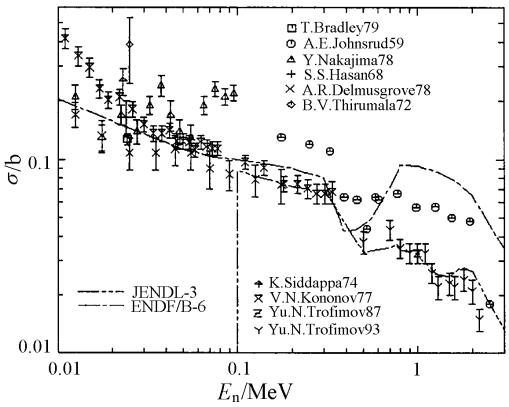

Fig. 3 Comparisons of the experimental data of (n,γ) cross sections for ^{148}Nd

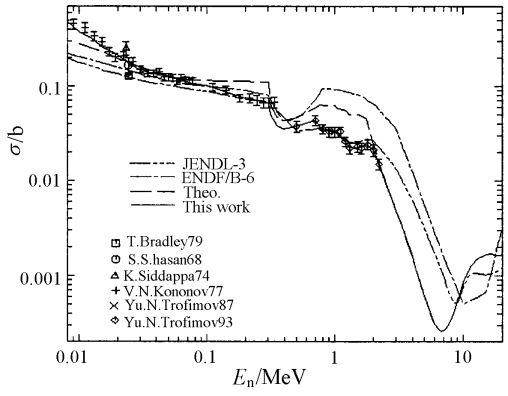

Fig. 4 Comparisons of the recommended (n,γ) cross sections in smooth and unresolved resonance regions with those in JENDL-3.2 and ENDF/B-6 libraries as well as the experimental data for ^{148}Nd

Fig. 5 shows the measured radiation capture cross sections of ^{150}Nd from 0.01 to 2.0 MeV. From Fig. 5 one can see that the experimental data by A. E. Johnsrud (1959) are too high and those by S. S. Hasan (1968) and B. V. Thirumala (1972) are too low. The measured data by V. N. Kononov (1977)[11], Yu. N. Trofimov (1987)[12], YU.N.Trofimov (1993)[13] were used for the data recommendation. Fig. 6 shows the comparisons of the recommended (n,γ) cross sections in smooth and unresolved resonance regions with those in JENDL-3.2 and ENDF/B-6 libraries as well as the experimental data for ^{150}Nd. Obviously the recommended data here are better in agreement with the experimental data than those in JENDL-3.2 and ENDF/B-6 libraries. The recommended data of this work are reasonable.

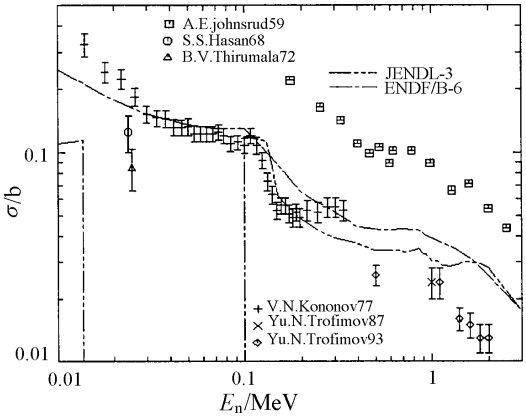

Fig. 5 Comparisons of the experimental data of (n,γ) cross sections for ^{150}Nd

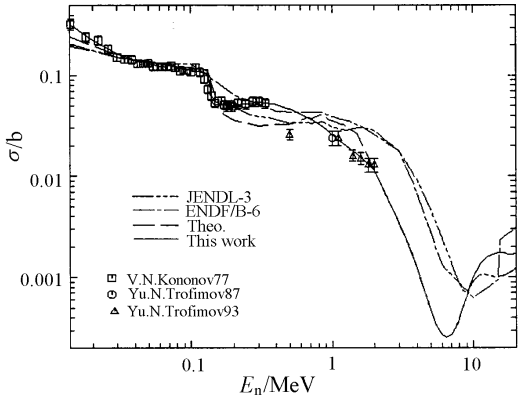

Fig. 6 Comparisons of the recommended (n,γ) cross sections with JENDL-3.2 and ENDF/B-6 as well as the experimental data for ^{150}Nd

2.2.3 Elastic Scattering Cross Sections

The recommended elastic scattering cross sections in smooth and unresolved resonance regions are compared with those in JENDL-3.2 and ENDF/B-6 libraries. The results of this work are reasonable.

2.2.4 Other Cross Sections

Fig. 7 shows that the calculated (n,2n) cross sections of ^{146}Nd are in good agreement with the experimental data and the calculated values are recommended. Fig. 8 shows the recommended (n,2n) cross sections of ^{142}Nd obtained on the basis of the experimental data and the calculated results. From the calculated (n, 3n) cross sections one can see that the (n, 3n) cross sections for different isotopes become larger as the isotope mass number increases.

The calculated (n,p) and (n,α) cross sections are in good agreement with the experimental data. Fig. 9 shows that the calculated (n,p) cross sections are in good agreement with the experimental data than those in JENDL-3.2 and ENDF/B-6 libraries. The calculated (n,p) and (n,α) cross sections for different isotopes become smaller as the isotope mass number increases and some experimental data are not suitable. The theoretical calculated cross sections for (n,3n), (n,p), (n,α), (n,t), (n,^{3}He), (n,n′p+pn') and (n,n′α+αn') reactions are recommended.

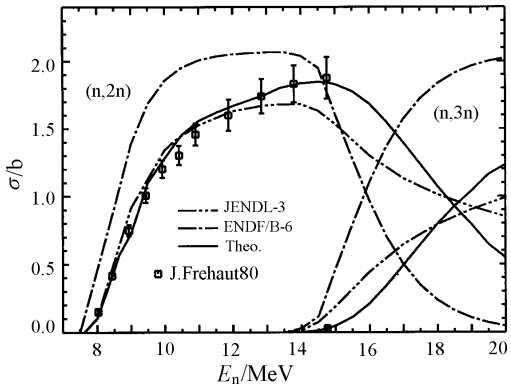

Fig.7 Comparison of (n,2n) and (n,3n) cross sections of ^{146}Nd between the calculated values and the experimental data

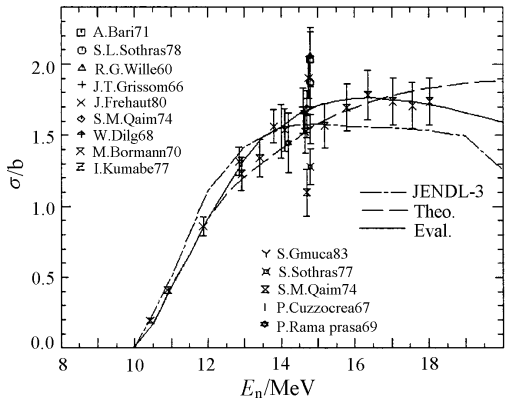

Fig.8 Comparison of (n,2n) cross sections of ^{142}Nd between the evaluated and the calculated values with the experimental data

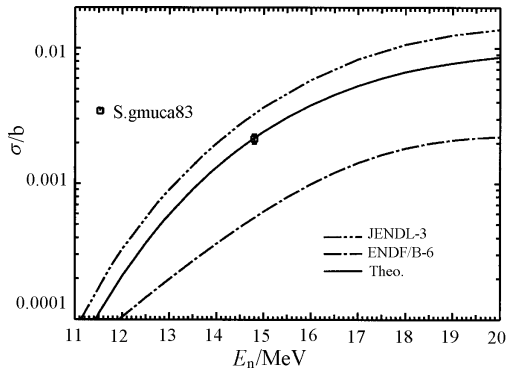

Fig.9 Comparison of (n,p) cross sections of ^{148}Nd between the calculated values and the experimental data

2.3 Secondary Neutron Angular Distributions

Figs.10~14 show that the calculated elastic scattering angular distributions at 2.5 and 7.0 MeV for ^{142,144,146,148,150}Nd are in good agreement with the experimental data. The theoretical calculated secondary neutron angular distributions for (n, el), (n, n'), (n,2n), (n,3n), (n,n'p+pn'), (n,n'α+αn') reactions are recommended.

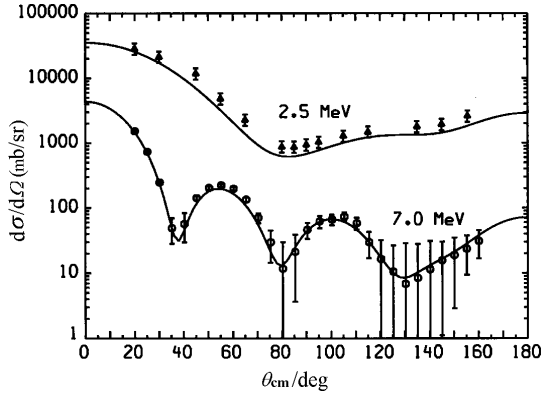

Fig.10 Comparison of neutron elastic scattering angular distributions of ^{142}Nd between the calculated values and the experimental data

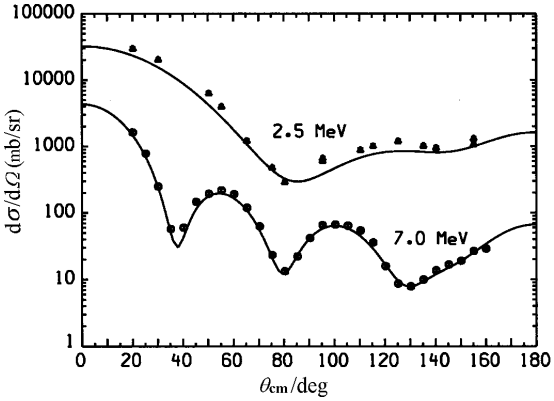

Fig.11 The same as Fig.10 but for ^{144}Nd

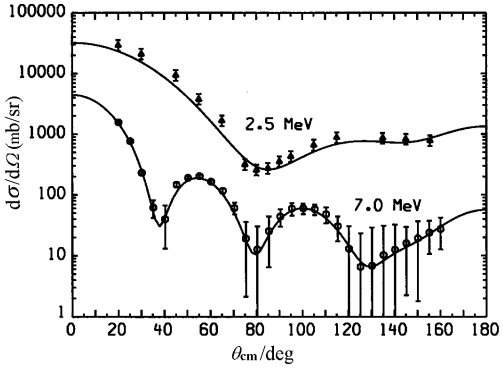

Fig. 12 The same as Fig.10 but for ^{146}Nd

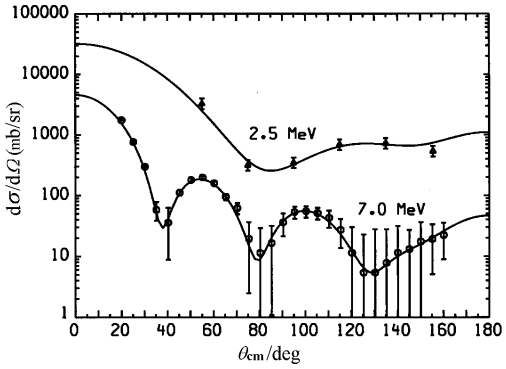

Fig. 13 The same as Fig.10 but for ^{148}Nd

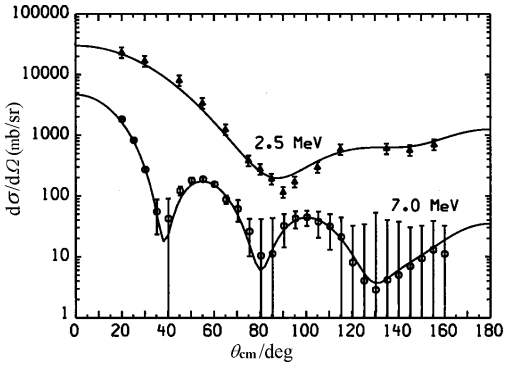

Fig. 14 The same as Fig.10 but for ^{150}Nd

2.4 Secondary Neutron Spectra

The theoretical calculated secondary neutron spectra for (n,n'), (n,2n), (n,3n), (n,n'p+pn'), (n,n'α+αn') reactions are recommended.

References

[1] SHEN Qingbiao, 'APMN-A Program for Automatically Searching a Set of Optimal Optical Potential Parameters in E≤300 MeV energy region', Commu. Nucl. Data Progress, Vol.25 (2001)

[2] P.D.Kunz, "Distorted Wave Code DWUCK4", University of Colorado, unpublished.

[3] ZHANG Jingshang, SUNF Code for Fast Neutron Data Calculations, Commu. Nucl. Data Progress, 17, 18 (1997).

[4] A. Gilbert and C. G. W. Cameron, Can. J. Phys., 43, 1446(1965).

[5] S.F.Mughabghab, M.Divadeenam, N.E.Holden, 'Neutron Cross Sections, Neutron Resonance Parameters and Thermal Cross Sections', Volume 1, Part A, NNDC, BNL, Upton, New York, Academic Press, 1981.

[6] R.E.Shamu, E.M.Bernstein, J.J.Ramirez, C.H.Lagrange, Phys.Rev. C22 (1980).1857.

[7] A.N.Djumin, A.I.Egorov, .N.Popova,V.A.Smolin, Izvestja Adad. Nauk SSSR, Ser. Fiz., Vol.37 (1973) 1019.

[8] T.Bradley et al., C. 79KNOX, 1979, p.344.

[9] S.S.Hasan et al., J.NC/B, 58(1968)402.

[10] K.Siddappa, J.AP, 83(1974)355.

[11] V.N,Kononov et al.,R.YK-22,1977,p.29.

[12] YU.N.Trofimov, C. 87KIEV, 3(1987)331.

[13] YU.N.Trofimov, J.YK, 1993,(1),p.17.

Calculation and Recommendation of n+^{136,138,140,142,Nat}Ce Reactions

Han Yinlu Shen Qingbiao Yu Baosheng Zhang Jingshang

China Nuclear Data Center, CIAE, Beijing

【**abstract**】*Based on experimental data, all reaction cross sections, elastic scattering angular distributions, double differential cross sections, γ-ray production cross section and γ-ray production energy spectrum of n+^{136,138,140,142,nat}Ce were calculated and recommended. The calculated results were compared with available experimental data and other evaluated data from ENDF/B-6 and JENDL-3 libraries.*

Introduction

Natural Ce consist of four isotopes, i.e. ^{136}Ce (0.19%), ^{138}Ce (0.25%), ^{140}Ce (88.48%) and ^{142}Ce (11.08%). Because some file are scare in present evaluated nuclear data libraries, it is necessary to calculate all cross sections.

1 Collection and Selection of Experimental Data

The experimental data of total cross section are given in Refs. [1~10] for natural Ce at incident neutron energies region 0.01~20 MeV, they are in basically agreement with each other. The experimental data of elastic scattering cross sections and elastic scattering angular distribution are given in Refs. [11~15], respectively. The experimental data of total cross section for ^{140,142}Ce are also given in Ref. [1] at incident neutron energies 2.0~57.0 MeV. The experimental data of total cross section for ^{nat}Ce are in agreement with those for ^{140,142}Ce. While for energy E_n<0.2 MeV, the experimental data of total cross section for ^{140}Ce were given in Ref. [16], and the data show resonance structure. There is a experimental datum of nonelastic cross section taken from Ref. [17]. All of above experimental data were used to guide adjusting optical potential parameters.

The experimental data of (n,γ) reaction cross section were given in Refs. [18,19] for ^{140}Ce, respectively. The experimental data of ^{142}Ce (n,γ) reaction cross section were given in Refs. [18~23]. Since the experimental data taken from Refs. [21,22] are larger than those taken from other Refs. for ^{142}Ce (n,γ) reaction cross section, the experimental data taken from Refs. [21,22] were not considered in our calculation. The experimental data of ^{nat}Ce (n,γ) reaction cross section were given in Refs. [24~26], the experimental data consist with each other.

The experimental data of (n,p) reaction cross section were given in Refs. [27~34] for ^{140}Ce, respectively. The experimental data Refs. [27,28, 30~32] consist with each other, and were considered in our calculation. The experimental data of ^{142}Ce(n,p) reaction cross section were taken from Refs. [29,32~37], and those taken from Refs. [29,32,37] were used to guide theoretically calculation. The experimental data of ^{140m}Ce(n,α) reaction cross section were given and were used as reference in the theoretically calculation. The experimental data for ^{142}Ce (n,α) reaction cross section were given in Refs. [28~30,33,34,38,39], and the experimental data taken from Ref. [30] were used to guide theoretically calculation.

The experimental data of ^{136}Ce(n,2n) reaction cross section are given in Refs. [27,28,35,40,41], respectively. The experimental data of ^{138}Ce (n,2n) reaction cross section were also given in Ref. [41]. The experimental data for ^{136,138}Ce (n,2n) reaction cross section were used to guide theoretically calculation. The experimental data of ^{140}Ce (n,2n) reaction cross section were given in Refs. [27,28,40~50], respectively. The experimental data taken from Refs. [27,44,49] were used to guide our calculation. The experimental data of ^{142}Ce (n,2n) reaction cross section were given in Refs. [27~29,32,37,40,41,43~46,48], respectively. The experimental data taken from Refs. [27,44,46] were used to guide our calculation.

2 Codes and Parameters

The code APOM[51] was used to obtain a set of optimum neutron optical potential parameters of Ce, by which the best neutron optical potential parameters can be searched automatically for fitting relevant experimental total, nonelastic scattering cross section, elastic scattering cross section and elastic scattering angular distributions. Because there are no experimental data of elastic scattering cross section and elastic scattering angular distribution for isotope, the experimental data of ^{nat}Ce were used to obtain a set of optimum neutron optical potential parameters of ^{140}Ce. Then, this set of optimum neutron optical potential parameters were used in n+^{136,138,140,142,nat}Ce reaction as fellows:

$$V=54.1110-0.3523E-0.0003763E^2-24.0(N-Z)/A$$
$$W_s=9.1953+0.1169E-12.0(N-Z)/A$$
$$W_v=-0.6170+0.1798E-0.001763E^2$$
$$U_{so}=6.2$$
$$r_r=1.1945,\ r_s=1.2931,\ r_v=1.5068,\ r_{so}=1.1945$$
$$a_r=0.7908,\ a_s=0.3330,\ a_v=0.5128,\ a_{so}=0.7908$$

Using this set of neutron optical potential parameters, adjusting charged particle optical potential parameters as well as giant dipole resonance parameters and level density parameters, all reaction cross sections, angular distributions, double differential cross sections, γ-ray production cross sections and γ-ray production energy spectrum were calculated for n+ ^{136,138,140,142,nat}Ce in incident neutron energies below 20 MeV by code NUNF[52]. The direct inelastic scattering data were calculated by the code DWUCK4[53] . The exciton model parameter K was 1500 MeV^3 for all isotopes.

3 Theoretical Results and Recommendation

The comparison of calculated results of neutron total, elastic scattering cross sections and elastic scattering angular distribution with experimental data for n+^{140,142,nat}Ce reaction are given in Figs.1~5, respectively. The calculated results of total cross sections and elastic scattering angular distribution are in good agreement with experimental data, while the calculated results of elastic scattering cross section pass through existing experimental data.

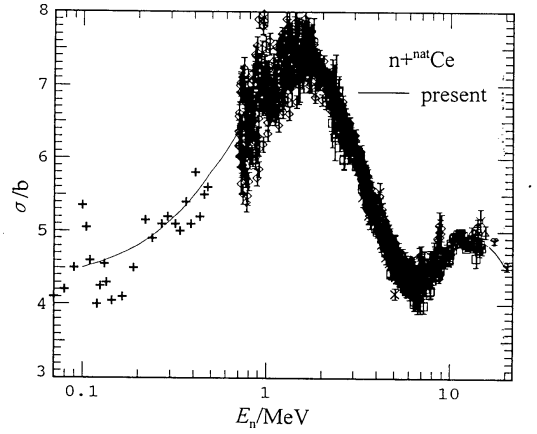

Fig. 1 The total cross section of n+^{nat}Ce reaction

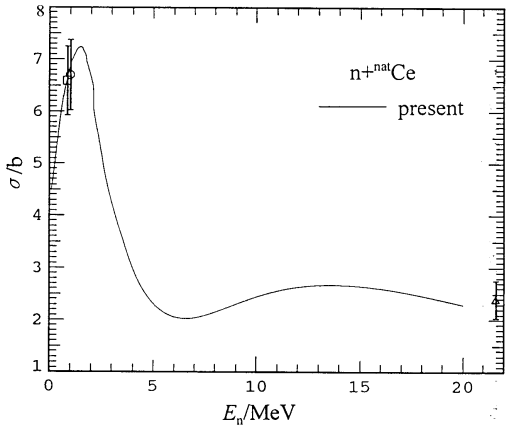

Fig. 2 The elastic scattering cross section of n+^{nat}Ce reaction

The comparison of calculated results of (n,γ) reaction cross section with experimental data for ^{140,142,nat}Ce are given in Figs. 6~8, respectively. The calculated results of ^{140,142}Ce(n,γ) reaction cross sections are in good agreement with experimental data in energy region 0.1~2 MeV, while for $E_n \geq 2$ MeV, it seems the present results is reasonable. The calculated results for ^{nat}Ce(n,γ) reaction cross sections are in good agreement with experimental data in energy region 0.2~15 MeV.

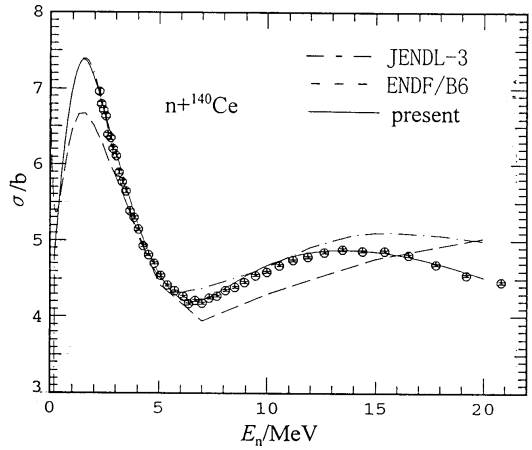

Fig. 3 The total cross section of n+^{140}Ce reaction

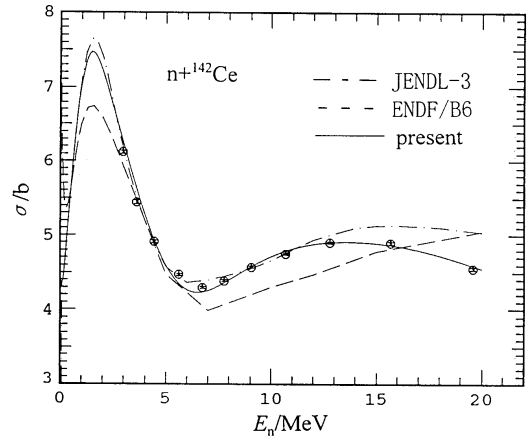

Fig. 4 The total cross section of n+^{142}Ce reaction

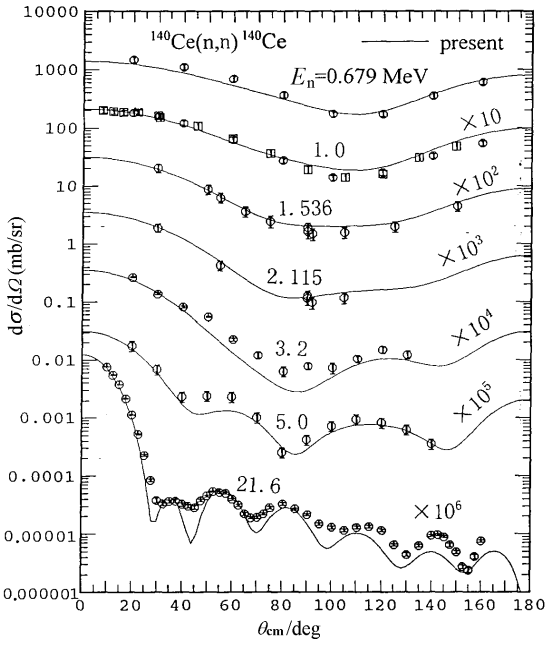

Fig. 5 The elastic scattering angular distribution of n+^{140}Ce reaction

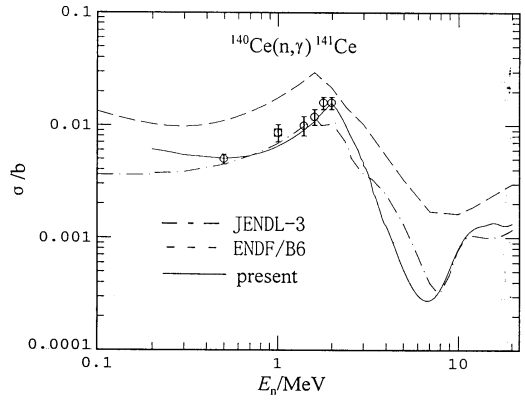

Fig. 6 The cross section of ^{140}Ce(n,γ) reaction

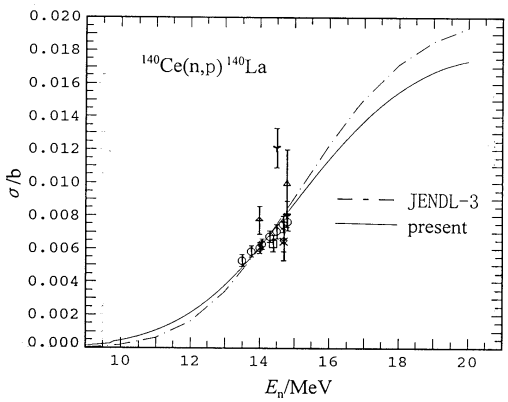

Fig. 9 The cross section of ^{140}Ce(n,p) reaction

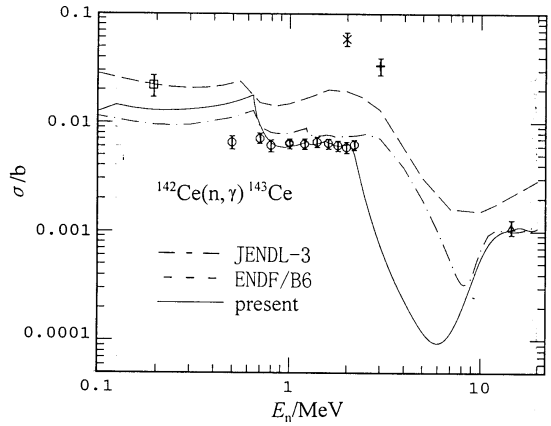

Fig. 7 The cross section of ^{142}Ce (n,γ) reaction

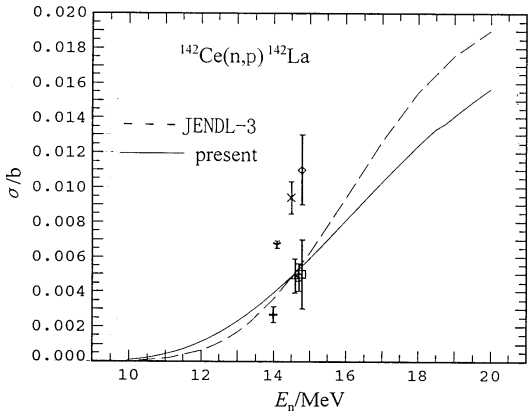

Fig. 10 The cross section of ^{142}Ce (n,p) reaction

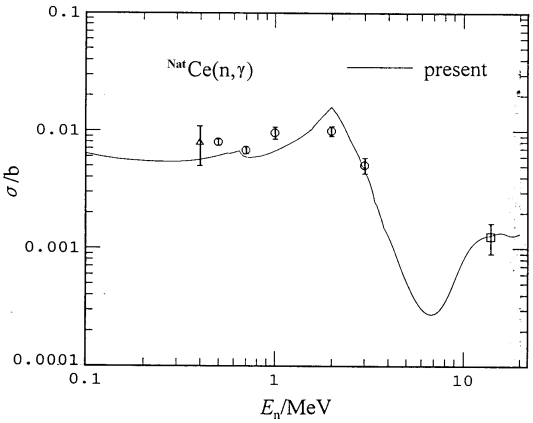

Fig. 8 The cross section of ^{Nat}Ce (n,γ) reaction

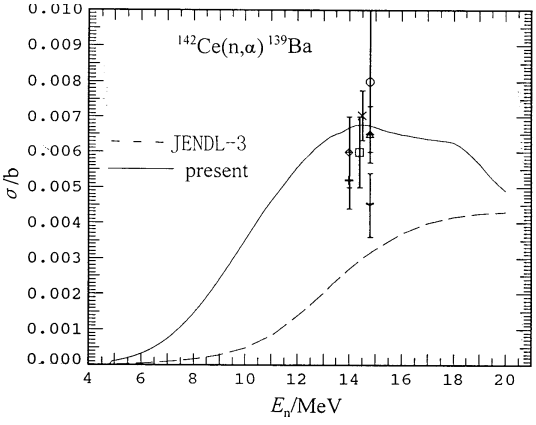

Fig. 11 The cross section of ^{142}Ce (n,α) reaction

In Figs. 9 and 10, the comparison of calculated results of ^{140,142}Ce(n,p) reaction cross sections with experimental data are given, respectively. The calculated curves pass through the experimental data within error bars. The comparison of calculated results and experimental data for ^{142}Ce(n,α) reaction cross sections are given in Fig.11.

The comparison of calculated results with experimental data for ^{136,138}Ce(n,2n) reaction cross sections are given in Figs.12 and 13, respectively. The calculated curves pass through the experimental data within error bars. The comparison of calculated results with experimental data for ^{140,142}Ce(n,2n) reaction cross sections are given in Figs.14 and 15,

respectively. The calculated results are in good agreement with the experimental data.

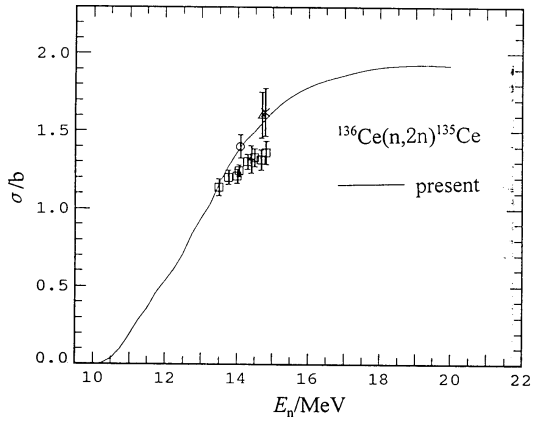

Fig. 12 The cross section of ^{136}Ce (n,2n) reaction

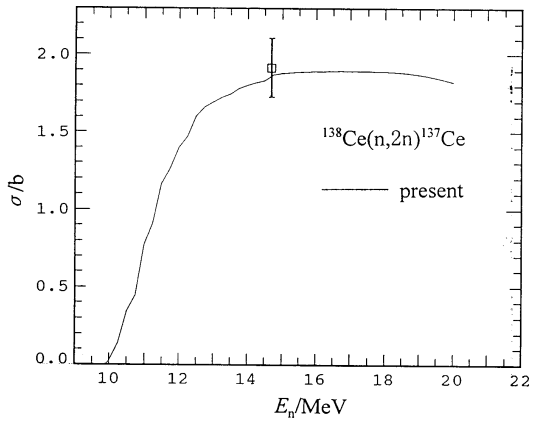

Fig. 13 The cross section of ^{138}Ce(n,2n) reaction

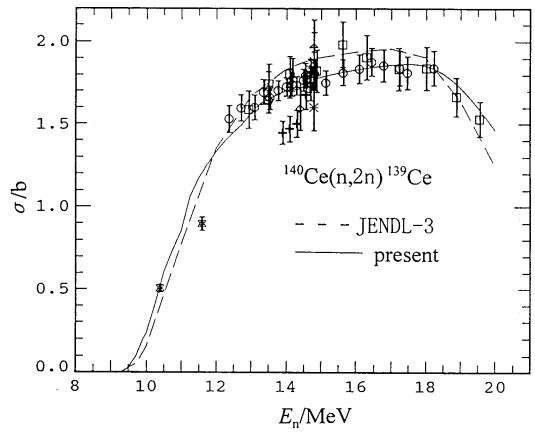

Fig. 14 The cross section of ^{140}Ce (n,2n) reaction

As example, the energy spectrum, γ-ray production cross section and γ-ray production energy spectrum for n+^{140}Ce reaction are given in Figs.16~19, respectively. The calculated results are reasonable.

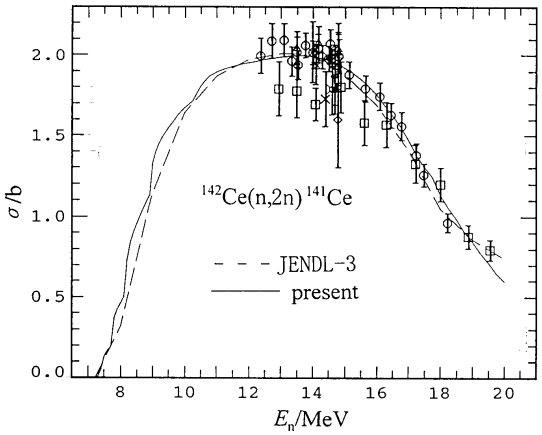

Fig. 15 The cross section of ^{142}Ce(n,2n) reaction

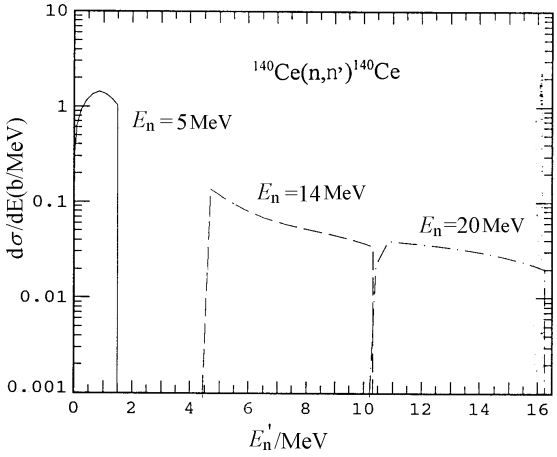

Fig. 16 The energy spectrum of ^{140}Ce (n,n') reaction

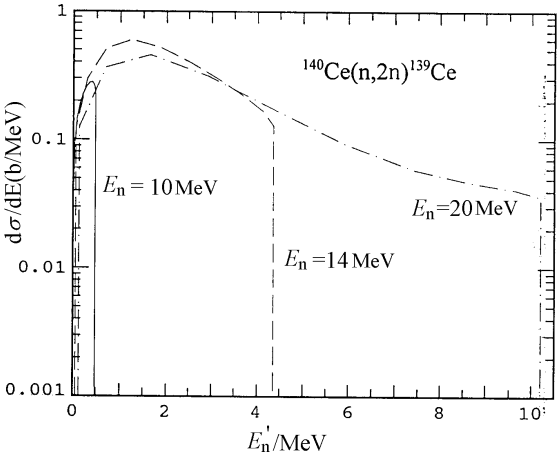

Fig. 17 The energy spectrum of ^{140}Ce (n,2n) reaction

Because theoretical calculated results are reasonable from above analysis, the calculated results are recommended in the energy range from 0.2 to 20 MeV, and those at energies from 1.0^{-5} to 0.2 MeV, were taken from JENDL-3.

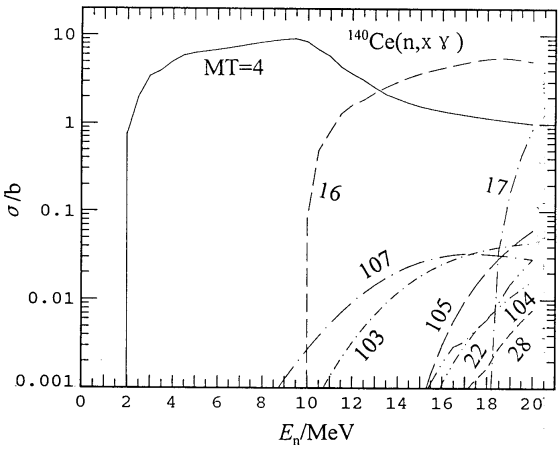

Fig. 18 The γ–ray production cross section of n+^{140}Ce reaction

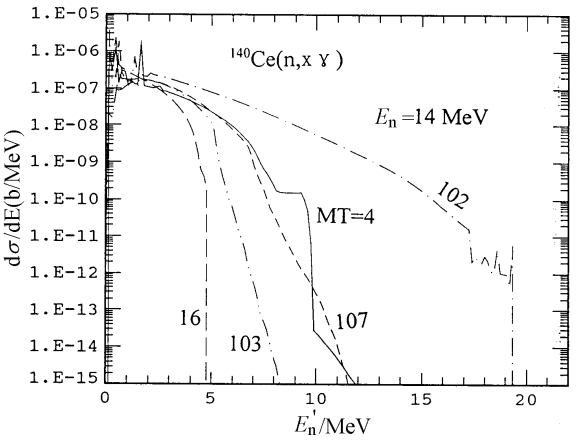

Fig. 19 The γ–ray production energy spectrum of n+^{140}Ce reaction

References

[1] H.S. Camarda, et al., Phys. Rev., C29,2106(1984).

[2] D.G. Foster JR, et al., Phys. Rev., C3,576(1971).

[3] J.H. Coon, et al., Phys. Rev., 88,562(1952).

[4] J.M. Peterson, et al., Phys. Rev., 120,521(1960).

[5] J.T. Wells, et al., Phys. Rev., 131,1644(1963).

[6] J.P. Conner, Phys. Rev., 109,1268(1958).

[7] D.W. Miller, et al., Phys. Rev., 88,83(1952).

[8] F. Manero, Anales de Fisica y Quimica, 64,63(1968).

[9] J.D. Kellie, et al., J. Phys., A7,1758(1974).

[10] I. Angell, et al., Acta Phys. Hungaricae, 30,115(1971).

[11] M. Ohkub, Conf. on Nucl. Data for Basic & Applied Sci., Santa Fe,1,1623,1985.

[12] A. Chatterjee, et al., Phys. Rev., 161,1181(1967).

[13] S.A. Cox, ANL-7210,3,1966.

[14] M. Walt, et al., Phys. Rev., 93,1062(1954).

[15] S.C. Buccino, et al., Z. Phys., 196,103(1966).

[16] R.L. Becker, et al., Nucl. Phys., 89,154(1966).

[17] N. Olsson, et al., Nucl. Phys., A472,237(1987).

[18] YU.N.Trofimov, All-Union Conf. on Neutron Phys., Kiev, 3,331,1987.

[19] YU.N.Trofimov, Voprocy At. Nauki I Tekhn., Yadernaye Konstanty, 4,36(1989).

[20] O. Schwerer, et al., Nucl. Phys., A264,105(1976).

[21] G. Peto, et al., J. Nucl. Ener., 21,797(1967).

[22] YU.N. Trofimov, Voprocy At. Nauki I Tekhn., Yadernaye Konstanty, 4(1987).

[23] W.S. Lyon, et al., Phys. Rev., 114,1619(1959).

[24] B.C.Diven, et al., Phys. Rev., 120,556(1960).

[25] F. Rigaud, et al., Nucl. Phys., A176,545(1971).

[26] J. Voignier, et al., Nucl. Sci. Eng., 93,43(1986).

[27] TENGDan, et al., Chinese J. Nucl. Phys., 7,307(1985).

[28] W.D. LU, et al., Phys. Rev., C1,350(1970).

[29] R.G. Wille, et al., Phys. Rev., 118,242(1960).

[30] A. Bari, J. of Radioanalytical Chemistry, 75,189(1982).

[31] E. Havlik, Acta Phys. Austriaca, 34,209(1971).

[32] S.M. Qaim, Phys. Rev. Lett., 25,335(1976).

[33] P. Cuzzocrea, et al., Nuovo Cimento, B52,476(1967).

[34] R.F. Coleman, et al., Proc. of the Phys. Soc., 73,215(1959).

[35] A.A.Filatenkov, et al., 97TRIEST,1,598,1997.

[36] R. Prasao, et al., Nuovo Cimento, A3,467(1971).

[37] O. Schwerer, et al.,Anz. Oesterr. Akad. Wiss Math-Naturwiss. KI.,113,153(1976).

[38] L. Chaturveroi, et al., INDC(SEC)-61,123(1977).

[39] V.N.Levkovskiy, et al., Yadernaya Fizika, 8,7(1968).

[40] A. Bari, Dissertation Abstr., B32,5091(1972).

[41] S.M.Qaim, Nucl. Phys., A224,319(1974).

[42] S. Sothras, Dissertation Abstr., B38,280(1978).

[43] W. Dilg, et al., Nucl. Phys., A118,9(1968).

[44] M. Bormann, et al., Nucl. Phys., A115,309(1968).

[45] J.Csikai, et al., Acta Phys. Hungaricae, 24,233(1968).

[46] KONG Xiangzhong, et al., INDC(CPR)-036/L,5,1995

[47] N.I. Molla, et al., 97TRIEST,1,517,1997.

[48] A.A.Filatenkov, et al., 97TRIEST,1,598,1997.

[49] ZHAO Wenrong, et al., Commu. Nucl. Data Prog.,19,7(1998).

[50] S.L. Sothras, et al., J. of Inorganic and Nucl. Chemistry, 40,585(1978).

[51] SHEN Qingbiao, Commun. Nucl. Data Prog., 7, 43 (1992)

[52] ZHANG Jingshang, Private Commun., 1998

[53] P.D. Kunz, DWUCK4 Code.

n+ $^{130,132,134\sim138}$Ba Nuclear Data Calculations

K. Kurban[1,2] ZHANG Zhengjun[2] SUN Xiuquan[2]
HAN Yinlu[3] SHEN Qingbiao[3]
1 Depart. of Physics, Xinjiang Normal University, Xinjiang
2 Depart. of Physics, Northwest University, Xian
3 China Nuclear Data Center, CIAE, Beijing

【abstract】 *According to the available neutron experimental data of $^{130,132,134\sim138}$Ba, a set of neutron optical potential parameters for all isotopes of Ba in the energy range from 0.01 to 20MeV was obtained. Based on this set of parameters the cross sections of all channels and the elastic scattering angular distributions of n+$^{130,132,134\sim138}$Ba were calculated. The theoretical results agree with the experimental data well, and the results were given in B6 format.*

1 The Experimental Data and Calculations

The natural element Ba consists mainly of ^{130}Ba (0.106%), ^{132}Ba (0.101%), ^{134}Ba (2.417%), ^{135}Ba (6.592%), ^{136}Ba (7.854%), ^{137}Ba (11.23%) and ^{138}Ba (71.70%). There are a lot of neutron experimental total, elastic scattering cross section and elastic scattering angular distribution data for natural Ba. Channels of ^{130}Ba(n,γ), ^{134}Ba(n,γ), ^{135}Ba(n,γ), ^{136}Ba(n,γ), ^{137}Ba(n,γ) and ^{138}Ba(n,γ) are with a few experimental data respectively, which present necessary references for adjusting model parameters in the calculation. There are also some experimental data of channels ^{134}Ba(n,p), ^{136}Ba(n,p), ^{137}Ba(n,p), ^{138}Ba(n,p) and ^{138}Ba(n,α). All experimental data were retrieved from the EXFOR library and selected before calculating.

Because ^{138}Ba is with an abundance of 71.70%, the relevant experimental data of natural Ba are used in the code APOM94[1], a set of neutron optimum optical potential parameters for ^{138}Ba fitting in energy range from 0.01 to 20. MeV were obtained and this set of parameters were used in calculations of neutron induced reactions on $^{130,132,134\sim138}$Ba. The code DWUCK4[2] was used to give neutron direct inelastic scattering cross section. The code SUNF[3] given out the final theoretical results in B6 format.

2 Important Parameters in Calculations

The neutron optimum optical potential parameters for $^{130,132,134\sim138}$Ba are given as follows:

$$V = 52.6533-0.31709E_n-0.00361E_n^2-24.0(N-Z)/A,$$
$$W_s = \max\{0.0, 10.0931+0.47731E_n-12.0(N-Z)/A\},$$
$$W_v = \max\{0.0, -1.5615+0.21883E_n-0.07471E_n^2\},$$
$$U_{so}=6.2,$$
$$R_r=1.19482, R_s=1.34769, R_v=1.31037, R_{so}=1.19482,$$
$$A_r=0.85731, A_s=0.31208, A_v=0.58002, A_{so}=0.85731,$$

Where E_n is the incident neutron energy, Z, N and A are the number of proton, neutron and mass of the target nucleus, respectively.

3 Analysis of the Theoretical Results

Fig. 1 shows the comparison for total cross sections between theoretical curve of n+$^{130,132,134\sim138}$Ba and experimental data of the natural Ba. The theoretical values are in good agreement with the experimental data. Fig. 2 shows the theoretical curves of elastic scattering cross sections of n+$^{130,132,134\sim138}$ Ba and the relevant experimental data of natural Ba. Fig. 3 shows the theoretical elastic scattering angular distribution curves of n+^{138} Ba and the corresponding experimental data of natural Ba at neutron incident energy E_n=0.5, 0.65, 0.80, 1.0, 3.20 and 4.10 MeV. Figs. 1~3 indicate that the neutron optical potential parameters are satisfied. Figs. 4a~b show the theoretical results of ^{130,132}Ba(n,γ) and ^{134}Ba(n,γ) cross sections reproduce the relevant experimental data well, respectively.

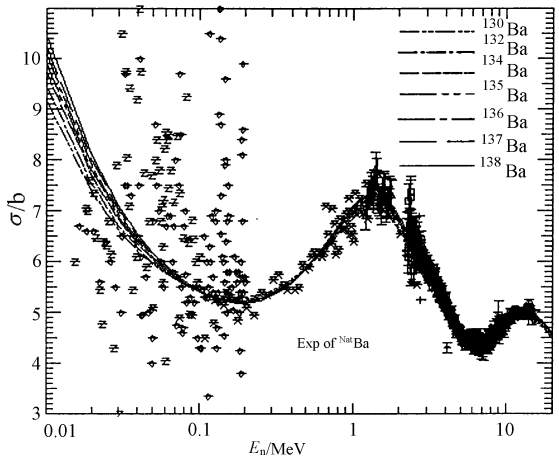

Fig. 1 Total cross sections

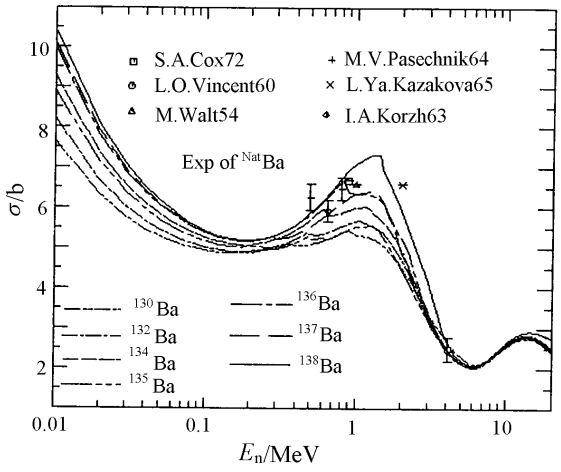

Fig. 2 Elastic scattering cross sections

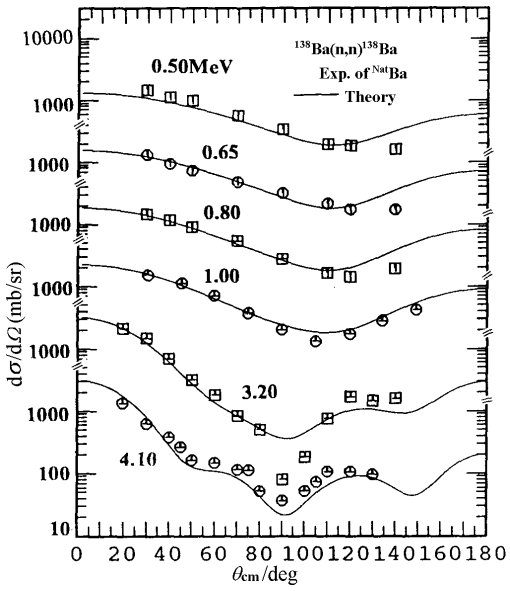

Fig. 3 Elastic scattering angular distributions

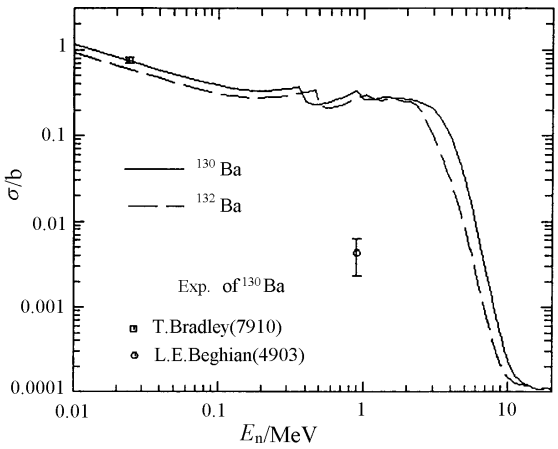

Fig. 4a Cross sections of ^{130,132}Ba(n,γ) reaction

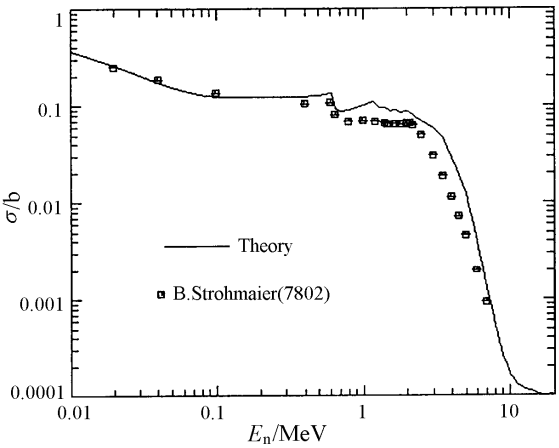

Fig. 4b Cross sections of ^{134}Ba(n,γ) reaction

From Figs.5a~b it can be seen that the theoretical results of ^{134}Ba(n,p) and ^{138}Ba(n,p) cross sections agree with the relevant experimental data well, respectively.

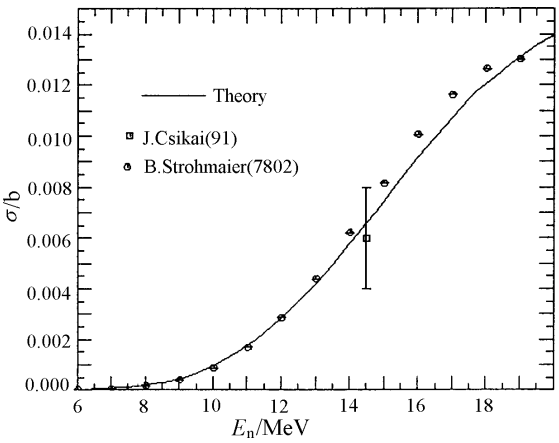

Fig. 5a Cross sections of ^{134}Ba(n,p) reaction

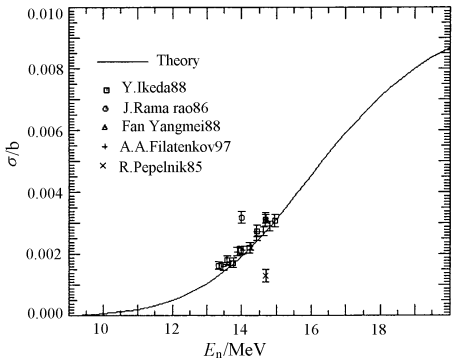

Fig. 5b Cross sections of ^{138}Ba(n,p) reaction

References

[1] SHEN Qingbiao, Commun. Nucl. Data Progress, 7, 43(1992)

[2] P.D.Kunz, Distorted Wave Code DWUCK4, University of Colorado, Unpublished.

[3] ZHANG Jingshang SUNF–a code for calculations of fission product nucei based on unified mode, CNDC, CIAE, Unpublished.

Calculations for n+ ^{93,95}Nb in Energy Range from 0.01 to 20 MeV

RONG Jian [1] ZHANG Zhengjun[2] HAN Yinlu [1] SHEN Qingbiao[1] SUN Xiuquan[2]

1 China Nuclear Data Center, CIAE, Beijing

2 Depart. of Physics, Northwest University, Shannxi,

Using the codes APOM94[1], DWUCK4 [2] and SUNF[3] all reaction data for n+^{93,95}Nb were calculated. The final theoretical results were given in B6 format.

The neutron optical potential parameters for ^{93}Nb and ^{95}Nb are given as follows:

V=54.86366−0.41574E_n−0.00416E_n^2−24.0(N−Z)/A,

W_s = max {0.0, 8.85209+0.58478E_n−12.0(N−Z)/A},

W_v = max {0.0,−1.5615+0.21883E_n−0.07471E_n^2},

U_{so}=6.2,

R_r=1.19115,R_s=1.37965, R_v=1.31036, R_{so}=1.19115,

A_r=0.77598,A_s=0.35701, A_v=0.58002, A_{so}=0.77598,

Where E_n is the incident neutron energy, Z, N and A are the numbers of proton, neutron and mass of the target nucleus, respectively

Fig.1 shows the comparisons for total cross sections between theoretical results of $^{93, 95}$Nb and experimental data. The theoretical values are in good agreement with the experimental data. Fig. 2 gives out the elastic angular scattering distributions of ^{93}Nb at E_n=1.0, 4.0, 7.0, 9.94, 14.7, 16.9, 20.0 MeV. Fig. 3 presents the comparisons between theoretical cross sections of ^{93,95}Nb(n,2n) cross section and the measured data of ^{93}Nb. Fig. 4 is theoretical results and the relevant experimental data of ^{93,95}Nb(n,γ) reaction. The comparisons and analysis of other reaction channels such as ^{93,95}Nb(n,el), ^{93,95}Nb (n, non), ^{93,95}Nb (n,inl), ^{93,95}Nb (n,3n), ^{93,95}Nb (n,α) and ^{93,95}Nb(n,p) are not given here, and the calculated results reproduce experimental data perfectly. For some channels without measured data the calculated results are reasonable as well.

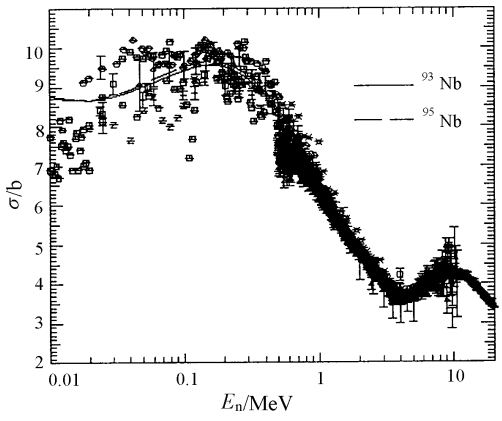

Fig. 1 Total cross sections of n+^{93,95}Nb

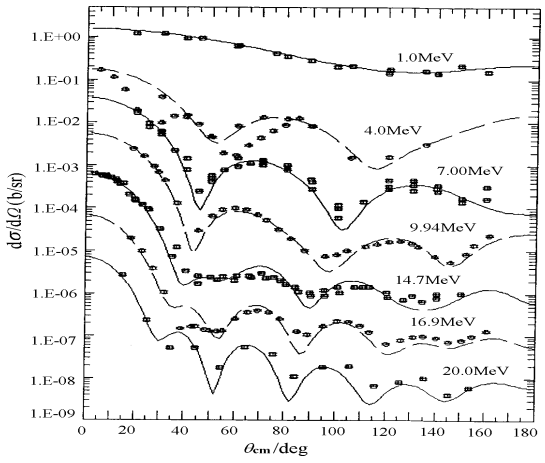

Fig.2 Elastic angular scattering distributions

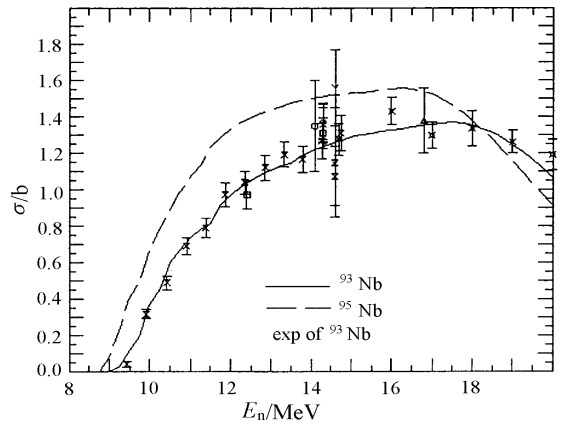

Fig.3 ^{93,95}Nb(n, 2n) cross sections

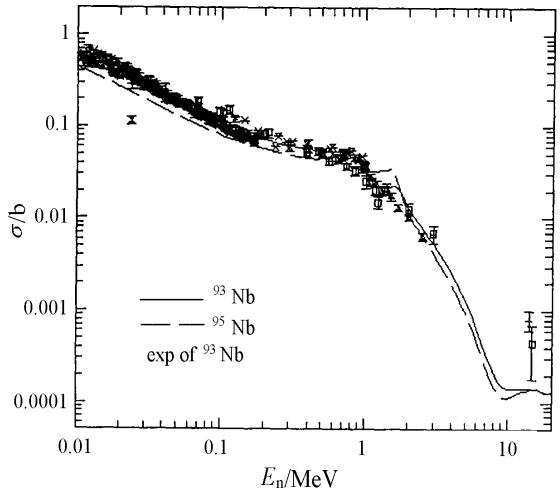

Fig.4 ^{93,95}Nb(n, γ) cross sections

References

[1] SHEN Qingbiao, Commun. Nucl. Data Progress, 7, 43(1992)

[2] P.D.Kunz, Distorted Wave Code DWUCK4, University of Colorado, Unpublished.

[3] ZHANG Jingshang. SUNF–a code for calculations of fission product nuclei based on unified mode, CNDC, CIAE, unpublished.

Calculation and Recommendation of n+^{175,176,Nat}Lu Reaction

HAN Yinlu SHEN Qingbiao YU Baosheng ZHANG Jingshang

China Nuclear Data Center, CIAE, Beijing

【**abstract**】*Based on the experimental data of total, elastic scattering cross sections and elastic scattering angular distribution of natural Hf as well as the experimental data of total cross sections of natural Lu, a set of neutron optical potential parameter was obtained. The cross sections, angular distribution, double differential cross sections, γ-ray production cross sections and γ-ray production energy spectrum were calculated for n+ ^{175,176,Nat}Lu at incident neutron energies below 20 MeV. The calculated results were compared with existing experimental data and the evaluated data from ENDF/B-6.*

Introduction

Natural Lu consists of two isotopes, i.e. ^{175}Lu (97.16%) and ^{176}Lu (2.08%). The experimental data for these nuclides are scare. It is necessary to calculate all cross sections.

1 Collection and Selection of Experimental Data

The experimental data of total cross section are given in Ref.[1] for natural Lu in the incident neutron energies region 2.1~14 MeV.

The experimental data of (n,γ) cross section are given in Refs.[2~6] for ^{175}Lu. The experimental data of Refs.[2~5] consist with each other. While the data of Ref.[6] are smaller and were not considered in our calculation. The experimental data of ^{176}Lu (n,γ) cross section are given in Refs.[3,7]. The data of Ref.[3] were used to guide theoretical calculation. The experimental data of ^{nat}Lu (n,γ) cross section are given in Refs.[8~11]. The data of Refs.[9,11] consist with the data of ^{175}Lu(n,γ) and were used to guide theoretical calculation.

The (n,p) cross sections is given in Refs.[12~14] for ^{175}Lu. The the data of ^{176}Lu (n,α) reaction cross sections were given in Ref.[13] . The data of Refs.[13,14] were used to guide theoretical calculation.

The experimental data of ^{175}Lu(n,2n) reaction cross sections are given in Refs.[15~22], and the data were analyzed in Ref.[22]. The data taken from Refs.[17,22] were used to guide theoretical calculation. The experimental data of ^{175}Lu (n,3n) cross sections were given in Refs.[16,17]. All experimental data were taken from EXFOR library.

2 Codes and Parameters

The code APOM[23] , was used to obtain a set of optimum neutron optical potential parameters for n+^{175,176}Lu. Because there are no experimental data for its isotopes, the experimental data of total cross section for ^{nat}Lu and the experimental data of total, elastic scattering cross sections and angular distribution of ^{nat}Hf, neighbors nuclei of Lu, were used to obtain the optimum neutron optical potential parameters. The optimum neutron optical potential parameters obtained for n+^{175,176}Lu reaction are:

V=51.4429+0.1546E−0.0206E^2−24.0(N−Z)/A

W_s=9.1002−0.3507E−12.0(N−Z)/A

W_v=−1.2155+0.1940E+0.016E^2

U_{so}=6.2

r_r=1.1906, r_s=1.3203, r_v=1.5881, r_{so}=1.1906

a_r=0.5789, a_s=0.6687, a_v=0.3615, a_{so}=0.5789

Using this set of neutron optical potential parameters, adjusting charged particle optical potential parameters as well as giant dipole resonance parameters and level density parameters, all neutron and γ-ray production data were calculated at in the incident neutron energies below 20 MeV with code NUNF[24]. The direct inelastic scattering data were calculated with the code DWUCK4[25] . The exciton model parameter K was as 800 MeV^3 for all isotopes.

3 Calculation Results and Analysis

The comparison of calculated total cross sections with experimental data for n+^{nat}Lu reaction are given in Fig.1. The calculated ones are in good agreement with experimental data for energy 2<E_n<15 MeV, while for other energy range, the calculated results are reasonable, since the property of neighbors nuclei of Lu are considered. Based on the fitting, a set of neutron optical potential parameters was determined for this work.

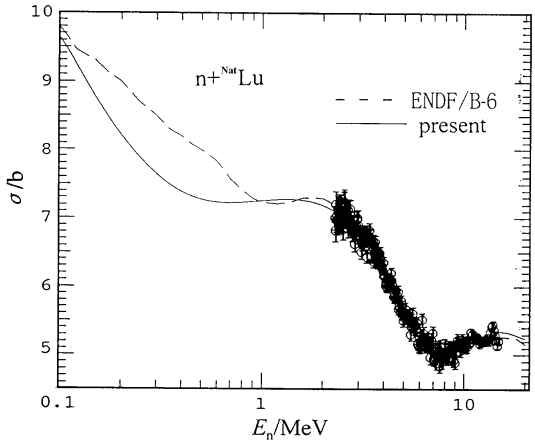

Fig.1 The total cross section of n+^{nat}Lu reaction

The comparison of calculated (n,γ) reaction cross sections with experimental data for ^{175,176,,Nat}Lu are given in Figs.2~4, respectively. For ^{175,176}Lu the calculated results are in good agreement with experimental data in energy region 0.01~2 MeV, while for E_n≥2 MeV, it seems the present results is reasonable. For ^{nat}Lu the calculated results are in good agreement with experimental data in energy region 0.01~3 MeV.

In Figs.5,6 the comparison of calculated results of ^{175}Lu(n,p), ^{176}Lu(n,α) cross sections with experimental data are given respectively. The calculated curves pass through the experimental data within error bars.

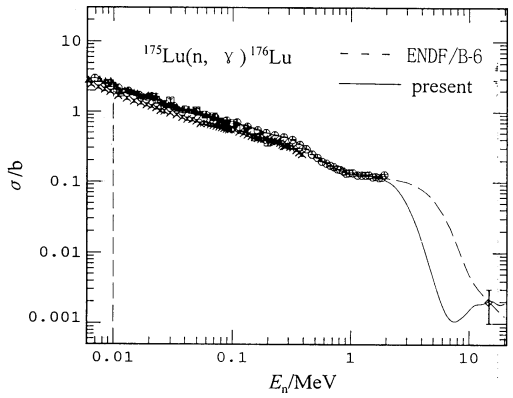

Fig.2 The cross section of ^{175}Lu (n,γ) reaction

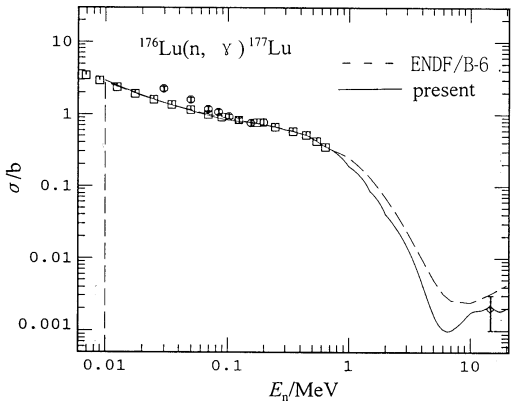

Fig.3 The cross section of ^{176}Lu (n,γ) reaction

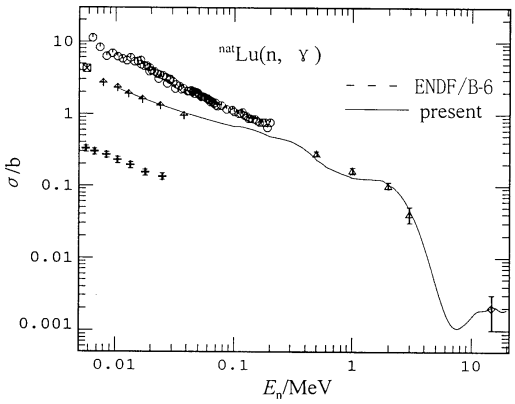

Fig.4 The cross section of ^{nat}Lu (n,γ) reaction

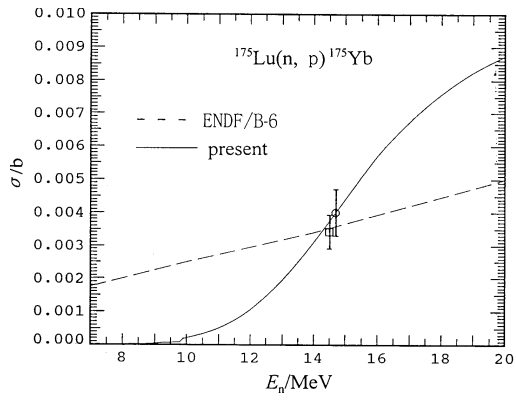

Fig.5 The cross section of ^{175}Lu (n,p) reaction

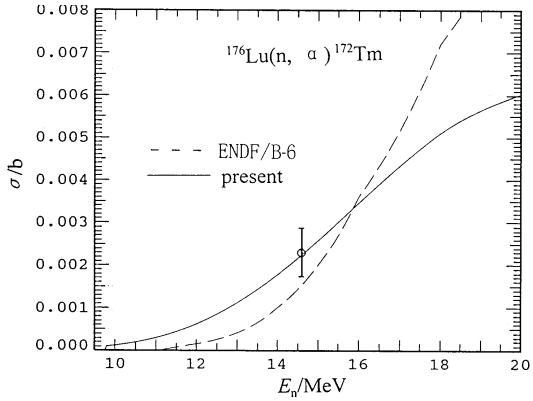

Fig.6 The cross section of ^{176}Lu (n,α) reaction

The comparison of calculated results with experimental data for ^{175}Lu(n,2n),(n,3n) reaction cross sections are given in Figs.7, 8. The calculated results are in good agreement with the experimental data.

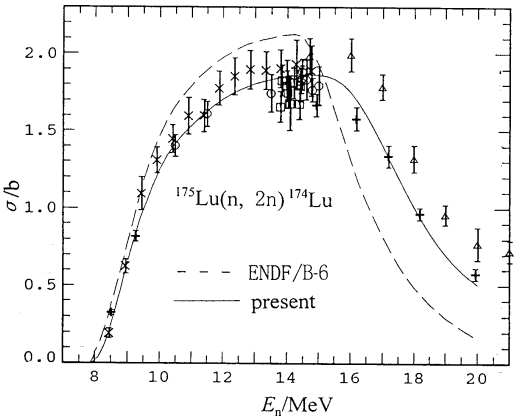

Fig.7 The cross section of ^{175}Lu (n,2n) reaction

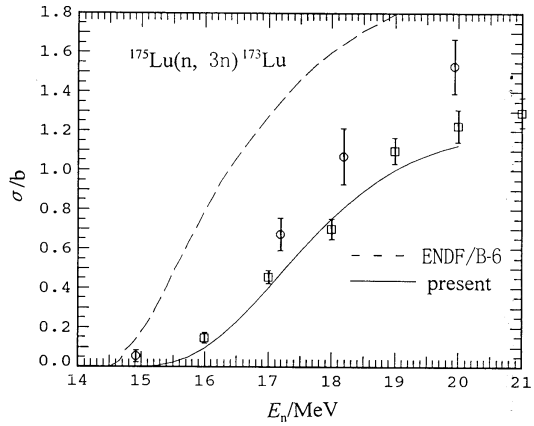

Fig.8 The cross section of ^{175}Hf (n,3n) reaction

As examples, the energy spectrum, γ-ray production cross section and γ-ray production energy spectrum for n+^{175}Lu reaction are given in Figs.9~12, respectively. The calculated results are reasonable.

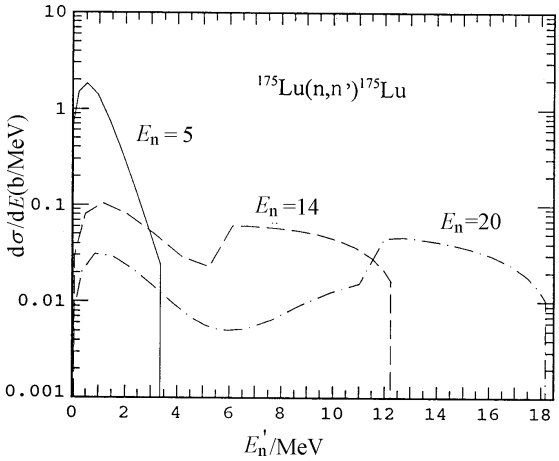

Fig.9 The energy spectrum of ^{175}Lu inelastic scattering to comtinous state

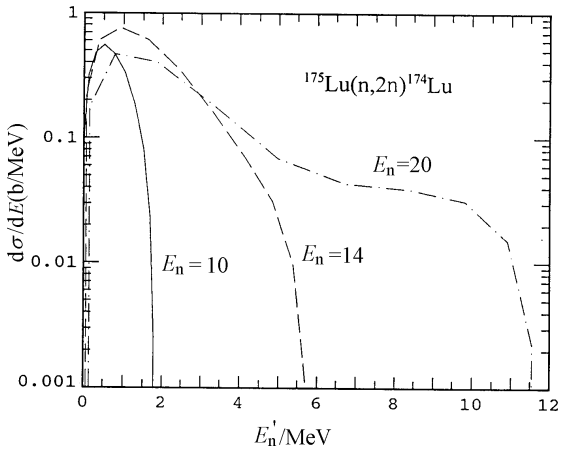

Fig.10 The energy spectrum of ^{175}Lu (n,2n) reaction

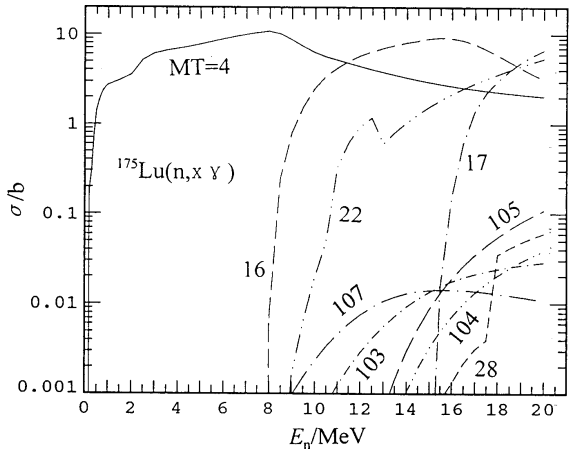

Fig.11 The γ–ray production cross section of n+^{175}Lu reaction

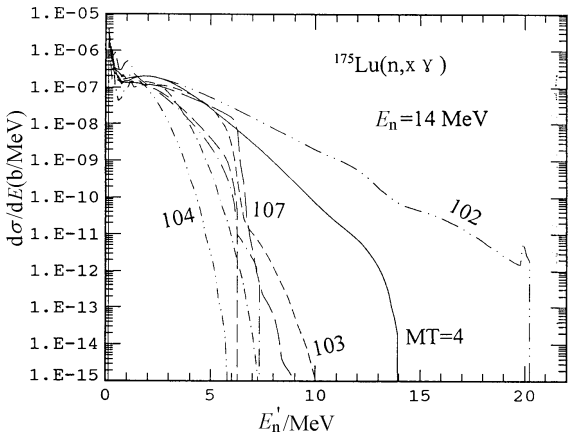

Fig.12 The γ–ray production energy spectrum of n+^{175}Lu reaction

Because theoretically calculated results are reasonable from above analysis, the calculated results are recommended in the energy range from 0.01 to 20 MeV, while for energy from 1.0^{-5} to 0.01 MeV, the evaluated data of ENDF/B-6 library were taken.

References

[1] D.G. Foster, et al., Phys. Rev., C3,576(1971).
[2] R.L. Macklin, et al., LA-7479-MS,1978.
[3] R.L. Macklin, et al., Phys. Rev., 159,1007(1967).
[4] R.G. Wille, et al., Phys. Rev., 118,242(1960).
[5] H. Beer, et al., Astrophyscal J., S46,295(1981).
[6] M.V. Bokhovko, et al., FEI-2169-91,1991.
[7] H. Beer, et al., Phys. Rev., C30,464(1984).
[8] J.H. Gibbons, et al., Phys. Rev., 122,182(1961).
[9] J. Voingier, et al., Nucl. Sci. Eng., 93,43(1986).
[10] V.A. Konks, et al., Yadernaja Fizika, 7,493(1968).
[11] V.A. Konks, et al., Nucl. Structure Conf., Antwerp, 576,1965.
[12] T. Sato, et al., Nucl. Sci. Tech., 12,681(1975).
[13] S.M. Qaim, Phys. Rev. Lett., 25,335(1976).
[14] R.F. Coleman, et al., Proc. Phys. Soc., 73,215(1959).
[15] D.R. Nethaway, Nucl. Phys., A190,635(1972).
[16] L.R. Veeser, et al., Phys. Rev., C16,1792(1977).
[17] B.P. Bayhurst, et al., Phys. Rev., C12,451(1975).
[18] J. Frehaut, et al., CEA-R-4627,1975.
[19] S.M. Qaim, Nucl. Phys., A224,319(1974).
[20] W. Dilg, et al., Nucl. Phys., A118,9(1968).
[21] J. Laurec, et al., CEA-R-5109,1981.
[22] YU Weixiang, et al., Commu. Nucl. Data Prog., 19,15(1978).
[23] SHEN Qingbiao, Commun. Nucl. Data Prog., 7, 43 (1992).
[24] ZHANG Jingshang, Private Communication，1998.
[25] P.D. Kunz, DWUCK4 Code.

Complete Neutron Data Calculations of n+ $^{133\sim135,137}$Cs in Energy Range from 0.01 to 20 MeV

ZHANG Zhengjun SUN Xiuquan

Depart. of Physics, Northwest University, Xian

HAN Yinlu SHEN Qingbiao

China Nuclear Data Center, CIAE, Beijing

After analyzing of the available neutron experimental data of n+$^{133\sim135,137}$Cs reactions, using the code APOM94, a set of neutron optical potential parameters in energy range from 0.01 to 20.0 MeV for all isotopes of Cs was obtained. Based on this set of optical potential parameters the cross sections of all channels and the elastic scattering angular distribution were calculated with the code SUNF. The theoretical results reproduced the experimental data well, and the results were given in B6 format.

The element Cs has 100% abundance of ^{133}Cs and isotopes ^{134}Cs, ^{135}Cs and ^{137}Cs are unstable. The available neutron experimental data of ^{133}Cs were retrieved and analyzed before theoretical calculating. There are a few experimental data of total cross sections. Beside these experimental data there are some experimental data for ^{133}Cs(n,2n), (n,γ), (n,p) and (n,α) reactions, which can be consulted in the calculation. For the unstable isotopes ^{134}Cs, ^{135}Cs and ^{137}Cs there is no experimental data. All the experimental data were taken from EXFOR library.

The neutron optical potential parameters for ^{133}Cs, ^{134}Cs, ^{135}Cs and ^{137}Cs are given as follows:

$$V = 52.3844-0.21446E_n-0.01099E_n^2-24.0(N-Z)/A,$$
$$W_s = \max\{0.0, 4.76901+0.70000E_n-12.0(N-Z)/A\},$$
$$W_v = \max\{0.0, -1.56148+0.21883E_n-0.07471E_n^2\},$$
$$U_{so}=6.2,$$
$$R_r=1.20242, R_s=1.38713, R_v=1.31037, R_{so}=1.20242,$$
$$A_r=0.77857, A_s=0.38613, A_v=0.58002, A_{so}=0.77857,$$

Where E_n is the incident neutron energy, Z, N and A are the numbers of proton, neutron and mass of the target nucleus, respectively. The exciton model parameter CK=900 MeV^3.

The theoretical results reproduce the experimental data well. Fig.1 shows the comparison for total cross sections between theoretical values of ^{133}Cs and experimental data. Fig.2 gives the comparison between theoretical cross sections of ^{133}Cs(n,γ) and experimental data. The theoretical values are in good agreement with the experimental data. The comparisons and analysis of other reaction channels such as ^{133}Cs(n,el), ^{133}Cs (n,non), ^{133}Cs (n,inl), ^{133}Cs (n,2n), ^{133}Cs (n,α) and ^{133}Cs (n,p) are not given here, and the calculated results reproduced experimental data. For some channels without measured data the calculated results are reasonable as well.

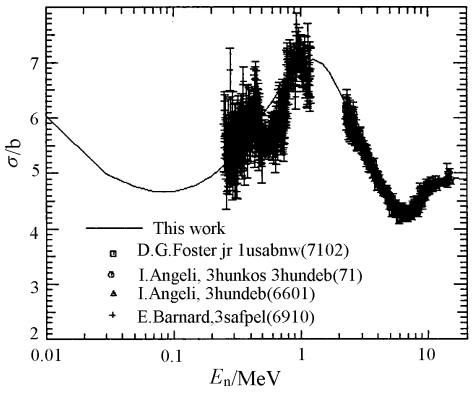

Fig.1 Total cross sections of ^{133}Cs

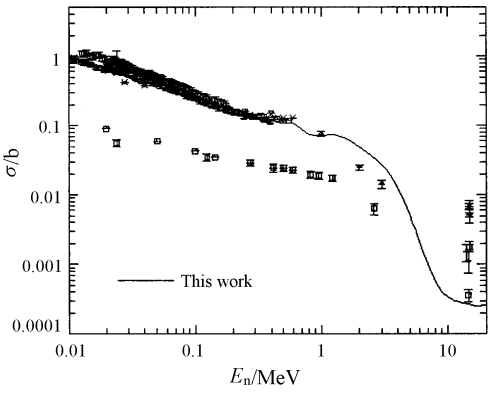

Fig.2 Cross sections of ^{133}Cs(n,γ)

References

[1] SHEN Qingbiao, Commun. Nucl. Data Progress, 7, 43(1992)

[2] P.D.Kunz, "Distorted Wave Code DWUCK4", University of Colorado, Unpublished.

[3] ZHANG Jingshang, SUNF–a code for calculations of fission product nucei based on unified mode, CNDC, CIAE, Unpublished.

n+ $^{99\sim105}$Ru $E_n \leq 20$MeV Nuclear Data Calculations

ZHANG Zhengjun[1] GE Zhigang[2] HAN Yinlu[2] SHEN Qingbiao[2] SUN Xiuquan[1]

1 Depart. of Physics, Northwest University, Xian

2 China Nuclear Data Center, CIAE, Beijing

The natural element Ru consists of ^{96}Ru(5.52%), ^{99}Ru(12.7%), ^{100}Ru(12.6%), ^{101}Ru(17.0%), ^{102}Ru(31.6%) and ^{104}Ru(18.7%), and ^{103}Ru. ^{105}Ru are unstable isotopes.

For element Ru there are no sufficient neutron experimental data for adjusting model parameters in calculations. There are only some experimental data of total cross sections of natural Ru for researching a set of optimum neutron optical potential parameters. Beside, there are some experimental data for reactions ^{100}Ru(n,γ), ^{101}Ru(n,γ), ^{102}Ru(n,γ), ^{104}Ru(n,γ), ^{104}Ru(n,2n), ^{102}Ru(n,α), ^{104}Ru(n,α), ^{100}Ru(n,p), ^{102}Ru(n,p) and ^{104}Ru(n,p) in energy region from 0.01 to 20.0 MeV. All experimental data used in this calculation were retrieved from the EXFOR library and selected before calculating.

Based on the available neutron experimental data of Ru and it's neighbor nuclei, a set of neutron optimum optical potential parameters for $^{99\sim105}$Ru in energy range from 0.01 to 20.0 MeV was obtained with code APOM94[1]. Using this set of parameters the cross sections of all reactions and the elastic scattering angular distribution of n+$^{99\sim105}$Ru were calculated with code SUNF[2]. The theoretical results agree with experimental data well, and the results were given in B6 format.

The neutron optical potential parameters for $^{99\sim105}$Ru are given as follows:

$$V=55.29658-0.45063E_n-0.00542E_n^2-24.0(N-Z)/A,$$
$$W_s=\max\{0.0,\ 9.58315+0.75008E_n-12.0(N-Z)/A\},$$
$$W_v=\max\{0.0,\ -1.5615+0.21883E_n-0.04927E_n^2\},$$
$$U_{so}=6.2,$$
$$R_r=1.18009, R_s=1.34427, R_v=1.40836, R_{so}=1.18009,$$
$$A_r=0.74069, A_s=0.39522, A_v=0.58501, A_{so}=0.74069.$$

Where E_n is the incident neutron energy, Z, N and A are the number of proton, neutron and mass of the target nucleus, respectively

Fig.1 shows the comparisons for total cross sections among theoretical curves of n+$^{99\sim105}$Ru and experimental data of ^{Nat}Ru. The theoretical values are reasonable and in good agreement with the experimental data. Fig.2 shows the theoretical curves of ^{99,101,103,105}Ru(n,γ) and experimental data of ^{101}Ru(n,γ). From Fig.2 one can also see the curves for ^{101}Ru(n,γ), ^{103}Ru(n,γ) and ^{105}Ru(n,γ) are reasonable. Fig.3 compares the theoretical cross section curves of reaction ^{104}Ru(n,p) with the corresponding experimental data. Theoretical results are in good agreement with experimental data. The comparisons and analysis of other reactions such as ^{102}Ru (n,2n), ^{X}Cs(n,α) and ^{X}Cs(n,p) are not presented here, but the calculated results reproduce experimental data. For some reactions without measured data the calculated results are reasonable as well.

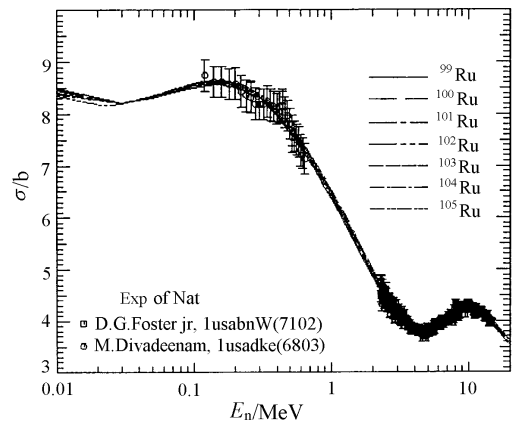

Fig.1 Total cross sections

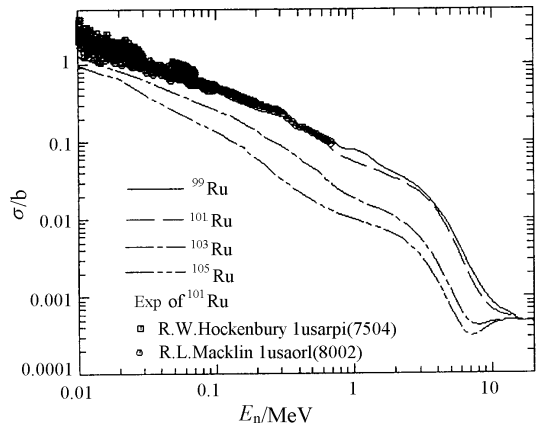

Fig.2 Cross sections of $^{99, 101, 103, 105}$Ru(n, γ)

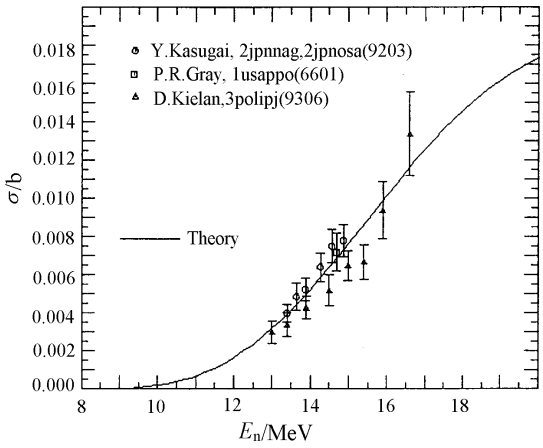

Fig.3 Cross section ^{104}Ru(n, p)

References

[1] SHEN Qingbiao, Commun. Nucl. Data Progress, 7, 43(1992)

[2] ZHANG Jingshang, SUNF–a code for calculations of fission product nuclei based on unified mode, CNDC, CIAE, Unpublished.

Reference Fission Yield Data Evaluation of ^{79}Se etc.17 Fission Product Nuclides from ^{235}U Fission

LIU Tingjin

China Nuclear Data Center, CIAE, Beijing

【**abstract**】*The reference fission yield data of ^{79}Se etc. 17 product nuclides from ^{235}U fission were evaluated based on available experimental data up to now. The data were processed with average code AVERAG and simultaneous evaluation code ZOTT. The evaluated data were compared with ENDF/B-6, JEF-2, JENDL-3 and CENDL/FY. The data were updated and improved.*

As reference fission yield data are used as standard and monitor, their accuracy and precision are very important, so they must be specially paid attention and evaluated. The relatively measured data should not be used in the evaluation as much as possible, because the standard could not be based on the other standards, which have not been approved to be reliable.

1 Experimental Data Evaluation.

The experimental data were retrieved from EXFOR Master Library and collected from the publications concerned. Altogether 102 entries (subentries, papers) were collected. The following data were abandoned:

(1) The quantity measured is not required;

(2) The data measured at the energy points are not required;

(3) Some thing is wrong in the measurement or data processing;

(4) The data are large discrepant with others and the measured method is not reliable or no information given in detail.

As a result, 32 papers were remained, which are listed in the Ref. [1~32]. All of these data were analyzed and evaluated in physics and made the necessary corrections and treatments:

(1) Standard corrections for Ref. [7,15,16, 31, 32] by using the reference data just evaluated by us;

(2) Decay data corrections for Ref.[28] by using the data taken from Table of Isotopes(eighth edition);

(3) Error adjusted or assigned for Refs. [2,3,6,9, 12~16, 18,20~25,29];

(4) Calculated the fission yield data from given ratio by using the reference data just evaluated by us for Refs. [12,25];

(5) Calculated the ratio from given relative data for Refs. [4,5] to avoid using other standard.

In addition, some things wrong were corrected for Ref. [32]. And also the data of some special nuclides in the above references were abandoned for the large differences with others. They are ^{79}Se (too large), ^{107}Pd (too small) in Ref. [19], ^{91}Zr (too large) in Ref. [22], ^{93,94}Rb (too small) in Ref. [28], ^{147}Pm (too large) in Ref. [31].

2 Data Processing

After the above analysis in physics and correction, the evaluated data with their adjusted errors were processed.

The all data with more than one set were averaged with weight by using code AVERAG[33]. Not only the weighted mean value but also the arithmetical mean value and reduced χ^2 were calculated. The weighted mean value is recommended and the latter two were used for reference and comparison. The averaged data are marked by letter “A” in Table 1, and also the data sets used for averaging were given in the Table.

The measured data together with the ratios relative to others were simultaneously evaluated by using code ZOTT[34]. The data concerned were divided into several groups, each group contain all data, which are correlative through the ratios, weather at numerator or at denominator. Concretely, they are four groups: ^{93,94,95}Rb; ^{99}Y, ^{99}Tc; ^{91,93}Zr and ^{105,107}Pd. The data evaluated simultaneously are marked by letter" S" in the Table 1.

If there are more than one set of absolute and ratio measurements, they were averaged first for each of them, and then evaluated simultaneously.

3 Result, Comparison and Recommendation

The evaluated results are presented in Table 1. The letter "T", "F" and "H" mean thermal energy spectrum, fission or fast reactor spectrum and around 14 MeV fast neutron respectively. The number under the "point" heading is the set number of the measured datum itself, and "+number" is the set number of the ratios at numerator, and "+number" is at denominator. There are only the data at thermal or thermal and fission spectrum for some nuclides, for there are no experimental data available. Also the data were collected for product nuclides ^{97}Br, ^{98m}Y, ^{134}Cs, ^{150}Sm and ^{155}Gd, but there are no any experimental data available at all. So there are no data given in Table 1 for them.

The evaluated data were compared with existing evaluated data from ENDF/B-6, JEF-2.2, JENDL-3.2

Table 1 The evaluated reference fission yield by this work

Nuclide	E	Yield Y	Y Error	Point	Proce.	Reco.
34-Se-79	T	4.3900E-02	3.0000E-03	1		R
37-Rb-93	T	3.3914E+00	1.1804E-01	1+1	S	R
37-Rb-94	T	1.6726E+00	4.2809E-02	+1(B6)	S	R
37-Rb-95	T	7.2229E-01	2.1583E-02	1+(2)	S	R
39-Y-99	T	2.0482E+00	6.1049E-02	+1(B6)	S	(R)
40-ZR-91	T	5.9288E+00	4.3812E-02	5+1	AS	R
40-ZR-91	F	5.6600E+00	5.1089E-02	3	A	R
40-ZR-91	H	4.9100E+00	2.4513E-01	2	A	R
40-ZR-93	T	6.3470E+00	4.6309E-02	5+(1)	AS	R
40-ZR-93	F	6.1579E+00	5.3653E-02	3	A	R
40-ZR-93	H	5.0863E+00	2.7621E-01	2	A	R
43-Tc-99	T	6.0756E+00	6.1049E-02	3+(1)	AS	R
45-Rh-103	T	2.9667E+00	3.2215E-02	4	A	R
45-Rh-103	F	3.2100E+00	1.2840E-01	1		R
45-Rh-103	H	3.4930E+00	2.0960E-01	1		R
46-Pd-105	T	9.4645E-01	8.8925E-03	4+(1)	AS	R
46-Pd-105	F	1.1700E+00	1.3000E-01	1		R
46-Pd-105	H	1.7010E+00	1.0210E-01	1		N
46-Pd-107	T	1.4574E-01	1.3758E-03	2+1	AS	R
50-Sn-126	T	5.7213E-02	2.6396E-03	2	A	R
50-Sn-126	F	1.0000E-01	5.0000E-03	1		R
53-I-129	T	7.5145E-01	3.7840E-02	6	A	R
53-I-129	F	1.0900E+00	5.5000E-02	1		(R)
53-I-129	H	3.2630E+00	1.9580E-01	1		R
53-I-138	T	1.5356E+00	1.3112E-01	2	A	R
53-I-139	T	6.3139E-01	1.0900E-01	2	A	R
55-Cs-135	T	6.5311E+00	4.3430E-02	6	A	R
55-Cs-135	F	6.5240E+00	4.2048E-02	6	A	R
55-Cs-135	H	5.6990E+00	3.4190E-01	1		R
61-Pm-147	T	2.2440E+00	1.8227E-02	5	A	R
61-Pm-147	F	2.1807E+00	8.2012E-02	2	A	R
61-Pm-147	H	2.0220E+00	1.2130E-01	1		N

NOTE: E Neutron energy: T Thermal energy, F Fission or fast reactor spectrum, H Around 14 MeV.
POINT Data point been measured.
PRO Processed: A Averaged, S Simultaneously evaluated.
REC Recommendation: R Recommended, N Not recommended.

Table 2 Some typical examples for comparison of this work with others

NUCLIDE	LIBRARY	YIELD Y	ERR(%)	DIF(%)	YIELD Y	ERR(%)	DIF(%)	YIELD Y	ERR(%)	DIF(%)
40-ZR- 91	THIS WORK	5.9288E+00	0.74		5.6600E+00	0.90		4.9100E+00	4.99	
40-ZR- 91	ENDF/B-6	5.8278E+00	0.70	1.70	5.7334E+00	0.70	-1.30	4.8227E+00	4.00	1.78
40-ZR- 91	JEF-2	5.8800E+00	8.46	0.82	5.3922E+00	13.37	4.73	4.6336E+00	8.81	5.63
40-ZR- 91	JENDL-3	5.9187E+00	0.00	0.17	5.6549E+00	0.00	0.09	4.8924E+00	0.00	0.36
40-ZR- 91	CENDL-FY	5.8762E+00	2.04	0.89	5.6500E+00	1.33	0.18	5.0083E+00	69.51	-2.00
40-ZR- 93	THIS WORK	6.3470E+00	0.73		6.1579E+00	0.87		5.0863E+00	5.43	
40-ZR- 93	ENDF/B-6	6.3463E+00	0.70	0.01	6.2540E+00	0.70	-1.56	5.1932E+00	6.00	-2.10
40-ZR- 93	JEF-2	6.3206E+00	2.90	0.42	5.8791E+00	5.85	4.53	5.1759E+00	11.62	-1.76
40-ZR- 93	JENDL-3	6.3902E+00	0.00	-0.68	6.1394E+00	0.00	0.30	5.2958E+00	0.00	-4.12
40-ZR- 93	CENDL-FY	6.3548E+00	2.42	-0.12	6.1358E+00	0.89	0.36	5.6994E+00	93.82	-12.05
45-Rh-103	THIS WORK	2.9667E+00	1.09		3.2100E+00	4.00		3.4930E+00	6.00	
45-Rh-103	ENDF/B-6	3.0309E+00	1.00	-2.17	3.2439E+00	1.40	-1.06	3.2048E+00	2.80	8.25
45-Rh-103	JEF-2	3.0237E+00	4.07	-1.92	3.2851E+00	10.10	-2.34	3.3855E+00	3.04	3.08
45-Rh-103	JENDL-3	3.0274E+00	0.00	-2.05	3.2749E+00	0.00	-2.02	3.2180E+00	0.00	7.87
45-Rh-103	CENDL-FY	3.2209E+00	16.36	-8.57	3.1865E+00	102.17	0.73	3.1847E+00	100.36	8.83
46-Pd-105	THIS WORK	9.4645E-01	0.94		1.1700E+00	11.11		1.7010E+00	6.00	
46-Pd-105	ENDF/B-6	9.6416E-01	1.40	-1.87	1.1963E+00	2.80	-2.25	1.8721E+00	4.00	-10.06
46-Pd-105	JEF-2	9.5770E-01	6.82	-1.19	1.2810E+00	14.13	-9.49	1.8310E+00	6.76	-7.64
46-Pd-105	JENDL-3	9.6384E-01	0.00	-1.84	1.2048E+00	0.00	-2.98	1.8861E+00	0.00	-10.88
46-Pd-105	CENDL-FY	9.6888E-01	2.05	-2.37	1.4404E+00	91.23	-23.11	1.8683E+00	100.37	-9.84
53- I-129	THIS WORK	7.5145E-01	5.04		1.0900E+00	5.05		3.2630E+00	6.00	
53- I-129	ENDF/B-6	5.4335E-01	1.00	27.69	8.3516E-01	4.00	23.38	3.3746E+00	8.00	-3.42
53- I-129	JEF-2	7.8234E-01	4.01	-4.11	1.1739E+00	26.79	-7.70	2.4260E+00	33.16	25.65
53- I-129	JENDL-3	7.1785E-01	0.00	4.47	8.2731E-01	0.00	24.10	3.3557E+00	0.00	-2.84
53- I-129	CENDL-FY	8.7909E-01	15.94	-16.99	1.1598E+00	12.30	-6.40	3.5533E+00	100.37	-8.90
53- I-139	THIS WORK	6.3139E-01	17.26							
53- I-139	ENDF/B-6	7.7756E-01	8.00	-23.15						
53- I-139	JEF-2	6.2688E-01	34.03	0.71						
53- I-139	JENDL-3	9.8141E-01	0.00	-55.44						
53- I-139	CENDL-FY	8.4390E-01	30.88	-33.66						
55-Cs-135	THIS WORK	6.5311E+00	0.66		6.5240E+00	0.64		5.6990E+00	6.00	
55-Cs-135	ENDF/B-6	6.5390E+00	64.00	-0.12	6.6013E+00	64.00	-1.18	5.7288E+00	64.00	-0.52
55-Cs-135	JEF-2	6.5803E+00	2.23	-0.75	6.3696E+00	3.68	2.37	5.7721E+00	10.41	-1.28
55-Cs-135	JENDL-3	6.5337E+00	0.00	-0.04	6.5711E+00	0.00	-0.72	5.9116E+00	0.00	-3.73
55-Cs-135	CENDL-FY	6.5300E+00	0.35	0.02	6.3696E+00	1.73	2.37	5.4936E+00	79.67	3.60
61-Pm-147	THIS WORK	2.2440E+00	0.81		2.1807E+00	3.76		2.0220E+00	6.00	
61-Pm-147	ENDF/B-6	2.2467E+00	1.00	-0.12	2.1389E+00	1.00	1.92	1.6232E+00	2.80	19.72
61-Pm-147	JEF-2	2.2665E+00	8.36	-1.00	2.1367E+00	13.88	2.02	1.6392E+00	9.62	18.93
61-Pm-147	JENDL-3	2.2534E+00	0.00	-0.42	2.0961E+00	0.00	3.88	1.6266E+00	0.00	19.56
61-Pm-147	CENDL-FY	2.3606E+00	5.99	-5.20	1.9044E+00	111.88	12.67	1.6302E+00	100.34	19.38

and CENDL/FY. Some typical results are presented in Table 2. The relative errors are given for each set of data (there is no error given for JENDL-3.2, so all of them are zero) and the differences (relative to present evaluated data) of this work with other evaluated data are also given. It can be seen that the most of our new evaluated data are consistent with all of the others within the error bar, which shows that all of these evaluated data are in good agreement with each other. But there are some exceptions:

(1) There are larger differences of present data with CENDL/FY for nuclides ^{93}Rb(T), ^{93}Zr(H), ^{105}Pd(F), ^{147}Pm(F), but the present data are consistent with others. It is shown that there may be some problems for CENDL/FY data, and besides the errors of CENDL/FY data are very large for these nuclides (except for 93Rb(T)). The same situation is for ^{129}I(T) with ENDF/B-6 and for ^{129}I(H) with JEF-2.2.

(2) There are larger differences between present data with CENDL/FY and JENDL-3.2 for nuclides ^{95}Rb(T) and ^{99}Y(T), with ENDF/B-6 and JENDL-3.2 for ^{129}I(F), with ENDF/B-6, JENDL-3.2 and CENDL/FY for ^{139}I(T). The reliability of this kind of data should be analyzed concretely and carefully. For ^{99}Y(T) and ^{129}I(F), there is only one set of measured data, not so reliable, so the data are recommended only as reference (marked in Table 1 by "(R)"). For ^{95}Rb(T), there are three sets of independent measured data, including two sets of ratios relative to ^{93,94}Rb(T) and the data of ^{93,94}Rb(T) are in good agreement with others, the data can be recommended. For ^{139}I(T), there are two sets of measured data and there are large differences with three sets of other evaluated data, it seems that they are divided into two groups, more attention should be paid to it and more measurements are expected to clarify the discrepancy.

(3) For ^{105}Pd(H) and ^{147}Pm(H), there is large discrepancy with all of others and in the same direction (the former small and the latter large). There is only one set of measured data for them, and possibly there is a systematical error. The data could not be recommended.

The error comparison of this work with others is given in Table 3. The number in the table is the data sets, whose relative errors are in the given region (including the up limit, for example 1%~2% means $1\%<\Delta Y\leq 2\%$). It can be seen that at thermal energy point, the error ΔY_{half}, less than which of the data set number is half, is 2% for this work and ENDF/B-6, is 9% for JEF2.2 and CENDL/FY. About one third of the error is less than 1% for this work and ENDF/B-6. At fission spectrum, ΔY_{half} is 3% for this work, 4% for ENDF/B-6, and 20% for JEF-2.2. For CENDL/FY, two third of the errors are larger than 20%. At around 14 MeV fast neutron energy point, ΔY_{half} is 10% for ENDF/B-6, 15% for JEF-2.2. All of the errors are less than 9%(4%~6%, 6%~9% each half) for this work and almost all of them are larger than 20% for CENDL/FY. It can be concluded that comparing with JEF-2.2 and CENDL/FY, the error of this work is considerably reduced especially at fission spectrum and fast energy point. Comparing with ENDF/B-6, the error of this work is at the same level at thermal energy point and fission spectrum, and is improved at fast neutron energy point.

Table 3 The error comparison of the evaluated data with others

E_n	ERROR(%)	<1	1~2	2~3	3~4	4~6	6~9	9~12	12~15	15~20	>20
T	THIS WORK	6	2	3	1	2	2	0	0	1	0
	ENDF/B-6	7	1	3	1	0	4	0	0	0	1
	JEF-2.2	0	0	2	1	2	4	2	1	0	5
	CENDL/FY	1	1	4	0	2	0	3	1	3	2
F	THIS WORK	3	0	0	2	2	0	1	0	0	0
	ENDF/B-6	4	1	1	3	0	2	1	0	1	4
	JEF-2.2	0	0	0	1	1	0	1	4	1	9
	CENDL/FY	1	2	0	1	0	0	0	1	0	12
H	THIS WORK	0	0	0	0	4	3	0	0	0	0
	ENDF/B-6	0	0	3	1	2	2	1	0	0	8
	JEF-2.2	0	0	0	1	0	3	3	1	0	9
	CENDL/FY	0	0	0	0	0	0	0	0	1	16

References

[1] M.Shima, CJP,56,1340(7810)

[2] W.J.Maeck, ICP-1142(7809)

[3] H.Farrar, NP,34,367(62)

[4] H.Farrar, CJP,40,1017(62)

[5] P.L.Reeder, 75WASH,1,401(7503)

[6] L.R.Bunney, JIN,27,273(65)

[7] R.J.Meyer, ANL-6900,338(6406)

[8] B.R.Erdal, JIN,31,2993(6910)

[9] R.P.Larson,Private Communication (6912) (EXFOR 13249002)

[10] F.L.Lisman, NSE,42,191(70)

[11] J.W.Mandler, BAP,18,768(7306)

[12] M.M.fowler, JIN,36,1201(7406)

[13] W.J.Maeck, 75WASH,1,378(7503)

[14] G.Diiorio, NIM/B,147,487(7712)

[15] D.R.Wiles, CJP,31,419(53)

[16] J.A.Petruska, CJP,33,64095511)

[17] L.E.Glendenin, Private Communication (55) (EXFOR 13428002)

[18] W.J.Maeck, ENICO-1028(8002)|7.0+05|

[19] H.Wohlfarth, Private Communication (7612) (EXFOR 21054087)

[20] L.Kosh, RCA,29,61(81)

[21] B.C.Purkayast, CJC,34,293(56)

[22] H.Thierens, NIM,134,299(7604)

[23] R.Brissot, NP/A,255,461(7512)

[24] M.Rajagopalan, NSE,58,414(7512)

[25] M.Weis, Private Communication (8010) (EXFOR 21687004)

[26] J.P.Bocquet, NP/A,189,556(7207)

[27] D.C.Aumann, RCA,30,(1),19(82)

[28] G.Rudstam, RCA,49,155(90)

[29] C.K.Mathews, PR/C,15,344(7701)

[30] M.Shmid, IA-1345(7908)

[31] V.K.Gorshkov, AE,3,(7),11(5707)

[32] V.YA.Gabeskir, AE,43,59(77)

[33] LIU Tingjin, CNDP, 19, 103(1998)

[34] D.Muir, Nucl. Su. and Eng., 101, 88(1989)

Evaluation of Complete Neutron Data of n+^{241,242}Pu from 10^{-5} eV to 20 MeV

YU Baosheng CAI Chonghai* SHEN Qingbiao

China Nuclear data Center, CIAE, Beijing

** Department of Physics, Nakai University, Tianjin*

【**abstract**】*A complete set of neutron nuclear data, including cross sections, angular distributions, secondary neutron spectra, of n+^{241,242}Pu from 10^{-5} eV to 20 MeV were evaluated based on available experimental data and theoretically calculated results. The data are given in ENDF/B-6 format.*

.

1 Resonance Parameters and Evaluated Files

The resonance parameters and ν value were taken from ENDF/B-6 due to the boundary is higher than other nuclear data libraries. The resolved region resonance for ^{241}Pu is from 1.0^{-5} eV to 0.3 keV and the unresolved region is from 0.3 to 40.2 keV. For ^{242}Pu, the region of resolved resonance is from 0 to 986 eV and the unresolved one is from 986 eV to 10 keV.

The smooth cross section at boundary should be reasonably in conjunction with the cross section calculated from resonance parameters. In general the conjunction of the cross-sections at boundary is quite well. When the conjunction is not smooth enough, the parameters were adjusted. In some cases, the similar adjustments were made for evaluated data in smooth region. After adjusting, the cross sections at boundary are good conjunction within fixed errors.

The comparisons of evaluated data files for ^{241}Pu are shown Table 1.

2 Evaluation and Adjusting Smooth Cross Sections

2.1 Total Cross Section

For ^{242}Pu, there are a few experimental data from thermal energy point up to 20 MeV. These data are mainly measured by T.E.Young[1] in the energy region of 2~770 eV, by G.F.Auchampaugh[2] from 0.0253 to 390 eV and by M.S.Moore[3] from 0.67 to 170 MeV, respectively.

The Moore's data[3] measured with 99.91% of ^{242}Pu sample by using time of flight method at Los Alamos Laboratory in 1979 was fitted as recommended total cross sections and compared with other evaluated data from ENDF/B-6 and JENDL-3 (shown in Fig.1a~1c).

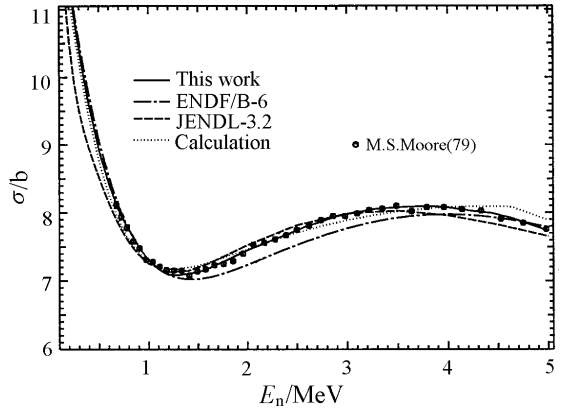

Fig. 1a ^{242}Pu(n,tot) cross section

2.2 Fission Cross Section for ^{241}Pu

The experimental data[4~14] of fission cross sections were measured by using absolute and ratio measurement techniques. The measured data were collected up to 2000.

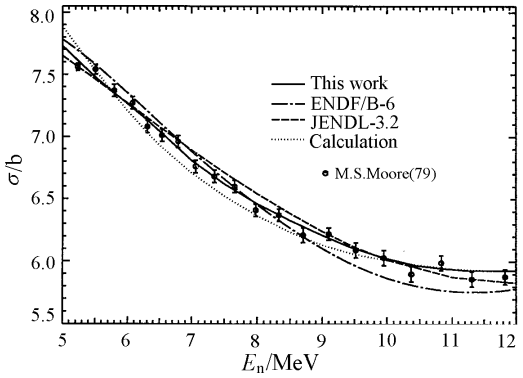

Fig. 1b ^{242}Pu(n,tot) cross section

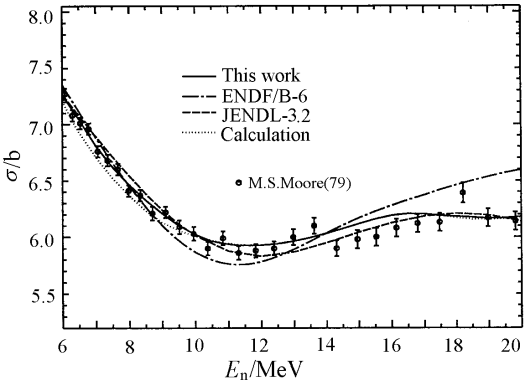

Fig. 1c ^{242}Pu(n,tot) cross section

The cross sections were measured by D.K.Butler[4] in energy region from 0.021 MeV to 1.825 MeV in 1961, by H.L.Smith[5] from 0.12 MeV to 21 MeV in 1962. They used enriched purity (~90%) ^{241}Pu sample and ionization fission chamber. The data were measured by O.D.Simpson[6] by using underground nuclear explosion in energy region from 20 eV to 0.978 MeV in 1966. The data of D.K.Butler[4] and H.L.Smith[5] are 20% higher at around 0.1 MeV and 2%~10% from 2 MeV to 14 MeV, the data of O.D.Simpson [6] are ~20% lower from 0.4 to 0.8 MeV than that of other ones. P.H.White[7,8] used an ion exchange technique to do some chemical separation for sample and used low geometry alpha counting and coulometric assay to determine the weight of the sample. The corrections of fission events from the other plutonium isotopes and from ^{241}Am in sample of ^{241}Pu were not considered. The data measured by P.H.White[7,8] could not produce the cross section structure.

After 1970, the fission cross section measurement was carried out by using the time of flight method to discriminate the time-independent background and

to determine the neutron energy. F.Fappeler [9] put the sample of ^{241}Pu and ^{235}U into the center of two identical gas scintillation chambers and the chambers were used to measure the neutron flux at symmetric positions. It is well known that the fission cross section of other plutonium isotopes is very high. Therefore, adoption of the high-purity isotopes sample and correction for other plutonium isotopes are important to obtain the accurate cross section. In order to obtain the accurate data for ^{241}Pu, the correction of the fission count rate has to be made for fission events from the other plutonium isotopes and ^{241}Am. The sample masses and isotopic compositions were determined by using the isotopic dilution method. The measurements were carried out at sufficiently fine energy intervals to show in detailed shape of fission cross section ratio. F.Fappeler [9] measured the data in the energy region from 5 keV to 1.2 MeV.

G.W.Carlson[11] measured the fission cross section ratio of ^{241}Pu/^{235}U over the neutron energy range from 1 keV to 30 MeV at the Lawrence Livermore Laboratory 100 MeV Linac. The ionization fission chambers and time of flight technique were used. In order to improve the knowledge of the ratio shape, the normalized value for the measured shape was determined from two independent auxiliary measurements. First the threshold method was applied to determine the fission cross sections of ^{238}U to ^{241}Pu. Combining the measured value for ^{238}U to ^{235}U and the new result for ^{238}U to ^{241}Pu. A normalization value for the ^{241}Pu/^{235}U was obtained. In the measurement, the isotopic composition of the ^{241}Pu was determined with ion exchange column. The fission measurement was made as soon as possible after chemical separation of ^{241}Am from the ^{241}Pu sample to minimize the effects of ^{241}Am.

I.Szabo[10] measured the data at a few energy points by using associated particle method. V.B.Aleksandrov[14] used mica-detector and admixture ^{241}Pu sample to measure the fission cross section at 1.2 MeV. He used the monoenergetic neutron source of ^{7}Li(p,n) reaction and made correction for the other plutonium isotopes and ^{241}Am in ^{241}Pu. The data of V.B.Aleksandrov[14] were in good agreement with one of G.W.Carlson[11]. The data measured by F.Fappeler[9], I.Szabo[10], V.B.Aleksandrov[14] and G.W.Carlson[11] were renormalized with ^{235}U data from ENDF/B-6 and a large weight was given.

Around 14 MeV, the discrepancy was found. The data by N.A.Khan[13] by means of registration of tracks from fragments in mica solid state detector at 14.8 MeV is systematically lower than G.W.Carlso's[11] at 14.7 MeV. The data of H.L.Smith[5] and P.H.White[7,8] are 10% and 19% higher than the one of G.W.Carlso[11] at 14.7 MeV. Therefore, a large weight was given to the data of G.W.Carlso[11] above 14.7 MeV.

The evaluation was based on all collected available ratio and absolute measured data, the results are shown in Fig.2.

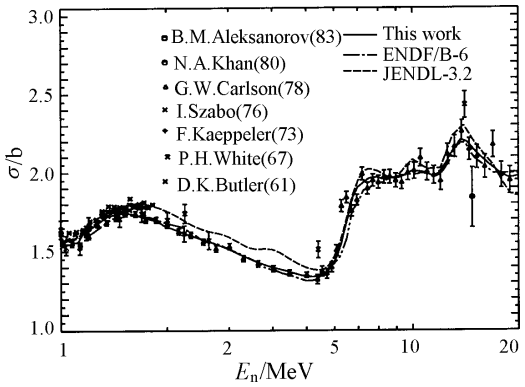

Fig.2 ^{241}Pu(n,f) cross section

2.3 Fission Cross Section for ^{242}Pu

There are 11 sets of mainly measured data[15~25]. The cross sections were measured by E.F.Fomushkin[15] in energy region from 0.44 MeV to 3.6 MeV in 1969 and by G.F.Auchampaugh[16] from 0.51 MeV to 4.0 MeV in 1971. They used plutonium-admixture or Pu-oxd sample and solid state detector. D.W.Bergen[17] measured the data by using underground nuclear explosion and ^{242}Pu sample enriched to 89% and solid state detector in energy region from 0.09 MeV to 2.9 MeV with errors ~17%. The data measured by E.F.Fomushkin[15] and G.F.Auchampaugh[16] have large fluctuations and the difference with others is more than 7%~20% and 10%~22%, respectively.

Table 1 Comparison of the evaluated nuclear data files

^{241}Pu	ENDF/B-6(1994)	JENDL-3(1993)	BROND-2(1982)	CENDL-3(1999)
File 2.	1.0E^{-5}~0.3keV, 0.3~40.2 keV	1.0E^{-5}~0.3 keV, 0.3~30 keV	1.0E^{-5}~ 100 keV	1.0E^{-5}~0.3 keV, 0.3~40.2 keV
Files. 3,4	1,2,4,16,17,18,51~65,91, 102	1,2,4,16,17,18,37,51 ~61,91,102	1,2,4,16,17,51~75, 91	1,2,4,16,17,18,51~ 71,91,103~105,107
File 5	16,17,18,91	16,17,18,37,91	16,17,18,91	16,17,18,91

The cross sections were measured by J.W. Behrens [18] in energy region from 0.1 MeV to 33.9 MeV , by J.W.Meadows[19] from 0.4 MeV to 9.9 MeV in 1978, by M.Cance[22] at 2.47 MeV in 1984 and by H.Weigmann[24] from 0.3 to 9.7 MeV, respectively. Their data are consistent with each other within errors.

The data measured by J.W. Behrens[18] with the white neutron source are consistent with those by J.W.Meadows[19], M.Cance[22] and H.Weigmann[24] using the mono-energetic neutron within errors. The ^{242}Pu samples used by J.W.Meadows[19] were deposited on 0.25 mm thick stainless steel plates by electrodeposition, the mass ratios of ^{242}Pu/^{239}Pu on sample were measured by absolute alpha counting. The effects from other isotopes were subtracted. The data measured by J.W. Behrens[18] are in agreement very well with those by M.Cance[22] and H.Weigmann[24]. Those data were given large weight for the energy region below 10 MeV.

The data of N.A.Khan[20] by means of registration of tracks from fragments in mica solid state detector at 14.8 MeV is systematically lower than the data of R.Arit[21] and I.D.Alkhazov[23] at 14.7 MeV and J.W.Meadows[25] at 14.74 MeV by using low mass ionization chamber. The sample enriched purity used by R.Arit[21] is 99.99% of ^{242}Pu and the isotopic abundance of ^{242}Pu and ^{239}Pu in samples were measured by J.W.Meadows[25]. Therefore, the data by R.Arit[21] and J.W.Meadows[25] was given large weight.

The evaluation is based on all collected ratio and absolute data, the result is shown in Fig.3.

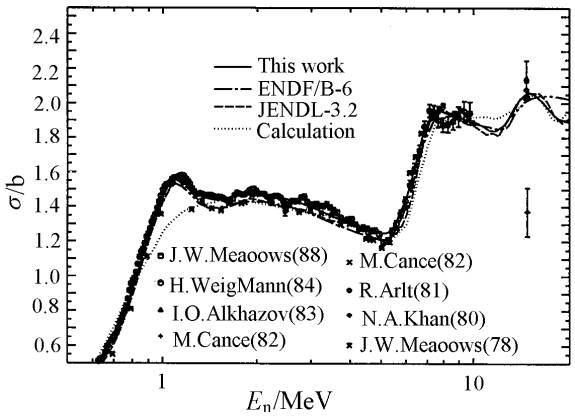

Fig. 3 ^{242}Pu(n,f) cross section

2.4 Radiation Capture Cross Section

For ^{241}Pu, there are some experimental data available in energy region from 0.01 eV to 30 keV, measured by L.W.Weston[26] using liquid NE-226 scintillation at Oak Ridge Electron Linear Accelerator in 1978. For ^{242}Pu, the data were measured by R. W. Hockenbury[27] used liquid scintillation in energy region from 6.3 keV to 0.87 MeV at Electron linear accelerator in 1974. Based on the experimental data the theoretically calculated and evaluated data were obtained. The evaluated data could reproduce the experimental data very well.

2.5 (n,2n) and (n,3n) Cross Sections

There are no experimental data for these reactions. The calculated data[28,29] were adopted. But for (n,2n) reaction, the cross section in high-energy region is too high and was corrected based on systematics. It was shown Fig. 4.

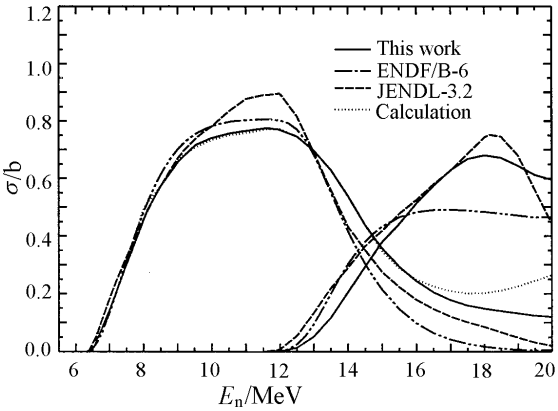

Fig. 4 ^{242}Pu(n,2n),(n,3n) cross section

2.6 Inelastic Scattering Cross Section

The total inelastic scattering cross sections were sum of partial inelastic scattering cross sections. Some partial calculated inelastic scattering cross sections were adjusted based on reasonable physics trend.

The data were investigated and compared with ENDF/B-6 and JENDL-3. It was found that the important effects on the evaluated results are from the energy interval ΔE_{hc} from the highest level to continuous state and whether adopted coupled channel calculation for first few levels. The comparison of our adopted levels with ENDF/B-6 and JENDL-3 is shown in Table 2.

For ENDF/B-6, there is a large ΔE_{hc}. Meanwhile the direct components were not considered. The valley around 1.3 MeV at inelastic scattering cross section consists with the continuous state boundary 1.195 MeV. The comparison of our evaluated data with ENDF/B-6 and JENDL-3 were shown in Figs.5.

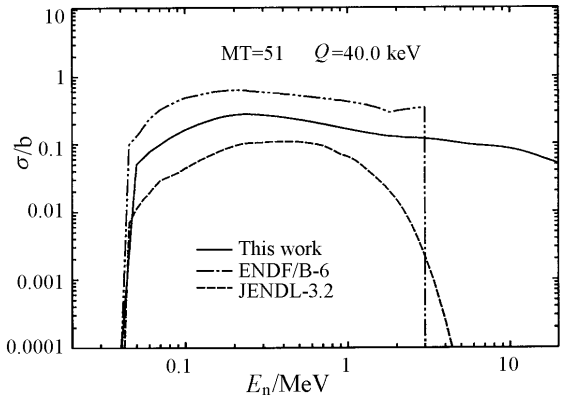

Fig. 5a ^{241}Pu(n,inl) cross section to first level

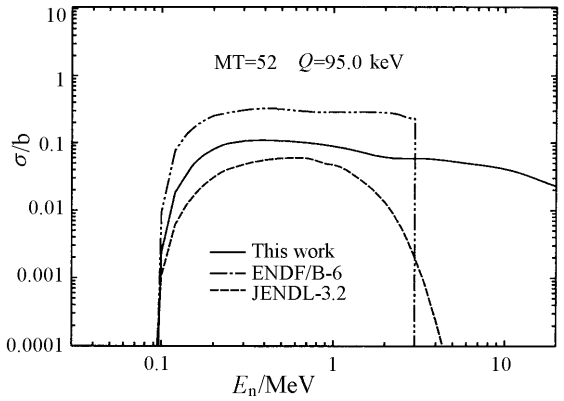

Fig. 5b ^{241}Pu(n,inl) cross section to second level

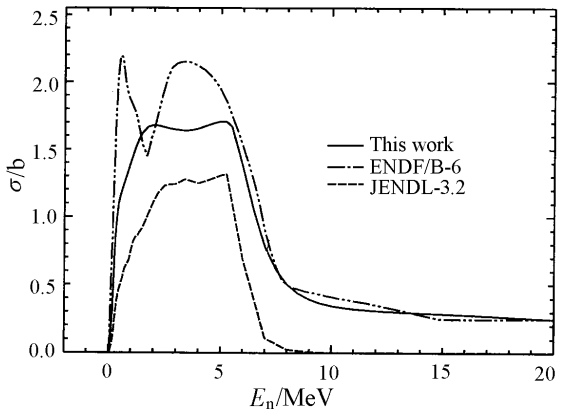

Fig. 5c ^{241}Pu(n,inl) total cross section

3 Summary Remarks

The complete neutron data for ^{241,242}Pu were recommended based on evaluated experimental data mentioned above and theoretically calculated results[28,29] from 10^{-5} eV to 20 MeV in ENDF/B-6 format. Some secondary neutron spectra are shown in Fig. 6.

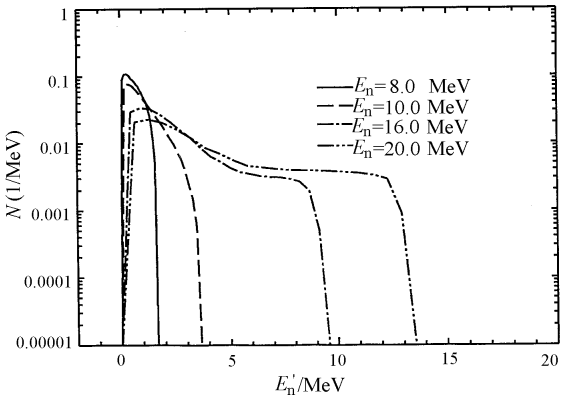

Fig.6a Normalized secondary neutron spectra for ^{242}Pu(n,2n) reaction

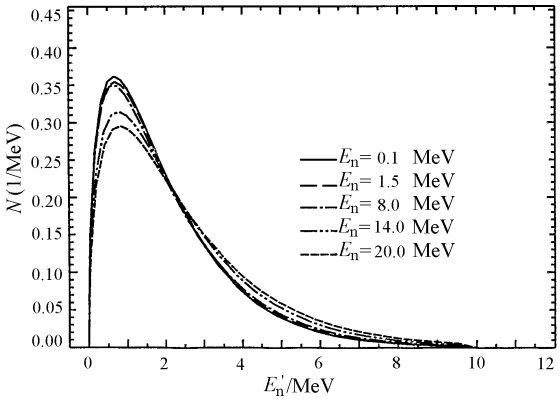

Fig. 6b Normalized secondary neutron spectra for ^{242}Pu(n,f) reaction

The data were checked by using ENDF utility codes, CHEKR, FIZCOM and PSYCHE in format and physics. Some problems were found and resolved.

The present evaluated data were compared with others. The total, fission and capture cross sections of present work are in good agreement with the measured data. The inelastic scattering cross sections are reasonable in physics.

Acknowledgments

The authors would like to thank Drs. TANG Guoyou, SHI Zhaomin for the benefit discussions.

Table 2 The comparison levels scheme used with ENDF/B-6 and JENDL-3

This Work		ENDF/B-6		JENDL-3	
No.	Energy / MeV	No.	Energy / MeV	No.	Energy / MeV
G.S.	0.0	G.S.	0.0	G.S.	0.0
1	0.04	1	0.04	1	0.0418
2	0.0957	2	0.095	2	0.09399
3	0.1611	3	0.163	3	0.1615
4	0.1616	4	0.169	4	0.1708
5	0.1709	5	0.174	5	0.2231
6	0.1749	6	0.231	6	0.23
7	0.2231	7	0.245	7	0.2427
8	0.2318	8	0.300	8	0.30
9	0.235	9	0.335	9	0.335
10	0.2427	10	0.448	10	0.367
11	0.3009	11	0.753	11	0.449
12	0.335	12	0.828	Eon.	0.489
13	0.337	13	0.894		
14	0.368	14	0.918		
15	0.376	15	0.941		
16	0.4044	Eon.	1.195		
17	0.444				
18	0.497				
19	0.5187				
20	0.561				
21	0.569				
Eon.	0.569				

References

[1] T.E.Young et al., Nucl. Sci. Eng., 40,389(1970)

[2] G.F.Auchampaugh et al., Phys.Rev.,146,840(1966)

[3] M.S.Moore et al., Int.Conf. on Nuclear Cross Sections for Technology, p-703, Knox vill(1979)

[4] D.K.Butler et al., Phys.Rev.,124,1129(1961)

[5] H.L.Smith et al., Phys.Rev.,125,1329(1962)

[6] O.D.Simpson et al., EXFOR DATA N0.12553002(1966)

[7] P.H.White et al., IAEA Conf.on Physics and Chemistry of Fission Salzburg. p-219, 22~26 Mar 1965 Austria,

[8] P.H.White et al., EANDC(UK)-775(1966)

[9] F.Kaeppele et al., Nucl.Sci.and Eng., 51,124(1973)

[10] I.Szabo et al., 76ANL P-208, Argonne,USA,28~30 June 1976

[11] G.W.Carlso et al., Nucl. Sci. and Eng., 68,128(1978)

[12] L.W.Weston et al., Nucl. Sci.and Eng., 65,454(1978)

[13] N..Khan et al., Nuclear Instrument and method, 173, 137(1980)

[14] B.M.Aleksandrov et al., J.YK,1/50,3(1983)

[15] E.F.Fomushkin et al., YF,10,917(1969)

[16] G.F.Auchampaugh et al., Nucl.Phis/A,171,31(1971)

[17] D.W.Bergen et al., Nucl.Phis/A,163,577(1971)

[18] J.W.Behrens et al., Nucl.Sci.Eng.,66,433(1978)

[19] J.W.Meadows et al., Nucl.Sci.Eng.,68,360(1978)

[20] N.A.Khan et al., J.Nucl.Instrum. and Method,173(1980)

[21] R.Arlt et al., Int.Conf. on Nuclear Cross Sections for Technology, P-990, Knox vill(1979)

[22] M.Cance et al., Int.Conf. on Nuclear Data for Science and Technology, P-51,Antwer(1982)

[23] I.D.Alkhazovet al., Conf. on Nuclear Spectroscopy and Nuclear Structure,2,201, Moscow,USSR(1983)

[24] H.Weigmann et al., EXFOR Data 21931(1983)

[25] J.W.Meadows et al., Annals of Nuclear Energy, 15,42 (1988)

[26] L.W.Weston et al., Nucl.Sic.Eng.,68,125(1978)

[27] R.W.Hockenbury et al., USNDC-11,220(1974)

[28] CAI Chonghai et al., CNDP,24,54(2000)

[29] SHEN Qingbiao et al., CNDP,24,60,(2000)

Evaluation of Complete Neutron Data for ^{23}Na

HUANG Xiaolong

China Nuclear Data Center, CIAE, Beijing

【**abstract**】*Based on the available experimental data and combined with the UNF theoretical calculation, the complete neutron data for ^{23}Na were re-evaluated and recommended in the neutron energy range from 10^{-5} eV to 20 MeV. The evaluated cross sections were compared with CENDL-2, JENDL-3 and ENDF/B-6.*

Introduction

The natural Na has one stable isotope ^{23}Na with the abundances of 100%. Its cross sections are very useful in nuclear reactor and other applications.

In present work, the complete neutron data for ^{23}Na were re-evaluated and recommended on the basis of the available experimental data and combined with the UNF theoretical calculated results. For convenience in plotting and discussion, the total, elastic scattering, non-elastic, total inelastic scattering, (n,γ), (n,p), (n,α), (n,t), (n,2n), (n,np+d), (n,n+α) cross sections and elastic scattering angular distributions were given in this paper only. As for other evaluations, there are main three sets of evaluated data from CENDL-2, JENDL-3 and ENDF/B-6. Present evaluated cross sections were compared with them.

1 Theoretical Calculation

In order to recommend the complete neutron data for ^{23}Na, the theoretical calculation was performed with the APOM94 and UNF code.

The code APOM94 was used to automatically get the optimal parameters of optical potential for neutron reaction channels. The experimental data of total cross sections, nonelastic scattering cross sections and elastic angular distributions were used to determine the optical potential parameters. Because the total cross sections have complex structure below 1 MeV, the final set of optical potential parameters for neutron channel was obtained in the energy region 1~20 MeV.

The contributions of the direct inelastic scattering were estimated with the code DWUCK4[1]. The selection of the discrete levels and their relevant input parameters were considered according to their contributions.

The UNF code was used to calculate the data of files 3, 4, 6, 12, 13 and 15. The direct inelastic scattering distributions and the optimum set of optical potential parameters mentioned above were taken as the input data of UNF code. The additional data such as nuclear level scheme, giant dipole resonance and level density are also required.

The parameters in the input data of UNF were adjusted on the basis of the relevant experimental data in the neutron energy region 0.35~20 MeV. Some major evaluated nuclear data files were considered as references during the calculations.

2 Evaluation and Recommendation

Files 3, 4, 6, 12, 13 and 15 were given in present re-evaluations. File 3 was given on the basis of the experimental data and the theoretically calculated results. Other files were taken from the theoretically calculated results. For convenience of discussion, the total cross section, elastic scattering cross section, non-elastic scattering cross section, total inelastic scattering cross section, (n,γ), (n,p), (n,α), (n,t), (n,2n), (n,np+d), (n,n+α) cross section and elastic scattering angular distributions were considered below.

2.1 Resonance Parameter

The resolved resonance parameters were directly taken from JENDL-3 in the energy region 10^{-5} eV to 350 keV. At 350 keV energy point, present recommended total cross section and (n,γ) reaction cross section are fully consistent with JENDL-3.

2.2 Total Cross Section

There is only one new datum measured by L.Koester et al.[8] in 1990 for total cross section. Other measurements were completed before 1980. In the energies between 350 keV and 14 MeV, the evaluation was done on the basis of the experimental data of D.C.Larson et al.[9] and S.Cierjacks et al.[10], above 14 MeV, based on the experimental data of D.C.Larson et al.[9] and A.Langsford et al.[11]. The above four measurements were directly taken as the recommended data in tracing their fine structures in the energy range from 350 keV to 20 MeV(Fig. 1).

Above the resolved resonance region, there are still some structure in the energy range (0.35 MeV~9 MeV) and become smooth above 9 MeV. The recommended data in the energy range from 1 MeV to 20 MeV were used to adjust the parameters in the calculation with APOM94 code.

2.3 Nonelastic Cross Section

All the experimental data measured by G.N.Lovchikova et al.[12], V.I.Strizhak[13], K.R.Poze et al.[14] and M.V.Pasechnik[15] were used to adjust the parameters in the calculation with APOM94 code.

Fig. 2 shows the evaluations of ENDF/B-6 and present recommended data, which were taken from the sum of all cross section of nonelastic channels. The recommended data of ENDF/B-6 is from the sum of the cross section of main nonelastic channels. Thus present evaluations are not in complete agreement with ENDF/B-6.

2.4 Elastic Scattering Cross Section

All the measurements were completed before 1980. And there are large discrepancies among these measurements. So the recommended elastic scattering cross section was obtained by subtracting the non-elastic cross section from the total cross section.

In Fig. 3 the evaluation of present work, JENDL-3 and CENDL-2 is given.

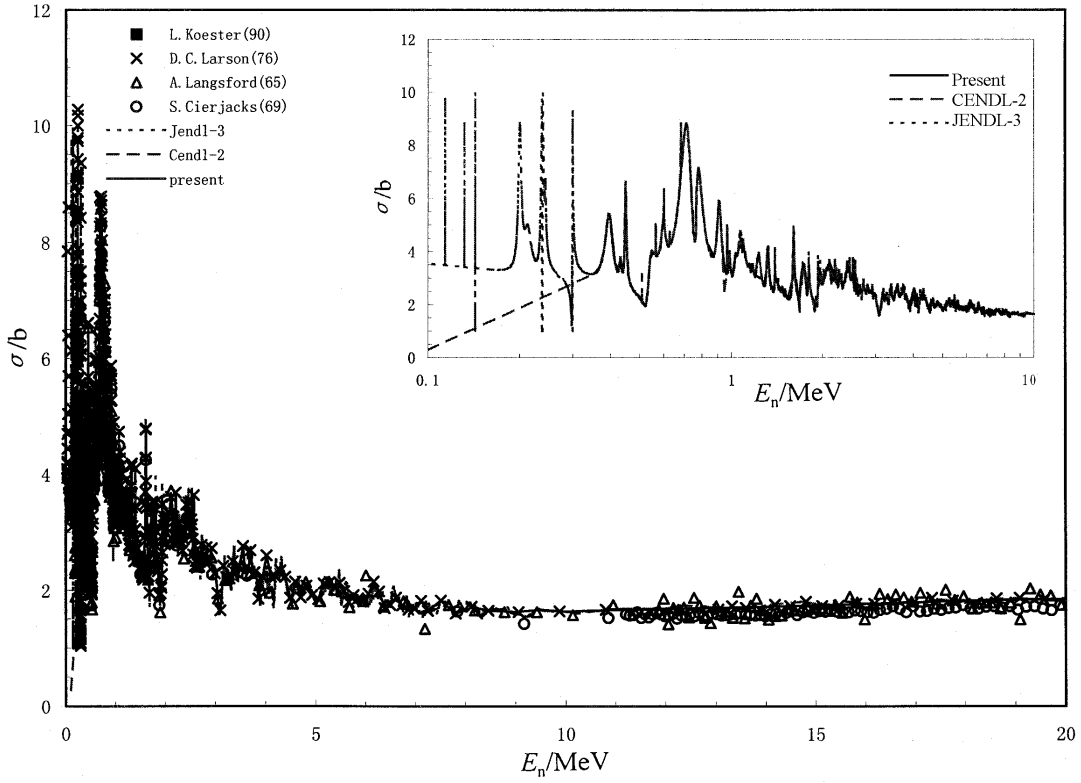

Fig. 1 The total cross section of n+^{23}Na reaction

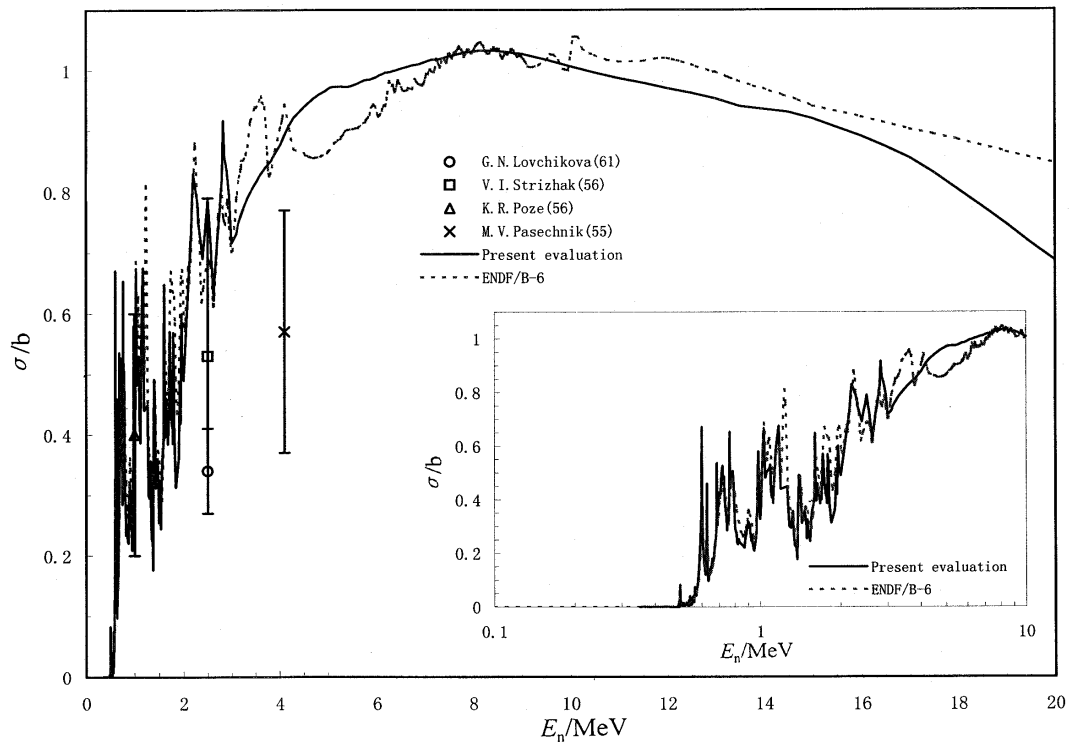

Fig. 2 The nonelastic cross section of n+^{23}Na reaction

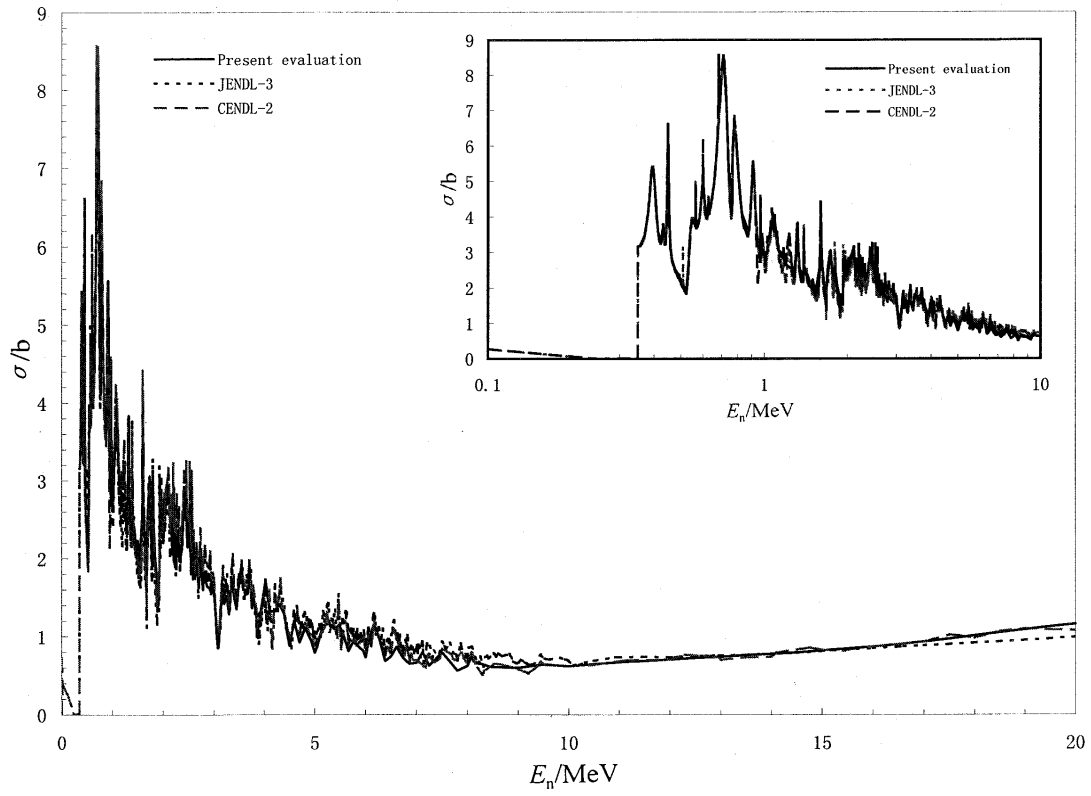

Fig. 3 The elastic cross section of n+^{23}Na reaction

2.5 (n,p) Cross Section

Below 11MeV, the evaluations were done based on the experimental data measured by H.Weigmann et al.[36], R.Bass et al.[37] and C.F.Williamson [39]. Above 14 MeV, the evaluations are from the fitting results of all measurements[27,39,43,44,45]. Between 11 MeV and 14 MeV, the recommended data were got by eye-guide. At 11 MeV and 14 MeV energy point, the data got by eye-guide are consistent well with the evaluated ones (Fig. 4).

2.6 (n,α) Cross Section

Below 11 MeV, the evaluations were done based on the experimental data measured by H.Weigmann et al.[36], R.Bass et al.[37], C.M.Bartle[38] and C.F. Williamson[39]. Above 14 MeV, the evaluations are from the fitting results of all measurements[27,39~45]. Between 11 MeV and 14 MeV, the recommended data were got by eye-guide. At 11 MeV and 14 MeV energy point, the data got by eye-guide are completely consistent with the evaluated ones (Fig.5)

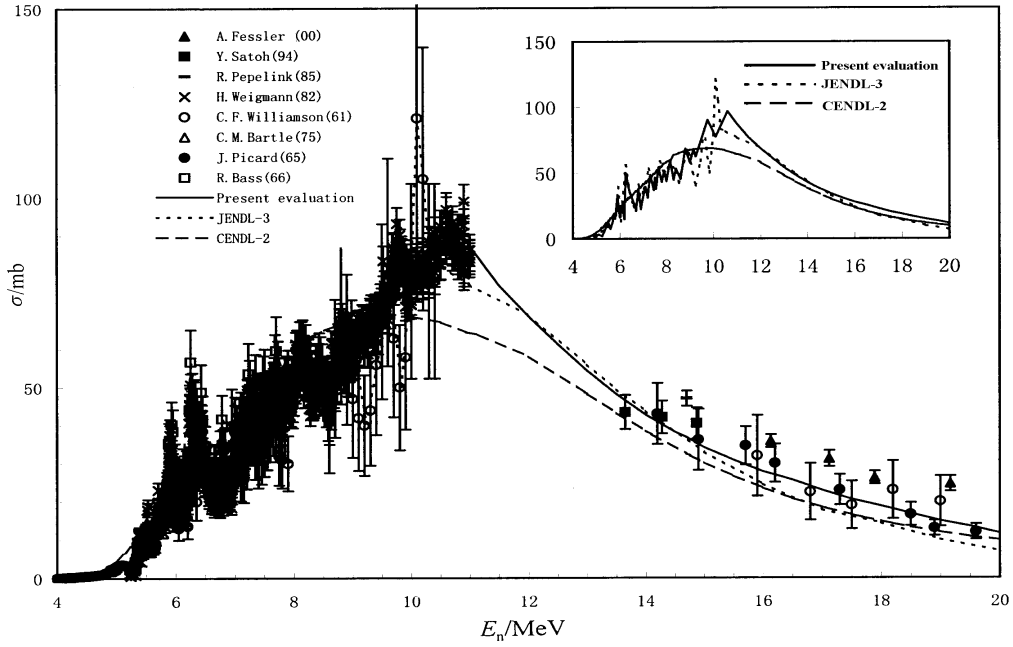

Fig. 4 The cross section of ^{23}Na(n,p) ^{23}Ne reaction

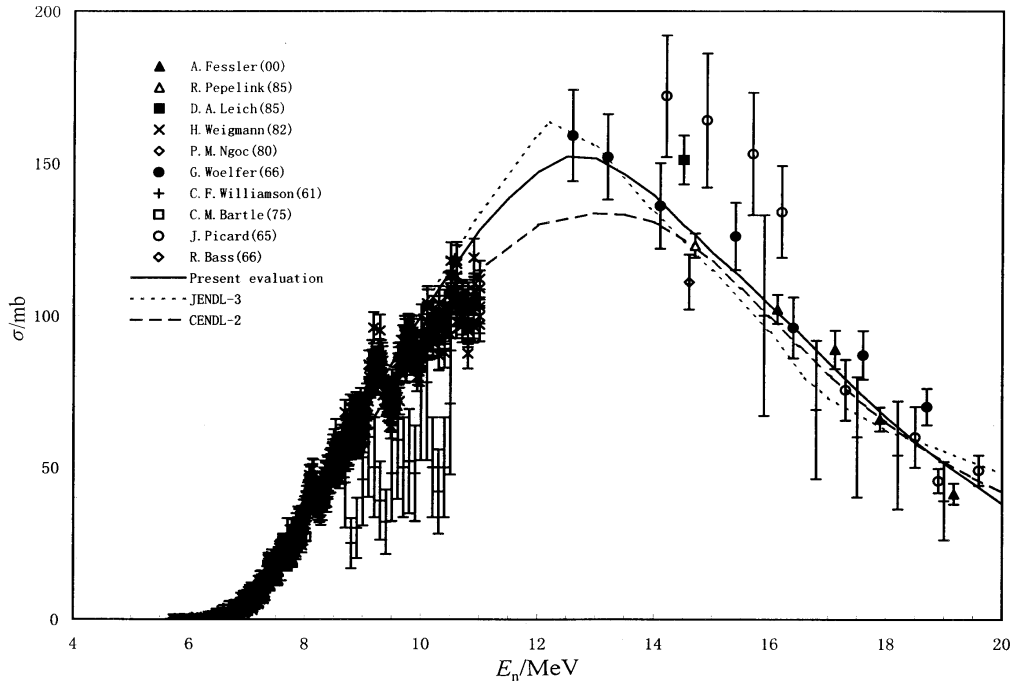

Fig. 5 The cross section of ^{23}Na(n,α) ^{20}F reaction

2.7 Inelastic Cross Section

16 discrete levels were adopted in the theoretical calculations. And the direct contribution was calculated by using the code DWUCK4 for the five lowest levels. The inelastic scattering cross section to the first level (MT=51, ε_n=0.44 MeV) was evaluated on the basis of the experimental data of J.H.Towle et al.[5], D.R.Donati et al.[16], D.A.Lind et al.[17], J.P.Chien et al.[18] and H.Maerten et al.[19] below 3 MeV and the UNF calculations above 3 MeV. For the inelastic scattering cross section to the other levels (MT=52~65) were recommended the data calculated by UNF.

The continuum part was calculated by using UNF code. The recommended total inelastic scattering cross section was the sum of the continuum part and the cross section of inelastic scattering to 15 discrete levels, which shown in Fig. 6. Above 3 MeV, present evaluations are from the results of theoretical calculations because there are large discrepancies among the measurements. So present evaluation doesn't exist some structure above 3 MeV energy region.

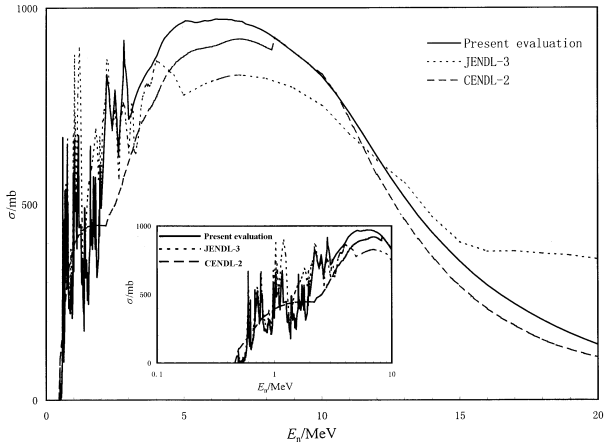

Fig. 6 The inelastic cross section of n+^{23}Na reaction

2.8 (n,γ) Cross Section

In Fig.7 the (n,γ) reaction cross section was presented. The evaluation of JENDL-3 was adopted below 350 keV and the UNF calculated result was taken above 350 keV. At 350 keV energy point, present evaluation is completely consistent with the result of JENDL-3.

2.9 (n,2n) Cross Section

For (n,2n) reaction the experimental data above 15 MeV are conflicting and can be divided into two groups. The evaluation of Lu Hanlin et al.[35] was directly taken as the present recommendation (Fig.8).

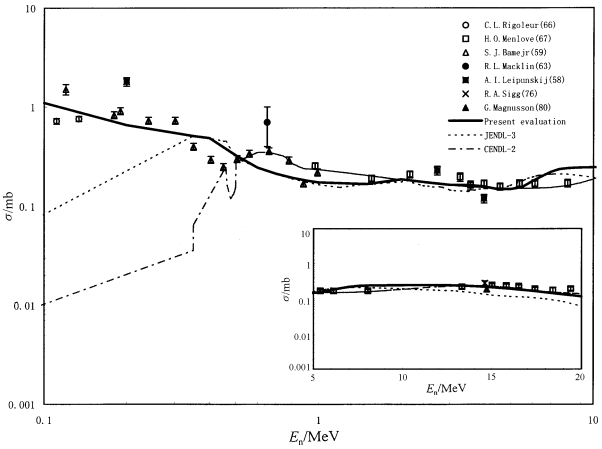

Fig. 7 The cross section of ^{23}Na(n,gamma) ^{24}Na reaction

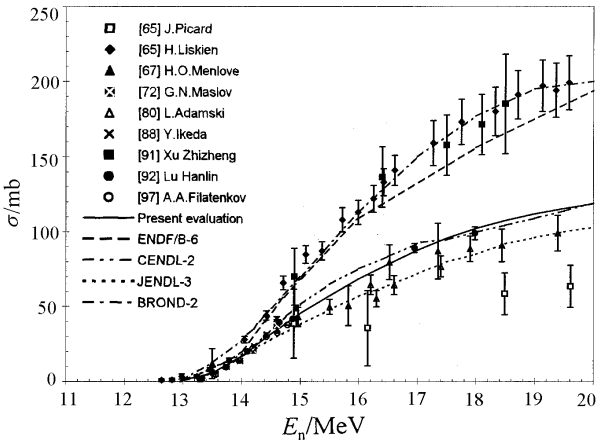

Fig. 8 The cross section of ^{23}Na(n,2n) ^{22}Na reaction

2.10 (n,t) Cross Section

The calculated results were normalized to the experimental data measured by D.A.Leich et al.[41] at 14.5 MeV. And the normalized data were taken as the recommended ones (Fig.9).

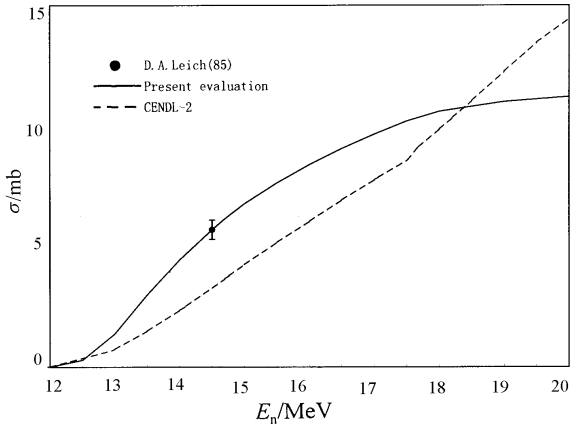

Fig. 9 The cross section of ^{23}Na(n,t) ^{21}Ne reaction

2.11 (n,np+d) Cross Section

The calculated results were normalized to the experimental data measured by D.A.Leich et al.[41] at 14.5 MeV. And the normalized data were taken as the recommended ones (Fig.10).

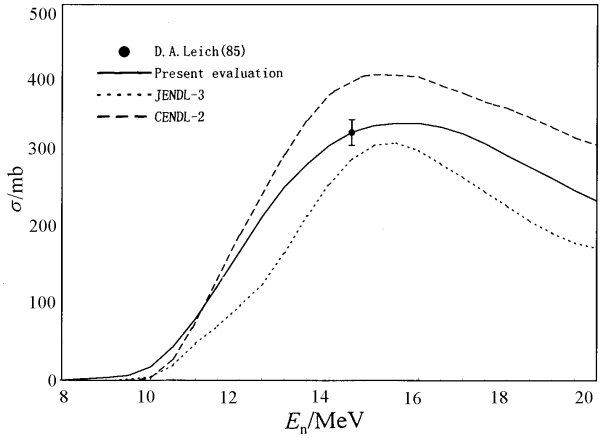

Fig. 10 The cross section of ^{23}Na(n,np+d) ^{22}Ne reaction

2.12 (n,n+α) Cross Section

The recommended data are taken from the theoretical calculated results.

2.13 Elastic Scattering Angular Distribution

The experimental data measured by P.Kuijper et al.[2], F.G.Perey et al.[3], U.Fasoli et al.[4], J.H.Towle et al.[5], T.H.Schweitzer et al.[6] and R.E.Coles[7] were used to adjust the parameters in the calculation with APOM94 code. The calculated results are in agreement with the measured data and taken as the recommended data. Some energy points were plotted and shown in Fig.11.

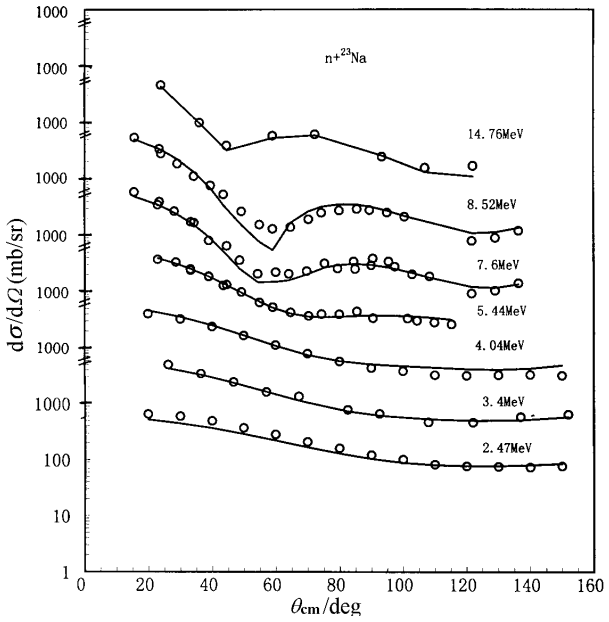

Fig. 11 The elastic scattering angular distribution of n+^{23}Na reaction

3 Summary

The complete neutron data for ^{23}Na are re-evaluated and recommended in the neutron energy range from 10^{-5} eV to 20 MeV. And the cross sections are compared with CENDL-2 and JENDL-3. Present evaluated data have some improvements compared with these two libraries.

As there is little measurements in last years, the reliability of present recommendation will have much room for improvements by the new measurement in the future. Nevertheless the present evaluations are still reasonable.

Acknowledge

The author appreciates Prof. Lu Hanlin for the useful discussions and kind helps in experimental data analysis and Prof. Zhang Jinshang and Shen Qingbiao for providing UNF code and APOM94 code.

Reference

[1] P.D.Kunz, DWBA code DWUCK4, University of Colorado(unpublished).
[2] P.Kuijper et al., Nucl. Phys. 181, 545(1972).
[3] F.G.Perey et al., ORNL-4518,1970.
[4] U.Fasoli et al., Nucl. Phys. A125, 227(1969).
[5] J.H.Towle et al., Nucl. Phys. 32, 610(1962).
[6] T.H.Schweitzer et al., IAEA-190, 243(1976).
[7] R.E.Coles, AWRE-O-03/71, 1971.
[8] L.Koester et al., Z.Phys. A337, 341(1990).
[9] D.C.Larson et al.,ORNL-TM-5614,1976.
[10] S.Cierjacks et al., KFK-1000, 1969.
[11] A.Langsford et al., 65Antwerp Conf. 529, 1965.
[12] G.N.Lovchikova et al., NEJTRONFIZ, 294(1961).
[13] V.I.Strizhak, Soviet Phys. 31, 907(1956).
[14] K.R.Poze et al., Soviet Phys. 3, 745(1956).
[15] M.V.Pasechnik, 55GENEVA, 2, 3(1955).
[16] D.R.Donati et al., Phys. Rev. C16, 939(1977).
[17] D.A.Lind et al., Ann. Phys. 12, 485(1961).
[18] J.P.Chien et al., Nucl. Sci. Eng. 26, 500(1966).
[19] H.Maerten et al., Nucl. Sci. & Eng., 114, 352(1993).
[20] C.L.Rigoleur et al., J.Nucl. Energy 20, 67(1966).
[21] H.O.Menlove et al., Phys. Rev. 163, 1299(1967).
[22] S.J.Bamejr et al., Phys. Rev. 113, 256(1959).

[23] R.L.Macklin et al., Phys. Rev. 107, 504(1957).
[24] A.I.Leipunskij et al., 58GENEVA, 15, 50(1958).
[25] R.A.Sigg, Thesis, 1976.
[26] G.Magunsson et al., Phys. Scripta 21, 21(1980).
[27] J.Picard et al., Nucl. Phys., 63, 673(1965).
[28] H.Liskien et al., Nucl. Phys., 63, 393(1965).
[29] G.N.Maslov et al., Report YF-9, 50, 1972.
[30] L.Adamski et al., Ann. Nucl. Energy, 7, 397(1980).
[31] Y.Ikeda et al., JAERI-1321, 1988.
[32] XU Zhizheng et al., 91Juelich Conf., Germany, 1991.
[33] LU Hanlin et al., J. Nucl. Phys., 14, 83(1992).
[34] A.A.Filatenkov et al., INDC(CCP)-402, 1997.
[35] LU Hanlin et al., C.J.Nucl. Phys. 14, 83(1992).
[36] H.Weigmann et al., 82ANTWER, 814, 1982.
[37] R.Bass et al., EANDC(E)-66, 64(1966).
[38] C.M.Bartle, Nucl. Instr. Meth. in Phys. Research 124, 547(1975).
[39] C.F.Williamson, Phys. Rev. 122, 1877(1961).
[40] G.Woelfer et al., Z. Phys. 194, 75(1966).
[41] D.A.Leich et al., 85HOUSTON Conf., 1985.
[42] P.M.Ngoc et al., ZFK-410, 192(1980).
[43] R.Pepelink et al., NEANDC(E)-262E, 1985.
[44] Y.Satoh et al., JAERI-95-008, 189(1994).
[45] A.Fessler et al., Nucl. Sci. & Eng. 134, 171(2000).

Evaluation of Neutron Cross Section for Isotopes ^{93,95}Nb and ^{99,100}Ru

SU Weining ZHAO Jingwu

Department of Physics, Nanjing University, Nanjing, 210093

Introduction:

Isotopes^{93,95}Nb and ^{99,100}Ru are important in nuclear physics and nuclear technology. Their data were given in libraries JENDL-3,ENDF/B-6 and JEF-2. The data of JENDL-3 are better. But comparing with the new experimental data, some of them are still deviated from the experiment data. The data were reevaluated and, as a result, they were improved.

1 Total Cross Section

For ^{93}Nb, nineteen sets of experimental data[1~19] were available. The data extended to 20 MeV. The data of Green are consistent with other experiments below 9 MeV. The data of Seth's is a little low at the low energy region, and consistent with other experimental data in the whole remained energy region. At 14 MeV, Seth's data are agreed with Coon's.

Because there are no experimental data for ^{99,100}Ru, the experimental data[1~20] of natural Ru were used. The first one is in the energy range 2MeV~14MeV (Foster). The second one is in the energy range 100 keV~800 keV (Divadeenam).

The calculated results of SUNF are coincidental with experimental data and are recommended for isotopes ^{93,95}Nb and ^{99,100}Ru. The same results are used for isotopes ^{93,95}Nb and ^{99,100}Ru respectively. The upper limit of resonance range is 100 keV and to make the conjunction between smooth and resonance range, resonance parameters were adjusted.

Fig. 1 shows the result comparing with JENDL-3 and ENDF/B-6 for ^{99,100}Ru.

2 (n,2n) Cross Section

There are eight sets of experimental data[21~28] for ^{93}Nb. At near 14 MeV, the data of Haering, Hermsporf and Lychagin agree with each other well. Paulsen's datum is at 17 MeV, which agrees with Veeser's. There are enough data for fitting, the fitted data were recommended.

There are no experimental data available for ^{95}Nb and ^{99,100}Ru, the calculated data were recommend.

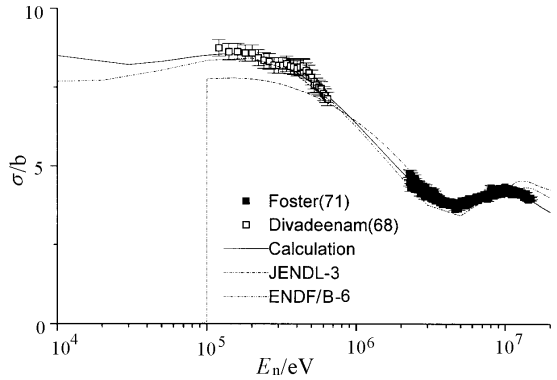

Fig.1 Total cross section for ^{99,100}Ru

3 (n,3n) Cross Section

There is only a set of experimental data[21] for ^{93}Nb. The fit curve was recommended.

There are no experimental data for ^{95}Nb and ^{99,100}Ru, the calculated data were recommended.

4 (n,α) Cross Section

There are seven sets of experimental data for ^{93}Nb[29~35]. At around of 14 MeV, the data of Mormann, Fischer and Kulisic's agree with each other. Tewes's data are higher than that of others above 12 MeV. Experimental data were fitted and the fitted result was recommended. In Fig. 2 is shown the evaluated result comparing with JENDL-3 and ENDF/B-6.

There are no experimental data for ^{95}Nb and ^{99,100}Ru, the calculated data were recommended.

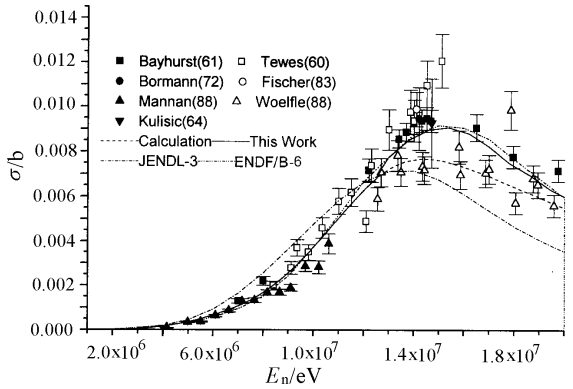

Fig.2 (n,α) cross section for ^{93}Nb

5 (n,t) Cross Section

There are two sets of experimental data[36,37] for ^{93}Nb. The datum of Sudar's is at 14 MeV, and consistent with to Qaim's. The fit curve was recommended. In Fig. 3 is shown the evaluation result comparing with ENDF/B-6 for ^{93}Nb.

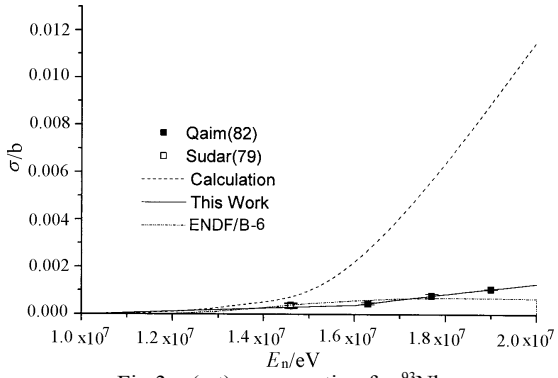

Fig.3 (n,t) cross section for ^{93}Nb

There is no experimental data for ^{95}Nb and ^{99,100}Ru, the calculated data were recommend.

6 (n,γ) Cross Section

There are fourteen sets of experimental data[38~51] available for ^{93}Nb. Rigaud's datum is at energy 14 MeV. It was used to revise the calculated data. The other data are consistent well with each other. They were used to improve the calculated data in the energy region from 1 MeV to 3 MeV. In the other energy region, the experimental data are consistent with calculation. The resonance parameters were adjusted to make the data conjunct at the upper resonance limit 100 keV. In Fig. 4 is shown the evaluation result comparing with JENDL-3 and ENDF/B-6 for ^{93}Nb.

There is no experimental data for ^{95}Nb and ^{99,100}Ru, the calculated data were recommend.

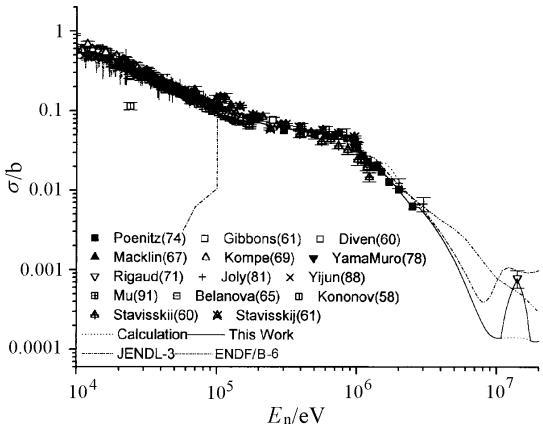

Fig.4 Capture cross section for ^{93}Nb

7 (n,p) Cross Section

There are two sets of experimental data[52,53] for ^{100}Ru, Prasad's is only one point at 14 MeV. The two

sets of data are deviated with each other. The calculated data were recommended which are consistent with Kasygai's data. In Fig. 5 is shown the evaluation result of comparing with JENDL-3 for ^{100}Ru.

There is no experimental data available for ^{99}Ru and ^{93,95}Nb, the calculated data were recommend.

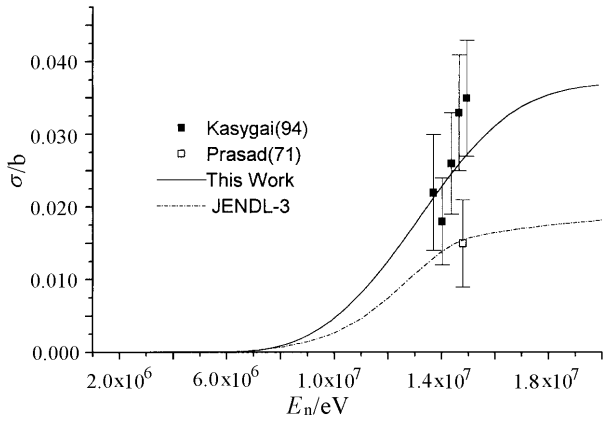

Fig.5 (n.p) cross section for ^{100}Ru

8 The Other Cross Sections

For isotopes ^{93,95}Nb, there are no experimental data for (n,nnp), (n,nα), (n,p), (n,d), (n,He) and (n,n') reactions and inelastic scattering to discrete level. For isotopes ^{99,100}Ru, there is no experimental data for (n,2n), (n,3n),(n,nnp), (n,nα), (n,t), (n,d), (n,^{3}He), (n, α) and (n,n') reactions and inelastic scattering to discrete level. The calculated data were recommended for all of these reactions. Non-elastic cross section is the summation of all nonelastic channel cross sections. Elastic cross section was obtained by subtracting non-elasticity cross section from total cross section.

References.

[1] D.G.Foster et al., Phys.Rev./C,3,576,1971
[2] L.Green et al., R,WaPd-TM-1073,1973
[3] A.B.Smith et al., J,ZP,264,379,1973
[4] J.H.Coon et al., Phys. Rev., 88, 562, 1952
[5] A.D.Carlson et al., Phys.Rev.,158,1142,1967
[6] H.W.Newson et al., Phys. Rev., 105, 198, 1957
[7] D.W.Miller et al., Phys. Rev., 88, 83, 1952
[8] K.K.Seth et al., J,PL,16,306,1965
[9] K.K.Seth et al., Phys. Rev., 110, 692, 1958
[10] W.P.Poenitz et al., R,ANL-NDM-80,1983
[11] R.W.Finlay et al., Phys Rev./C, 47, 237, 1993
[12] F.Manero, J,ARS,64,373,1968
[13] R.E.Coles, R,AWRE-O-66/71,1971
[14] C.A.Uttley et al., C,66PARIS, 1, 165, 1966
[15] O.Aizawa et al., C,85SANTA, 1, 561, 1985
[16] V.V.Filippov et al., C,68DUBNA,ASS-68/17, 1968
[17] V.V.Filippov, C,83KIEV,3,107,1983
[18] B.Ya.Guzhovskiy et al., C, 94 GATlIN,, 254,1994
[19] G.V.Gorlov et al., J,YF, 6, 910, 1967
[20] M.Divadeenam et al., J,DA/B, 28, 3834, 1968
[21] L.R.Veeser et al., Phys. Rev./C, 16, 1792, 1977
[22] A.Paulsen et al., J,ZP,238,23,1970
[23] J.Frehaut et al., W,FREHAUT,1980
[24] D.S.Mather et al., R,AWRE-O-72/72,, 1972
[25] M.Haering et al., J,ZP,244,352,1971
[26] D.Hermsdorf et al., J,JNE, 27, 747, 1973
[27] A.A.Lychagin et al., r,FEI-1385, 1983
[28] G.A.Prokopets, J,YF,32,(1),37,1980
[29] B.P.Bayhurst et al., J,JIN,23,173,1961
[30] H.A.Tewes et al., R,UCRL-6028-T, 1960
[31] M.Bormann et al., Nucl. Phys./A, 186, 65,1972
[32] R.Fischer et al., J, ANE, 9,409, 1983
[33] A.Mannan et al., Phys.Rev./C,38,(2),630,1988
[34] R.Woelfle et al., J,ARI,39,(5),407,1988
[35] P.Kulisic et al., Nucl.Phys.,54,17,1964
[36] S.M.Qaim et al., Phys. Rev./C, 25,(1), 203, 1982
[37] S.Sudar et al., Nucl.Phys./A,319,157,1979
[38] W.P.Poenitz, R,ANL-NDM-8,1974
[39] J.H.Gibbons et al., Phys. Rev., 122, 182, 1961
[40] B.C.Diven et al., Phys. Rev., 120, 556, 1960
[41] R.L.Macklin et al., Phys.Rev.,159,1007,1967
[42] D.Kompe, Nucl.phys./A,133,513,1969
[43] N.Yamamuro et al., J,NST,15,637,1978
[44] F.Rigaud et al., Nucl. pev./A, 173, 551, 1971
[45] S.Joly et al., R,CEA-R-5089,1981
[46] XIA Yijun et al., J,CNp, 10, (3), 227, 1988
[47] Yunshan mu et al., J, NSE, 108, (3), 302,1991
[48] T.S.Belanova et al., J,AE, 19, (1), 3, 1965
[49] V.N.Kononov et al., J,AE, 5, 564,1958
[50] Yu.Ya.Stavisskii et al., J,AE,9,401,1960
[51] Ju.Ja.Stavisskij et al., J,AE,10,(3),264,1961
[52] Y.Kasugal et al., C, 94GATLIN,, 935, 1994
[53] R.Prasad et al., J,NC/A,3,(3),467,1971

Internal Conversion Electron Data Calculation

ZHOU Chunmei HUANG Xiaolong WU Zhendong

China Nuclear Data Center,CIAE, Beijing

【**abstract**】*Calculation method of internal conversion electron energy and their absolute intensity in γ transition is introduced briefly, and its application is also given by using ^{232}Th decay as example.*

For nuclear decay, nucleus is in its excited states. It deexcites by means of emitting γ-rays, and decays to its ground state. During deexcitation, the transition energy may be transferred to the electrons in different atomic-electronic shells outside nucleus by Coulomb interaction between a nucleus and its surrounding atomic electrons. For the γ transitions, there are γ rays emitted and competing internal conversion electrons. These electrons are called as internal conversion electrons in γ transitions. The calculation method of internal conversion electron energy and its absolute intensity in γ transition is introduced briefly, and its application is also given by using ^{232}Th decay as example.

1 Calculation Method

1.1 Internal Conversion Electron Energy Calculation

In order to calculate the internal conversion electron energy, it is assumed that γ transition energy is E_γ, atomic-electron binding energy in i-th atomic-electronic shell is E_i, emitting electron energy from i-th atomic-electronic shell is E_{ei}. According to the basis of energy balance, then

$$E_{ei}=E_\gamma-E_i \tag{1}$$

where, i=K,L,M,N,..., atomic-electronic shell.

The data of atomic-electronic binding energies E_i in different shells for different elements (different nuclear proton numbers Z) have been evaluated and can be taken from reference [1]. These atom-electronic binding energies are tabulated for different elements (nuclear proton number Z) and in different atomic-electronic shells (K,L,M,N,..., shell).

1.2 Internal conversion electronic absolute intensity calculation

Assumed that absolute intensity of E_γ in nuclear decay is P_γ, its internal conversion coefficients are α_i (i=K,L,M,N,.., shell), and absolute intensities of internal conversion electrons are P_{ei}, then

$$P_{ei}=P_\gamma\cdot\alpha_i \tag{2}$$

Obviously, the following expression can be easy deduced from Eq. (2)

$$P_e=\sum_i P_{ei}=\sum_i P_\gamma\cdot\alpha_i=P_\gamma\sum_i\alpha_i=P_\gamma\cdot\alpha \tag{3}$$

$$\alpha=\sum_i\alpha \tag{4}$$

Where α is total internal conversion coefficient for E_γ transition; P_e is total internal conversion electronic absolute intensity (photon numbers per 100 parent decays).

1.3 Internal Conversion Coefficients Calculation

As mentioned above, in order to calculate internal conversion electronic intensities of different shells and their total intensity, their partial and total conversion coefficient α_i, α must be known.

The internal conversion coefficient data of different elements (different nuclear proton numbers Z) in different atomic-electronic shells have been evaluated[2]. In the tables and charts the γ transition energies, their transition electric and magnetic multiplicities are given. The code HSICC has been written to calculate the internal conversion coefficients[3]. The calculation is based on spline-fitting method interpolating.

1.4 γ-ray Absolute Intensity Calculation

In order to calculate the electronic intensities, the γ-ray absolute intensity P_γ must be known. Usually the relative intensities of radionuclide are measured. The γ-ray absolute intensities are required in practical applications. So the normalization factor N (multiplier for conversing relative photon intensity to photons per 100 decays of parent through the decay branching) of γ-ray intensities must be known in decay data evaluations by using data analysis and calculation. The γ-ray absolute intensities (γ-ray emitting probabilities per 100 parent decays) can be calculated by using the normalization factor.

At present, Table of Isotopes (8-th edition) (1996) by R.B.Firestone et al. is the best evaluated decay data collection. The relative γ-ray intensities and normalization factor of all radionuclei are given in this book. The data can be retrieved from Evaluated Nuclear Structure Data File (ENSDF), which are done by the evaluators of International Network of Nuclear Structure and Decay Data Evaluation from different countries.

1.5 Main Calculation Codes and Calculation Flow Chart

The main calculation codes and their functions are listed in the Table 1. These codes are mainly from International Network of Nuclear Structure and Decay Data Evaluation.

In Fig. 1, flow chart of internal conversion electronic energies and their absolute intensities calculation is given. There are three steps:

(1) Start. Evaluated nuclear decay data file, atomic-electronic binding energies data file and evaluated internal conversion coefficients data file are prepared in the required format of calculation codes;

(2) Calculation. At first, internal conversion coefficients and γ-ray emitting absolute intensities for each γ-ray are calculated. Then internal conversion electronic energies and their absolute intensities are calculated;

(3) Output. The results of calculations are output in tables and drawings, respectively.

2 Application

The application of internal conversion electronic data calculation are shown by taking ^{232}Th decay ($T_{1/2}$=14.05×10^9 a) as an example. The data[5] are given in Table 2, and the scheme is shown in Fig.2[5].

From Table 2, it can be seen that the normalization factor of γ-ray relative intensities is 1.0, and other data relative to internal conversion electronic data calculation are also given.

The internal conversion coefficients are calculated by using HSICC code. The energies of internal conversion electrons can be got by using formula (1) on the basis of γ-ray energy in Table 2 and atomic-electronic binding energies of different shells of ^{232}Th. The absolute intensities of internal conversion electrons are calculated by using formula (2) from data in Table 2. In Table 3, radiation data of ^{232}Th decay are given, in which are included the radiation data of α, γ, and their internal conversion electrons. From Table 3 it can be seen that the electronic intensities calculation is very important for heavy nucleus.

In Fig. 2, the γ-ray energies, intensities, their multipolarities and total internal conversion electron intensities are given.

Table 1 Main codes and their functions of electronic data calculation

Codes name	Functions
HSICC	calculation of internal conversion coefficients
GABS	calculation of γ intensity normalization factor
RADLST	calculation of internal conversion electronic data
ENSDAT	table and drawing of data output

Table 2 γ-ray data of ^{232}Th decay

E_γ/keV	E_L/keV	I_γ	γ-mult.	Internal Conversion Coefficients				
				α_K	α_L	α_M	$\alpha_{N...}$	α
63.81±0.01	63.82	0.263±0.013	E2		59.92	16.22	5.824	82.0
140.88±0.01	204.69	0.021±0.004	E2	0.287	1.47	0.399	0.145	2.30

I_γ absolute intensities, multiplied 1.0, per 100 parent decays.

Table 3 Radiation data of ^{232}Th decay

Radiation type	Energies/keV		Absolute intensities / %	
α_1	3830.	10	0.063	10
α_2	3950.	8	21.7	13
α_3	4012.3	14	78.2	13
γ_1	63.810	10	0.263	13
eCe_{1L}	44.573	10	15.8	10
eCe_{1M}	58.988	10	4.27	25
eCe_{1N}	62.602	10	1.53	9
γ_2	140.880	10	0.021	4
eCe_{2K}	36.958	13	0.0060	12
eCe_{2L}	121.643	10	0.031	6
eCe_{2M}	136.058	10	0.0084	17
eCe_{2N}	139.672	10	0.0030	6

eCe_{1L} is a emitting electron of L -shell from γ_1-ray.

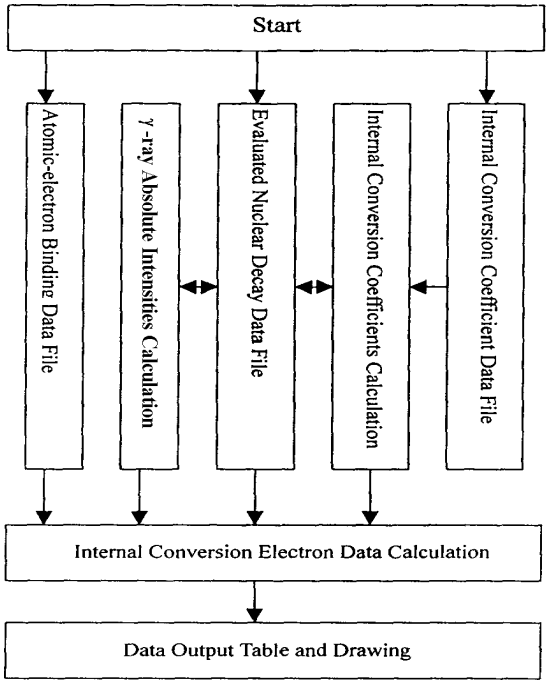

Fig. 1 Flow chart of internal conversion electronic data calculation

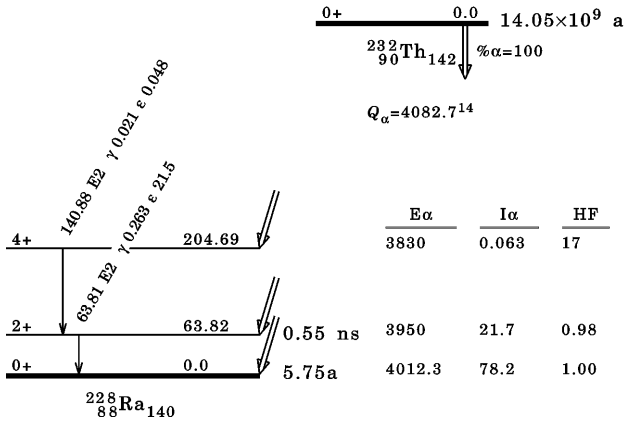

Fig. 2 ^{232}Th decay scheme

It is noted that in Fig. 2, γ0.263 is γ-ray intensity 0.263, and ε21.5 is total internal conversion electronic intensity 21.5.

3 Conclusion

The calculation method of internal conversion electronic energies and their absolute intensities is given.

In general, the error propagation method is adopted in the uncertainty calculation. The uncertainties in table 3 were calculated on the basis of error propagation method.

References

[1] F.B.Firestone, et al., Table of Isotopes (8-edition) (1996), Atomic-Electron Binding Energies, P.F37-F39.

[2] F.B.Firestone, et al., Table of Osotopes (8-edition) (1996), Theoretical Internal conversion Coefficients, P.F1-F32.

[3] T.W.Burrows, ENSDF Physics Analysis Programs, Private communications (1998).

[4] F.B.Firestone, et al., Table of Isotopes (8-edition) (1996), Vol.I A=1-150, Vol. II A=151-266.

[5] A.Artna-Cohen, Nuclear Data Sheets, 80, 723 (1997).

Evaluation of Neutron Cross Section Data for ^{121,123}Sb and ^{127,135}I

ZHAO Jingwu SU Weining

Department of Physics, Nanjing University, Nanjing

Introduction

The data of isotopes, ^{121,123}Sb and ^{127,135}I were evaluated in several evaluated nuclear data libraries. But there are some discrepancies in these libraries. The data of JENDL-3 is better than others and contain all files. Even so the data of JENDL-3 are also disagree with the experimental data, especially new ones. The neutron cross sections were reevaluated in this work. This evaluation is based on both experimental data and calculated data with SUNF code and compared with the experimental data and other evaluated data from JENDL-3, ENDF/B-6.

1 Total Cross Section

There are no any experimental data for ^{121,123}Sb. The experimental data of natural Sb were used. Except for the data in low energy range, there are only thirteen sets of experimental data[1~13], of which the three from Miller[7], Bockelman[9] and Tabony[11] are disperse, the other ten are consistent with each other in energy range 100 keV to 20 MeV. These data were fitted by polynomial. The calculated data were recommended in the energy range above 14 MeV.

There are over twenty sets of experimental data for ^{127}I. Except for the data in low energy range, there are only seven sets of experimental data available. The data from Foster[1], Manero[14], Gorlow[15] and Miller[7] are consistent with each other in high energy range and are also consistent with the data from Angeli[16] at 14 MeV. The data from Bockelman[9] and Merrison[17] are consistent with each other in low energy range and are also consistent with the data from Miller at 1 MeV. The data were fitted with polynomial. The calculated data are recommended in the energy range above 14 MeV.

Due to no experimental data for ^{135}I, the calculated data were recommended.

In Fig.1 is shown the evaluated result and compared with JENDL-3 and ENDF/B-6 for natural Sb.

In Fig.2 is shown the evaluated result and compared with JENDL-3 and ENDF/B-6 for ^{127}I.

2 (n,2n) Cross Section

There are seven sets of experimental data[18~24] for ^{121}Sb. The data of Ref. [18] is too low. The data[22,23] are not consistent with each other at 14 MeV. The average value was recommended at 14 MeV. The data of Ref. [24] are unreasonable (under threshold energy). The three sets of remained data determine the shape of cross section curve and were fitted by polynomial.

There are seven sets of experimental data[21~23,25~28] for ^{123}Sb. The data of Ref. [22] is too large. The experimental of Ref. [23,24,27,28] are not consistent with each other at 14 MeV. The average value was recommended at 14 MeV. The other two sets of experiment data determine the shape of cross section curve and were fitted by polynomial. In Fig. 3 is shown the evaluated result and compared with JENDL-3 for ^{123}Sb.

There are fourteen sets of experimental data for ^{127}I. The data of Martin[29] and Bormann[30] are in the low group and are thought to be the cross sections to ground state or isometric state. The data from Paul[31] and Qaim[32] are with the same error. The data of ref. [33~39] are consistent with each other at 14 MeV. The data from Santry[40] and Lu Hanlin[41] determine the shape of the cross section curve and are consistent with the data from Cohen[42] near threshold energy. The data were fitted by polynomial. In Fig. 4 is shown the evaluated result for ^{127}I.

Due to no experimental data for ^{135}I, the calculated result was recommended.

3 (n,γ) Cross Section

There are eight sets of experimental data[24,43~49] in low energy for ^{121}Sb. Two of them[24,43] are too low or too high. The other six sets of data are consistent with each other and were fitted by polynomial. The calculated result with SUNF code was recommended in the energy region above 3 MeV.

There are five sets of experimental data[43,45~47,50] in low energy for ^{123}Sb. The data of Ref. [32] is too large at 14 MeV. The data of Ref. [43,47] are too high or too low. The data were fitted by polynomial. The calculated result was recommended in the energy region above 3 MeV. In Fig. 5 is shown the evaluated result and compared with JENDL-3 and ENDF/B-6.

There are over sixty sets of experimental data for ^{127}I. Except for the experimental data in low energy range, there are still 23 sets of data available. Most of the data[51~60] are in the range below 3 MeV. The data from Humme[51], Martin[52] and Brzosko[53] are discrepant, the others are consistent with each other. The data from Johnsrud[62] extend to 5 MeV and the data from Brzosko to 4 MeV. The data of Refs. [61~65] are at 14 MeV. The recommended datum is 1mb at 14 MeV. The data were fitted by polynomial. In Fig. 6 is shown the evaluated result for ^{127}I.

Due to no experimental data for ^{135}I, the calculated result with SUNF code was recommended.

4 (n,3n) Cross Section

There are two sets of experimental data for ^{127}I. The datum from Qaim[32] is at near threshold energy and is extremely large. The data from Liskien[66] was taken. The calculated data were recommended, which is passed through the experimental data.

Due to no experimental data for ^{135}I and ^{121,123}Sb, the calculated result with SUNF code was recommended.

5 (n,p) Cross Section

There are two sets of experimental data for ^{127}I. The data from Allan[67] is too low and the data from Coleman[68] were taken. The calculated data were recommended, which is passed through the experimental data.

Due to no experimental data for ^{135}I and ^{121,123}Sb, the calculated result with SUNF code was recommended.

6 Other Cross Section

There are no experimental data for (n,np), (n,na), (n,t), (n,d), (n,^{3}He), (n,α), (n,n') and inelastic scattering to discrete level for ^{121,123}Sb and ^{127,135}I. The calculated data were recommend. Nonelastic cross section was the summation of all nonelastic channel cross sections. Elastic cross section was obtained by subtracting the nonelastic cross section from total cross section.

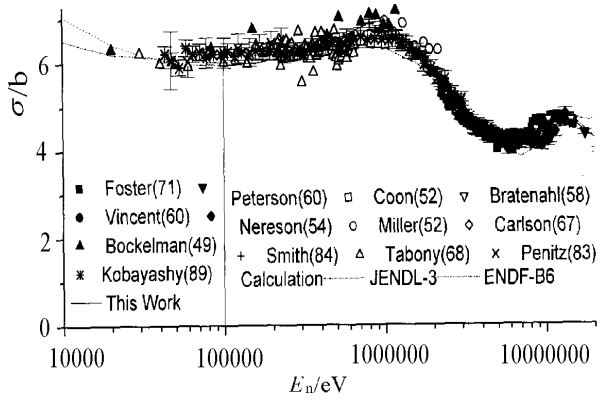

Fig. 1 Natural Sb total cross section

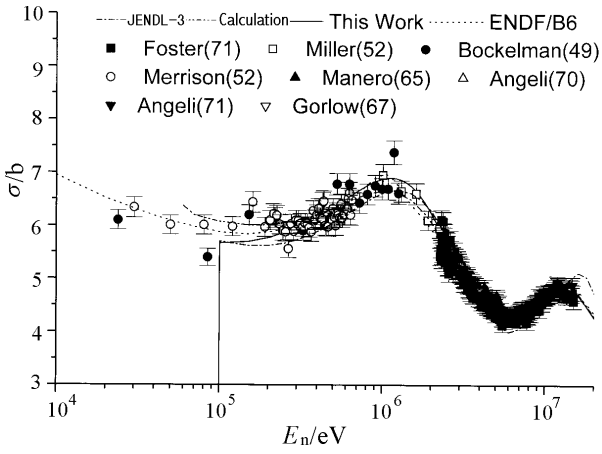

Fig. 2 ^{127}I total cross section

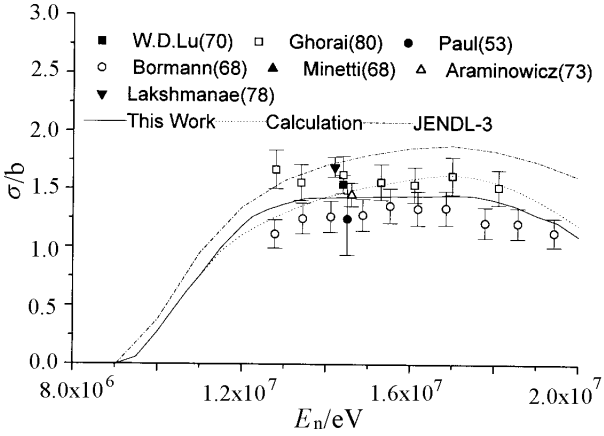

Fig. 3 ^{123}Sb(n,2n) cross section

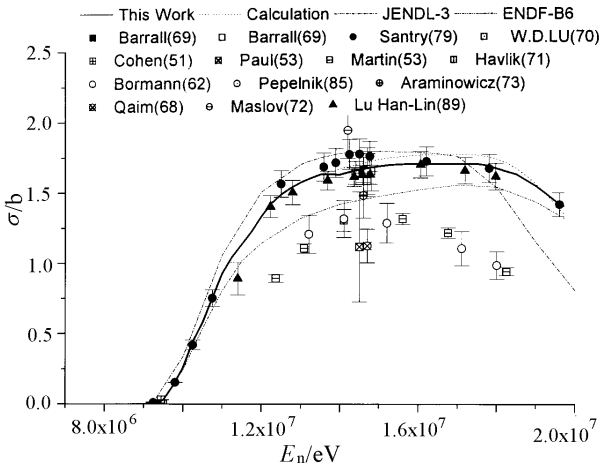

Fig. 4 ^{127}I(n,2n) cross section

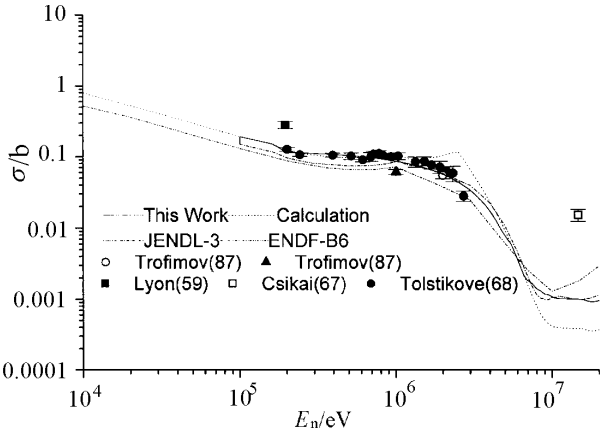

Fig. 5 ^{123}Sb capture cross section

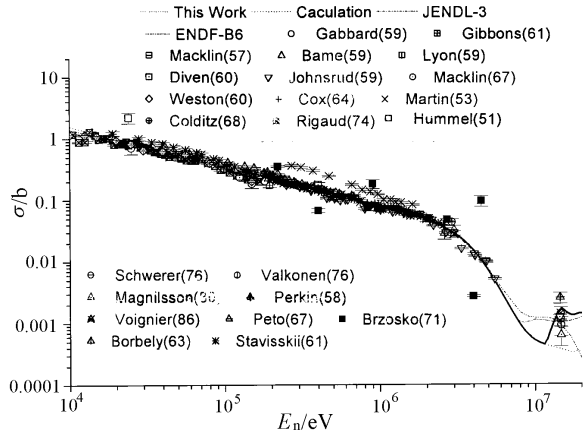

Fig. 6 ^{127}I capture cross section

Reference

[1] D.G.Foster et al., Phys. Rev./C, 3, 576, 1971
[2] J.M.Peterson et al., Phys. Rev., 120, 521,1960
[3] J.H.Coon et al., Phys. Rev., 88, 562,1952
[4] A.Bratenahl et al., Phys. Rev., 110, 927,1958
[5] L.D.Vincent et al., R, WADD-TR-60-217, 1960
[6] N.Nereson et al., Phys.Rev.,94,1678,1954
[7] D.W.Miller et al., Phys. Rev., 88, 83,1952
[8] A.D.Carlson et al., Phys. Rev., 158, 1142, 1967
[9] C.K.Bockelman et al., Phys. Rev., 76, 277,1949
[10] A.B.Smith et al., Nucl. Phys./A, 415,1,1984
[11] R.H.Tabony et al., Appl.Phys., 46, 401, 1968
[12] W.P.Poenitz et al., R, ANL-NDM-80, 1983
[13] K.Kobayashi et al., P, NEANDC (J)-140,42,1989
[14] F.Manero, Phys. Rev., 65, 419,1965
[15] G.V.Gorlov et al., Jadernaja Fizika, 6,91,1967
[16] I.Angeli et al., Acta Physica Hungarica, 28, 87, 1970
[17] A.W.Merrison et al., Proc.Roy.Soc.,215, 278,1952
[18] B.L.Cohen, Phys.Rev.,81,184,1951
[19] J.H.Mc Crary et al., J, BAP, 5, 246 (HA5), 1960
[20] Y.Kanda, J,JPJ,24,17,1968
[21] M.Bormann et al., Nucl. Phys./A, 115, 309,1968
[22] B.Minetti et al., J,ZP, 217,83,1968
[23] J.Araminowicz et al., P,INR-1464,14,1973
[24] V.S.Dementi et al., J,DOK, 27, 926, 1940
[25] W.D.Lu et al., Phys. Rew./C, 1,350,1970
[26] S.K.Ghorai et al., J,JP/G,6,393,1980
[27] E.B.Paul et al., J,CJP,31,267,1953
[28] N.Lakshmana et al., J,PRM, 11, (5), 595,1978
[29] H.C.Martin et al., Phys. Rev., 89, 1302, 1953
[30] M. Bormann et al.. Physik,166, 477,1962
[31] E.B.Paul et al., Phys., 31, 267, 1953
[32] S.M.Qaim et al., Nucl. Chem., 30, 2577, 1968
[33] R.C.Barrall et al., R, AFWL-TR-68-134,1969
[34] W.D.Lu et al., Phys. Rev., 1, 350,1970
[35] J.D.Jenkins et al., Nucl. Soc., 14, 381,1971
[36] E.Havlik, Acta Physica Austriaca,34,209,1971
[37] R.Pepelnik et al., C, 85SANTA, 1,211 (JA46),1985
[38] J.Araminowicz et al., R,INR-1464,14,1973
[39] G.N.Maslov et al., R,YK-9, 50, 1972
[40] D.C.Santry, C,79KNOX,,(DC-9),1979
[41] LU Hanlin et al., R,INDC(CPR)-16,1989
[42] B.L.Cohen, Phys. Rev.,81,184,1951
[43] W.S.Lyon et al., Phys. Rev., 114, 1619, 1959
[44] D.J.Hughes et al., Phys.Rev.,75,1781,1949
[45] V.A.Tolstikov, et al., J,AE,24,(6),576,1968
[46] Yu.N.Trofimov, J,YK,(4),1987
[47] Yu.N.Trofimov, C,87KIEV,3,331,1987
[48] H.Von Halban et al., J,Nat,142,392,1938
[49] L.E.Beghian et al., J,Nat,163,366,1949
[50] J.Csikai et al., Nucl. Phys./A, 95, 229,1967
[51] V.Hummel et al., Phys. Rev.,82,67,1951
[52] J.S.Brzosko et al., Acta Physica Polonica Section B,2,489,1971
[53] F.Gabbard et al., Phys. Rev., 114, 201, 1959
[54] J.H.Gibbons et al., Phys. Rev.,122, 182,1961
[55] S.J.Bame et al., Phys. Rev.,113,256,1959
[56] B.C.Diven et al., Phys. Rev., 120, 556, 1960
[57] R.L.Macklin et al., Phys. Rev.,159,1007,1967
[58] S.A.Cox, Phys. Rev., 133, 378, 1964
[59] G.A.Linenberger et al., R, LA-467,1946
[60] R.L.Macklin, Nucl.Sci. and Eng.,85,350,1983
[61] G.Magnusson et al., Physica Scripta, 21,(1),21, 1980
[62] A.E.Johnsrud et al., Phys. Rev., 116, 927,1959
[63] F.Rigaudv, Nucl.Sci. and Eng., 55,17, 1974
[64] O.Schwerer et al., Nucl. Phys., 264,105, 1976
[65] M.Valkonen, R,Ju-RR-1/1976,1976
[66] H.Liskien, Nucl. Phys.,118,379,1968
[67] D.L.Allan, Nucl. Phys.,24,274,1961
[68] R.F.Coleman et al., Proc. Phys. Soc., 73,215,1959

NAT–A Code for Composition of the Nuclear Data File of Natural Element from Its Isotope Files

SHEN Qingbiao

China Nuclear Data Center, CIAE, Beijing

Introduction

The nuclear data of the natural elements are very useful in some nuclear engineering design. The data of natural element can be composed from its isotope data. The NATURAL command of the CRECTJ-6 code[1] can do this but some problems existed. (1) It can not treat the angular distributions (MF=4) for MT=51~90; (2) It could not really compose the energy spectra (MT=5) of the isotopes to one set of the energy spectra of the natural element; (3) If the sum of the (n, n′) levels of all isotopes exceeds 40, it can not make the contributions of the (n,n′) levels above 40-th level to the angular distributions (MF=4, MT=91) and the energy spectra (MF=5,MT=91). We developed a code NAT, which can composite natural element data from its isototopes for MF=2,3,4,5 and solved above problems describing as follows.

1 Angular Distributions (MF=4)

The NAT code can treat the angular distributions given in the form of Legendre polynomials. The coefficient of *l*-th term a_l except the inelastic scattering to discrete levels is calculated as follows:

$$a_l = \sum_{i=1}^{n} (a_l)_i (\sigma)_i f_i \Big/ \sum_{i=1}^{n} (\sigma)_i f_i \qquad (1)$$

Where $(\sigma)_i$ is the corresponding cross section, f_i is the abundance of the *i*-th isotope. This calculation is performed at all incident neutron energies *E*, where the data are given for certain isotope.

The coefficient of *l*-th term a_l of the inelastic scattering to discrete levels does not need to be changed. If the sum *K* of the levels of all isotopes exceeds 40, the continuum level inelastic scattering coefficient of *l*-th term a_l of the natural element is calculated as follows:

$$a_l = (a_{l,\mathrm{c}}\sigma_{\mathrm{in,c}} + \sum_{k=41}^{K} a_{l,k}\sigma_{\mathrm{in},k}) / (\sigma_{\mathrm{in,c}} + \sum_{k=41}^{K} \sigma_{\mathrm{in},k}) \qquad (2)$$

where $a_{l,\mathrm{c}}$ is the original continuum level inelastic scattering coefficient of *l*-th term of the natural element treated with Eq. (1); $a_{l,k}$, k=41,42,……,K are the inelastic scattering coefficient to the discrete levels of *l*-th term of the natural element obtained by the method mentioned above; $\sigma_{\mathrm{in},k}$, k=41,42,……,K are the inelastic scattering cross sections of the natural element for the levels ordered 41,42,……,K; and $\sigma_{\mathrm{in},c}$, is the original continuum level cross section of the natural element, which is the sum of the isotopes cross sections multiplied by its abundance.

2 Energy Spectra (MF=5)

The NAT code can treat the energy spectra given in the tabulated form. The emitted particle normalized spectra of the natural element *S(E′)* is calculated as follows:

$$S(E') = \sum_{i=1}^{n} (S(E'))_i (\sigma)_i f_i \Big/ \sum_{i=1}^{n} (\sigma)_i f_i \qquad (3)$$

Where E' is the neutron output energy. This calculation is performed at all neutron incident energies *E*, where the data are given for certain isotope. If the sum of the levels of all isotopes exceeds 40, the discrete level cross sections $\sigma_{\mathrm{in},k}$, above 40-th level should be spread according to the normalized Gaussian distribution:

$$f_k(E') = \frac{1}{\sqrt{2\pi}\Gamma_k} \exp\left(-\frac{(E'-E_k)^2}{2\Gamma_k^2}\right) \qquad (4)$$

Where $\Gamma_k = 0.05E_k^{2/3}$ in MeV, E_k is the output

energy of *k*-th level, *E'* is the neutron output energy after energy spread. Then the continuum level normalized neutron spectra can be calculated as follows:

$$S(E') = (S_{\mathrm{in,c}}(E')\sigma_{\mathrm{in,c}} + \sum_{k=41}^{K} f_k(E')\sigma_{\mathrm{in},k})/(\sigma_{\mathrm{in,c}} + \sum_{k=41}^{K}\sigma_{\mathrm{in},k}) \quad (5)$$

where $S_{\mathrm{in,c}}$ (E') is the original continuum level inelastic scattering normalized neutron spectra of the natural element treated with Eq. (3).

In Figs. 1 and 2 are shown the comparisons of the (n,2n) and (n,n′) output neutron normalized spectra for ^{151}Eu, ^{153}Eu, and ^{Nat}Eu at incident energy 10.5 MeV. It can be seen that the composition spectra of ^{Nat}Eu by the NAT code are reasonable.

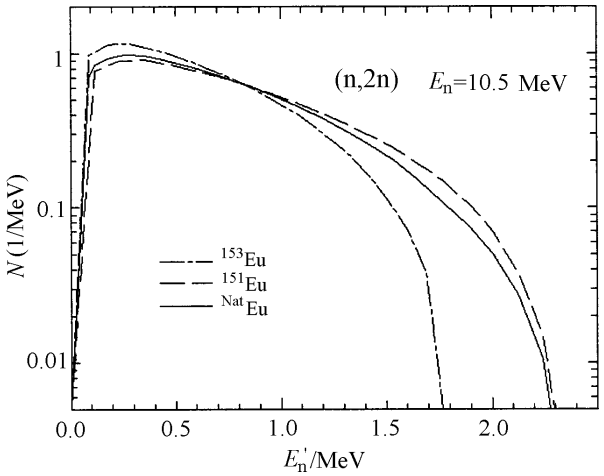

Fig. 1 Comparison of the (n,2n) output neutron spectra for ^{151,153}Eu,and at ^{Nat}Eu at incident energy 10.5 MeV

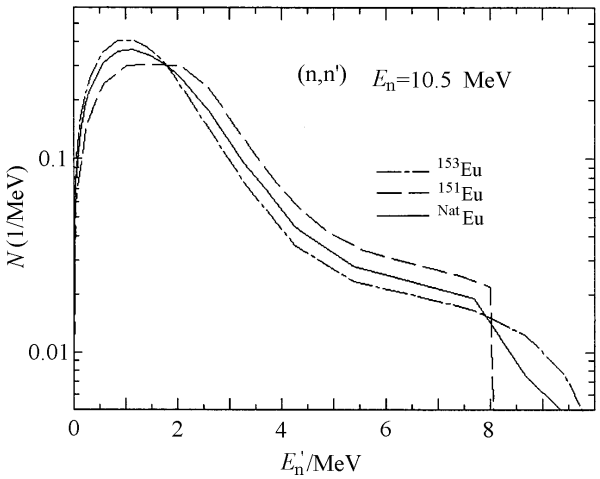

Fig. 2 Same as Fig. 1 but for (n,n′) reaction

The NAT code has been used for 8 elements: Ga, Rb, Sb, Ba, Nd, Sm, Eu, Gd, whose numbers of the isotopes are 2, 2, 2, 7, 7, 7, 2, and 7, respectively, and the satisfied results were obtained.

The author would like to thank Profs. Liu Tingjin, Zhuang Youxiang, Zhang Jingshang for their helpful discussions.

Reference

[1] Tsuneo Nakagawa, JAERI-Data/Code 99-041, Sep.1999.

The Developments of CWIMS Code and Its 69-group Library

LIU Ping ZHANG Baocheng

China Nuclear Data Center, CIAE, Beijing

【**abstract**】*Because of the limitation of original WIMS 69-group library, the reaction cross-sections and scatting matrices in the epithermal energy ranges are only given for one temperature. According to the requirement of user and for wide applications, the suitable adjustments of WIMS library were done, and the new WIMS library---CWIMS library is temperature-dependent in the whole energy ranges. Meanwhile the WIMS/D4 code was modified according to the new WIMS format library. Some auxiliary codes of new version WIMS/D4--- CWIMS, such as CSCN—Select and Collapse the CWIMS library and W10T2—Change CWIMS library from BCD to binary or from binary to BCD format were designed. In order to demonstrate the reliability of the CWIMS library and CWIMS code, five thermal assemblies -- TRX-1 and 2, BAPL-1,2 and 3 were calculated by using the CWIMS code and its own library. The calculated results were compared with those of experiments and old WIMS library.*

Introduction

WIMS/D4[1] is a non-commercial lattice code, which was developed by Britain. It's very popular all around the world. WIMS/D4 is mainly used for the calculations of thermal reactors, and it has its own WIMS 69-group cross-sections library. Because of the limitation of the library format, the reaction cross-sections and scattering matrices are only given for one temperature in the epithermal energy ranges, namely they are temperature-independent. Such processing is obviously unreasonable for some nuclides, and some errors could be coursed sometimes. It's the limitation of the library format. In order to solve the problem and for wide applications. It's necessary to change the format of original WIMS library and modify the WIMS/D4 code, so that the new format WIMS library can sufficiently consider the temperature effect in the whole energy ranges.

The processing was carried out by using NJOY[2] nuclear data processing code system. CENDL-2.1 evaluated nuclear data libraries were used for generating the CWIMS library.

In order to demonstrate the reliability of the CWIMS library and CWIMS code, it's necessary to do benchmarks testing. So, the integral parameters of five thermal assemblies -- TRX-1 and 2, BAPL-1, 2 and 3 were calculated by using the CWIMS code and CWIMS library. The calculated results were compared with those of experiments and old WIMS library.

1 Generation of CWIMS 69-group cross-sections library

The CWIMS library includes 83 nuclides.

1.1 Evaluated Nuclear Data Library

CENDL-2.1 were used for generating the CWIMS library.

1.2 Processing Code System

The famous nuclear data processing code system NJOY was used, including the RECON, BROADR, THERMR, UNRESR and GROUPR modules. The module WIMSR of NJOY was modified for preparing the new format WIMS library and called CWIMSR module.

RECONR: Reconstruction of resonance cross sections

The main input parameter is resonance reconstruction tolerance, a value of 0.2% was used for it for all materials in this work.

BROADR: Doppler-broadens and thinning point-wise cross sections

The main input parameter is the tolerance for thinning. A 0.2% maximum tolerance criterion was applied for all materials in this work.

UNRESR: Processing point-wise cross sections in the unresolved energy range

THERMR: Generating neutron scattering cross sections in the thermal energy range

GROUPR: Producing multi-group cross-sections and group-to-group scattering matrices

The neutron group structure is EPRI-CPM 69-group structure. The Legendre order is one, and the EPRI-CELL LWR spectrum for cross section averaging was adopted.

CWIMSR: Preparing libraries for the code CWIMS

CWIMS libraries use a standard 69-group structure with 14 fast groups, 13 resonance groups and 42 thermal groups. The energy-independent Goldstein-cohen (λ) values for intermediate-reconstruction were applied. They are shown in Table 1 for some materials.

Table 1 List of applied λ values.

Materials	λ Values
H	1.0
D	1.0
O	1.0
Al	1.0
^{235}U	0.2
^{238}U	0.2

2 Data Testing Calculations

The integral parameters of 5 thermal assembles -- TRX-1, 2; BAPL-1, 2, 3 were calculated by using CWIMS code and its 69-group library. They are given in Table 2.

K_{eff} —effective multiplication factor;

ρ^{28} —ratio of epithermal to thermal ^{238}U capture reaction rate;

δ^{25} —ratio of epithermal to thermal ^{235}U fission reaction rate;

δ^{28} —ratio of ^{238}U fission to ^{235}U fission reaction rate;

C^* —ratio of ^{238}U capture to ^{235}U fission reaction rate.

TRX-1,2 used uranium metal fuel in ^{235}U enriched to 1.305 wt. %; BAPL-1,2,3 used uranium oxide fuel enriched 1.311 wt. %; TRX and BAPL were water (H_2O)-moderated. Details of these lattices are given in Table 2. The results and comparisons are shown in Table 3 and Table 4.

The results show that the calculated results based on CWIMS library are in good agreement with those of experiments, and are much better than those results of WIMS86 library with WIMS/D4.

Table 2 Brief Characteristics of TRX-1, 2 and BAPL-1, 2, 3

Lattice	Fuel	Cladding	Moderator	Rod Radius(cm)	Pitch(cm)
TRX-1	1.3 wt. % U-metal	Al	H_2O	0.4915	1.8060
TRX-2	1.3 wt. % U-metal	Al	H_2O	0.4915	2.1740
BAPL-1	1.3 wt. % UO_2	Al	H_2O	0.4864	1.5578
BAPL-2	1.3 wt. % UO_2	Al	H_2O	0.4864	1.6528
BAPL-3	1.3 wt. % UO_2	Al	H_2O	0.4864	1.8057

Table 3 Integral parameter comparison

Lattice	Integral parameters	Experimental values	WIMS/D4 (WIMS86)	CWIMS (CENDL-2.1)	WIMS/D4 (ENDF/B6)
TRX-1	K_{eff}	1.0000(~.30)	1.0023	99832	0.98853
	ρ^{28}	1.32(~1.6)	1.279	1.3658	1.377
	δ^{25}	0.0987(~1.0)	0.099	0.09800	0.0977
	δ^{28}	0.0946(~4.3)	0.0965	0.09989	0.0974
	C^*	0.797(~1.0)	0.780	0.79277	0.808
TRX-2	K_{eff}	1.0000(~.10)	0.9965	0.9992	0.99113
	ρ^{28}	0.837(~1.9)	0.808	0.8543	0.863
	δ^{25}	0.0614(~1.3)	0.061	0.060134	0.0600
	δ^{28}	0.0693(~5.1)	0.0695	0.07105	0.0690
	C^*	0.647(~.93)	0.636	0.63822	0.650
BAPL-1	K_{eff}	1.0000(~.10)	1.0029	1.00328	0.99431
	ρ^{28}	1.390(~.72)	1.358	1.40728	1.429
	δ^{25}	0.084(~2.4)	0.084	0.08267	0.0824
	δ^{28}	0.078(~5.1)	0.0755	0.077124	0.0751
	C^*	0.0000	0.800	0.80065	0.819
BAPL-2	K_{eff}	1.0000(~.10)	1.0005	1.00229	0.99459
	ρ^{28}	1.120(~.89)	1.133	1.1714	1.188
	δ^{25}	0.068(~1.5)	0.0687	0.0675	0.0672
	δ^{28}	0.070(~5.7)	0.0652	0.06644	0.0645
	C^*	0.0000	0.732	0.7299	0.746

Cont. Table 3

Lattice	Integral parameters	Experimental values	WIMS/D4 (WIMS86)	CWIMS (CENDL-2.1)	WIMS/D4 (ENDF/B6)
BAPL-3	K_{eff}	1.0000(~1.0)	0.9981	1.0019	0.99565
	ρ^{28}	0.906(~1.1)	0.894	0.92046	0.933
	δ^{25}	0.052(~1.9)	0.0529	0.0519	0.0516
	δ^{28}	0.057(~5.3)	0.0538	0.05456	0.0528
	C*	0.0000	0.657	0.65256	0.666

Table 4 Integral parameter comparison (C/E)[1)]

Lattices	Integral Parameters	Experimental Values	CWIMS (CENDL-2.1)(C/E)	WIMS/D4(ENDF/B6)(C/E)
TRX-1	K_{eff}	1.0000(~.30)	0.99832	0.98853
	ρ^{28}	1.32(~1.6)	1.03469	1.04318
	δ^{25}	0.0987(~1.0)	0.99291	0.98987
	δ^{28}	0.0946(~4.3)	1.05592	1.02960
	C*	0.797(~1.0)	0.994693	1.01380
TRX-2	K_{eff}	1.0000(~.10)	0.9992	0.99113
	ρ^{28}	0.837(~1.9)	1.02067	1.03106
	δ^{25}	0.0614(~1.3)	0.97938	0.97720
	δ^{28}	0.0693(~5.1)	1.02525	0.99567
	C*	0.647(~.93)	0.98643	1.00464
BAPL-1	K_{eff}	1.0000(~.10)	1.00328	0.99431
	ρ^{28}	1.390(~.72)	1.01243	1.02806
	δ^{25}	0.084(~2.4)	0.98417	0.98095
	δ^{28}	0.078(~5.1)	0.98877	0.96282
	C*	0.0000	0.80065	0.819
BAPL-2	K_{eff}	1.0000(~.10)	1.00229	0.99459
	ρ^{28}	1.120(~.89)	1.04589	1.06071
	δ^{25}	0.068(~1.5)	0.9926	0.98824
	δ^{28}	0.070(~5.7)	0.94914	0.92143
	C*	0.0000	0.7299	0.746
BAPL-3	K_{eff}	1.0000(~1.0)	1.0019	0.99565
	ρ^{28}	0.906(~1.1)	1.01596	1.02980
	δ^{25}	0.052(~1.9)	0.99808	0.99231
	δ^{28}	0.057(~5.3)	0.95719	0.92632
	C*	0.0000	0.65256	0.666

Note：1) C/E = Calculated result/Experimental result

References

[1] Macfarlane,R., E. et Al:, NJOY 97 Code System for Producing Pointwise and Multi-group Neutron andPhoton Cross Section from ENDF/B Data, LANL, Contribution to RSIC Peripheral Shielding Routine Collection, PSR-355,1997.

[2] Askew, J. R., Fayers, F. J., Kemshell P. B., J. British Nucl. Energy Soc., Vol. 5, No. 4, P. 564, October 1966

Activities and Cooperation in Nuclear Data Field in China During 2000

ZHUANG Youxiang
China Nuclear Data Center, CIAE, Beijing
e-mail: yxzhuang@iris.ciae.ac.cn

1 Meetings Held in China in 2000

1) Working Meeting on Fission Nuclide, Mar. 6~8, Beijing;
2) The Standing Committee Meeting of China Nculear Data Committee, Aug. 4, Beijing;
3) The Working Group Meeting of Multi-group Constant and Benchmark Test, Aug. 23~28, Nanchang;
4) Working Meeting on Nuclear Data Measurement, Nov. 27~Dec. 2, Kunming.

2 The International Meetings and Workshops in Nuclear Data Field Attended by Staffs of CNDC in 2000.

1) Workshop on Nuclear Reaction Data and Nuclear Reactor, Physics, Design and Safety. Mar. 13~Apr. 14, Yu Hongwei, Jin Yongli and Wei Kexing, ICTP, Italy;
2) IAEA Advisory Group Meeting on Network of Nuclear Reaction Data Centers, May 14~19, Zhuang Youxiang, Obninsk, Russia;
3) The 23rd Meeting of International Nuclear Data Committee, May 24~26, Liu Tingjin, Vienna, Austria;
4) NEA Working Party on International Nuclear Data Evaluation Co-operation, and International Advisory Committee on ND 2001, Jun. 19~21, Liu Tingjin, JAERI, Japan;
5) Advisory Group Meeting on the Co-ordination of International Network of Nuclear Structure and Decay Data Evaluators, Dec. 4~8, Zhou Chunmei and Huo Junde, Vienna, Austria.

3 The Foreign Scientists in Nuclear Data Field Visited CNDC/CIAE in 2000.

1) Dr. Charles Dunford, NNDC, U.S.A., Jun. 25~29.
2) Dr. Tokio Fukahori, JAERI, Japan, Sep. 3~10.

4 Staff of CNDC Worked in or visited Foreign Country.

1) Rong Jian, JAEIR, starting from Aug.1, schednled one year;
2) Han Yinlu, KAERI, from Oct. 10, 1998 to Apr.7, 2000;
3) Zhuang Youxiang, Zhou Chunmei and Huang Xiaolong visited the Central Research Institute of Management, Economics and Information, Moscow Russia, Oct. 2~10, 2000.

CINDA INDEX

Nuclide	Quantity	Energy/ eV		Lab	Type	Documentation				Author, Comments
		Min	Max			Ref	Vol	Page	Date	
^{10}B	(n,α)	4.0+6	6.7+6	BJG	Expt	Jour CNDP	25	1	Jun 2001	TANG Guoyou +, DA, SIG,TBL,IOCH
^{23}Na	Evaluation	1.0-5	2.0+7	AEP	Eval	Jour CNDP	25	61	Jun 2001	HUANG Xiaolong+, SIG,DA,DA/DE
^{64}Zn	(n,α)	5.0+6	6.7+6	TSI	Expt	Jour CNDP	25	6	Jun 2001	YUAN Jing +, DA, SIG,TBL,IOCH
^{75}As	(n,γ)	2.9+4	1.1+6	SIU	Expt	Jour CNDP	25	8	Jun 2001	XIA Yijun+ , SIG, ACTIVATION
^{93}Nb	Calculation	1.0+3	2.0+7	AEP	Theo	Jour CNDP	25	43	Jun 2001	RONG Jian +, SIG, DA, DE
^{93}Nb	Evaluation	1.0+3	2.0+7	NAN	Eval	Jour CNDP	25	67	Jun 2001	SU Weining+, SIG
^{95}Nb	Calculation	1.0+3	2.0+7	AEP	Theo	Jour CNDP	25	43	Jun 2001	RONG Jian +, SIG, DA, DE
^{95}Nb	Evaluation	1.0+3	2.0+7	NAN	Eval	Jour CNDP	25	67	Jun 2001	SU Weining+, SIG
^{99}Tc	Calculation	1.0+3	2.0+7	NKU	Theo	Jour CNDP	25	28	Jun 2001	CAI Chonghai +, SIG, DA, DE
^{99}Ru	Calculation	1.0+3	2.0+7	UNW	Theo	Jour CNDP	25	49	Jun 2001	ZHANG Zhengjun +, SIG, DA, DE
^{99}Ru	Evaluation	1.0+3	2.0+7	NAN	Eval	Jour CNDP	25	67	Jun 2001	SU Weining+, SIG
^{100}Ru	Calculation	1.0+3	2.0+7	UNW	Theo	Jour CNDP	25	49	Jun 2001	ZHANG Zhengjun +, SIG, DA, DE
^{100}Ru	Evaluation	1.0+3	2.0+7	NAN	Eval	Jour CNDP	25	67	Jun 2001	SU Weining+, SIG
^{101}Ru	Calculation	1.0+3	2.0+7	UNW	Theo	Jour CNDP	25	49	Jun 2001	ZHANG Zhengjun +, SIG, DA, DE
^{102}Ru	Calculation	1.0+3	2.0+7	UNW	Theo	Jour CNDP	25	49	Jun 2001	ZHANG Zhengjun +, SIG, DA, DE
^{103}Ru	Calculation	1.0+3	2.0+7	UNW	Theo	Jour CNDP	25	49	Jun 2001	ZHANG Zhengjun +, SIG, DA, DE
^{104}Ru	Calculation	1.0+3	2.0+7	UNW	Theo	Jour CNDP	25	49	Jun 2001	ZHANG Zhengjun +, SIG, DA, DE
^{105}Ru	Calculation	1.0+3	2.0+7	UNW	Theo	Jour CNDP	25	49	Jun 2001	ZHANG Zhengjun +, SIG, DA, DE
^{121}Sb	Evaluation	1.0+3	2.0+7	NAN	Eval	Jour CNDP	25	73	Jun 2001	ZHAO Jingwu+, SIG
^{123}Sb	Evaluation	1.0+3	2.0+7	NAN	Eval	Jour CNDP	25	73	Jun 2001	ZHAO Jingwu+, SIG
^{127}I	Evaluation	1.0+3	2.0+7	NAN	Eval	Jour CNDP	25	73	Jun 2001	ZHAO Jingwu+, SIG
^{135}I	Evaluation	1.0+3	2.0+7	NAN	Eval	Jour CNDP	25	73	Jun 2001	ZHAO Jingwu+, SIG
^{130}Ba	Calculation	1.0+3	2.0+7	UNW	Theo	Jour CNDP	25	41	Jun 2001	K. Kurban +, SIG, DA, DE

CINDA INDEX

Nuclide	Quantity	Energy/ eV		Lab	Type	Documentation				Author, Comments
		Min	Max			Ref	Vol	Page	Date	
^{132}Ba	Calculation	1.0+3	2.0+7	UNW	Theo	Jour CNDP	25	41	Jun 2001	K. Kurban +, SIG, DA, DE
^{134}Ba	Calculation	1.0+3	2.0+7	UNW	Theo	Jour CNDP	25	41	Jun 2001	K. Kurban +, SIG, DA, DE
^{135}Ba	Calculation	1.0+3	2.0+7	UNW	Theo	Jour CNDP	25	41	Jun 2001	K. Kurban +, SIG, DA, DE
^{136}Ba	Calculation	1.0+3	2.0+7	UNW	Theo	Jour CNDP	25	41	Jun 2001	K. Kurban +, SIG, DA, DE
^{137}Ba	Calculation	1.0+3	2.0+7	UNW	Theo	Jour CNDP	25	41	Jun 2001	K. Kurban +, SIG, DA, DE
^{138}Ba	Calculation	1.0+3	2.0+7	UNW	Theo	Jour CNDP	25	41	Jun 2001	K. Kurban +, SIG, DA, DE
^{133}Cs	Calculation	1.0+3	2.0+7	UNW	Theo	Jour CNDP	25	48	Jun 2001	ZHANG Zhengjun +, SIG, DA, DE
^{134}Cs	Calculation	1.0+3	2.0+7	UNW	Theo	Jour CNDP	25	48	Jun 2001	ZHANG Zhengjun +, SIG, DA, DE
^{135}Cs	Calculation	1.0+3	2.0+7	UNW	Theo	Jour CNDP	25	48	Jun 2001	ZHANG Zhengjun +, SIG, DA, DE
^{137}Cs	Calculation	1.0+3	2.0+7	UNW	Theo	Jour CNDP	25	48	Jun 2001	ZHANG Zhengjun +, SIG, DA, DE
^{136}Ce	Calculation	1.0+3	2.0+7	AEP	Theo	Jour CNDP	25	35	Jun 2001	HAN Yinlu +, SIG, DA, Da/DE, γ-production
^{138}Ce	Calculation	1.0+3	2.0+7	AEP	Theo	Jour CNDP	25	35	Jun 2001	HAN Yinlu +, SIG, DA, Da/DE, γ-production
^{140}Ce	Calculation	1.0+3	2.0+7	AEP	Theo	Jour CNDP	25	35	Jun 2001	HAN Yinlu +, SIG, DA, Da/DE, γ-production
^{142}Ce	Calculation	1.0+3	2.0+7	AEP	Theo	Jour CNDP	25	35	Jun 2001	HAN Yinlu +, SIG, DA, Da/DE, γ-production
^{Nat}Ce	Calculation	1.0+3	2.0+7	AEP	Theo	Jour CNDP	25	35	Jun 2001	HAN Yinlu +, SIG, DA, Da/DE, γ-production
^{142}Nd	Calculation	1.0+3	2.0+7	AEP	Theo	Jour CNDP	25	29	Jun 2001	SHEN Qingbiao +, SIG, DA, DE
^{143}Nd	Calculation	1.0+3	2.0+7	AEP	Theo	Jour CNDP	25	29	Jun 2001	SHEN Qingbiao +, SIG, DA, DE
^{144}Nd	Calculation	1.0+3	2.0+7	AEP	Theo	Jour CNDP	25	29	Jun 2001	SHEN Qingbiao +, SIG, DA, DE
^{145}Nd	Calculation	1.0+3	2.0+7	AEP	Theo	Jour CNDP	25	29	Jun 2001	SHEN Qingbiao +, SIG, DA, DE
^{146}Nd	Calculation	1.0+3	2.0+7	AEP	Theo	Jour CNDP	25	29	Jun 2001	SHEN Qingbiao +, SIG, DA, DE
^{147}Nd	Calculation	1.0+3	2.0+7	AEP	Theo	Jour CNDP	25	29	Jun 2001	SHEN Qingbiao +, SIG, DA, DE
^{148}Nd	Calculation	1.0+3	2.0+7	AEP	Theo	Jour CNDP	25	29	Jun 2001	SHEN Qingbiao +, SIG, DA, DE
^{150}Nd	Calculation	1.0+3	2.0+7	AEP	Theo	Jour CNDP	25	29	Jun 2001	SHEN Qingbiao +, SIG, DA, DE

CINDA INDEX

Nuclide	Quantity	Energy/ eV		Lab	Type	Documentation				Author, Comments
		Min	Max			Ref	Vol	Page	Date	
^{175}Lu	Calculation	1.0+3	2.0+7	AEP	Theo	Jour CNDP	25	44	Jun 2001	HAN Yinlu +, SIG, DA, Da/DE, γ-production
^{176}Lu	Calculation	1.0+3	2.0+7	AEP	Theo	Jour CNDP	25	44	Jun 2001	HAN Yinlu +, SIG, DA, Da/DE, γ-production
^{Nat}Lu	Calculation	1.0+3	2.0+7	AEP	Theo	Jour CNDP	25	44	Jun 2001	HAN Yinlu +, SIG, DA, Da/DE, γ-production
^{174}Hf	Calculation	1.0+3	2.0+7	AEP	Theo	Jour CNDP	25	23	Jun 2001	HAN Yinlu +, SIG, DA, Da/DE, γ-production
^{176}Hf	Calculation	1.0+3	2.0+7	AEP	Theo	Jour CNDP	25	23	Jun 2001	HAN Yinlu +, SIG, DA, Da/DE, γ-production
^{177}Hf	Calculation	1.0+3	2.0+7	AEP	Theo	Jour CNDP	25	23	Jun 2001	HAN Yinlu +, SIG, DA, Da/DE, γ-production
^{178}Hf	Calculation	1.0+3	2.0+7	AEP	Theo	Jour CNDP	25	23	Jun 2001	HAN Yinlu +, SIG, DA, Da/DE, γ-production
^{179}Hf	Calculation	1.0+3	2.0+7	AEP	Theo	Jour CNDP	25	23	Jun 2001	HAN Yinlu +, SIG, DA, Da/DE, γ-production
^{180}Hf	Calculation	1.0+3	2.0+7	AEP	Theo	Jour CNDP	25	23	Jun 2001	HAN Yinlu +, SIG, DA, Da/DE, γ-production
^{Nat}Hf	Calculation	1.0+3	2.0+7	AEP	Theo	Jour CNDP	25	23	Jun 2001	HAN Yinlu +, SIG, DA, Da/DE, γ-production
^{235}U	Fission Yield	2.2+7		AEP	Expt	Jour CNDP	25	4	Jun 2001	FENG Jing +, Fission Yield
^{235}U	Fission Yield	2.5-2	1.5+7	AEP	Eval	Jour CNDP	25	51	Jun 2001	LIU Tingjin, Reference Fission Product Yield
^{238}U	Fission Yield	1.9+7		AEP	Expt	Jour CNDP	25	10	Jun 2001	YANG Yi +, Fission Yield
^{241}Pu	Evaluation	1.0-5	2.0+7	AEP	Eval	Jour CNDP	25	55	Jun 2001	YU Baosheng +, SIG, DA, DE
^{242}Pu	Evaluation	1.0-5	2.0+7	AEP	Eval	Jour CNDP	25	55	Jun 2001	YU Baosheng +, SIG, DA, DE